INFN Angela Bonaccorso
Istituto Nazionale di Fisica Nucleare
SEZIONE DI PISA

The many facets of breakup reactions with exotic beams

G. Blanchon, D.M. Brink, F. Carstoiu, A. Garcia-Camacho, R. Kumar, J.Margueron, N. Vinh Mau

JAPAN-ITALY EFES Workshop
on Correlations in Reactions and Continuum
TORINO - Italy 6-8 September 2010

cf. Y. Suzuki &Co., H. Sagawa &Co., T. Nakamura &Co.

Introduction

Breakup reactions are a versatile mean of studying both projectile and target nuclear properties

In exotic nuclei they are used to study projectile structure via inverse kinematics experiments

Also transfer to the continuum from target sometime or projectile fragmentation to study resonance states in unbound nuclei

High energy scattering and the eikonal approximation. Optical potentials.

Elastic scattering of halo nuclei and the optical potential including breakup.

Transfer to the continuum, projectile fragmentation.

Coulomb breakup. All orders vs first order approximation. The proton vs neutron case.

Accuracy of reaction theory and experimental data analysis vs structure theory.

Binding energy per nucleon (MeV)

Colour codes:

0 - 0.56	0.56 - 1.13
1.13 - 1.69	1.69 - 2.25
2.25 - 2.81	2.81 - 3.38
3.38 - 3.94	3.94 - 4.5
4.5 - 5.06	5.06 - 5.63
5.63 - 6.19	6.19 - 6.75
6.75 - 7.31	7.31 - 7.88
7.88 - 8.44	8.44 - 9
Unknown or out of range	

Min: 0
Max: 9
Steps: 16

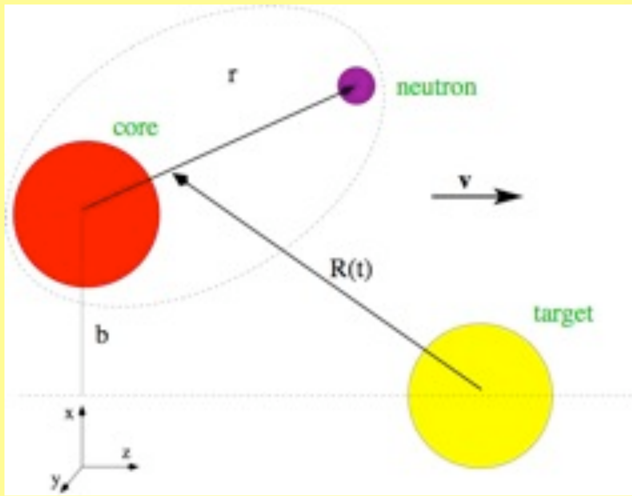

Transfer (...to the continuum)
(inclusive breakup with final state interaction with the target)

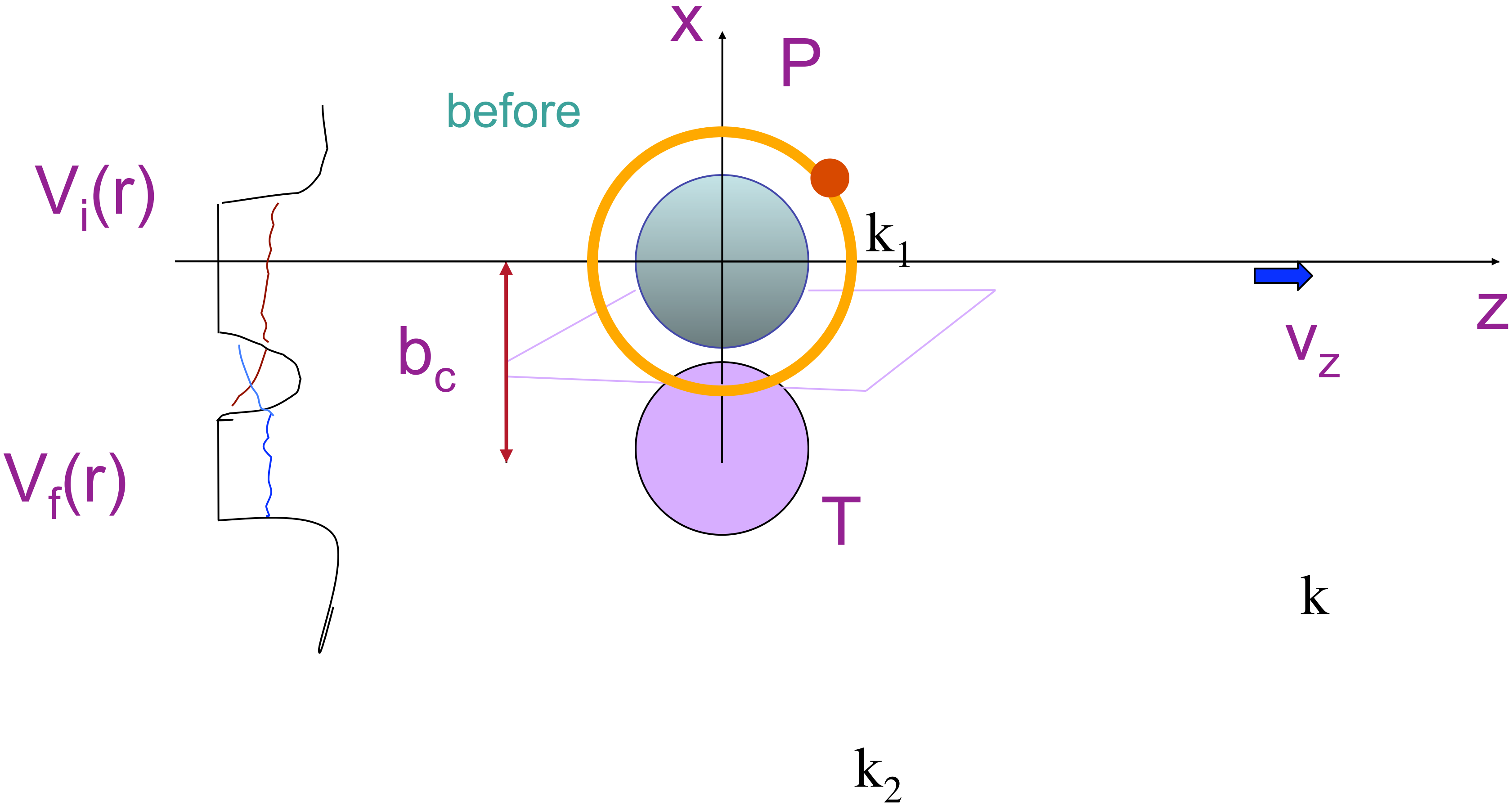

$k_2 - k_1 = k \quad \varepsilon_f - \varepsilon_i = mv^2/2$

diffraction and stripping

$\varepsilon_f^{opt} > 0$ for small ε_i

Transfer (...to the continuum)
(inclusive breakup with final state interaction with the target)

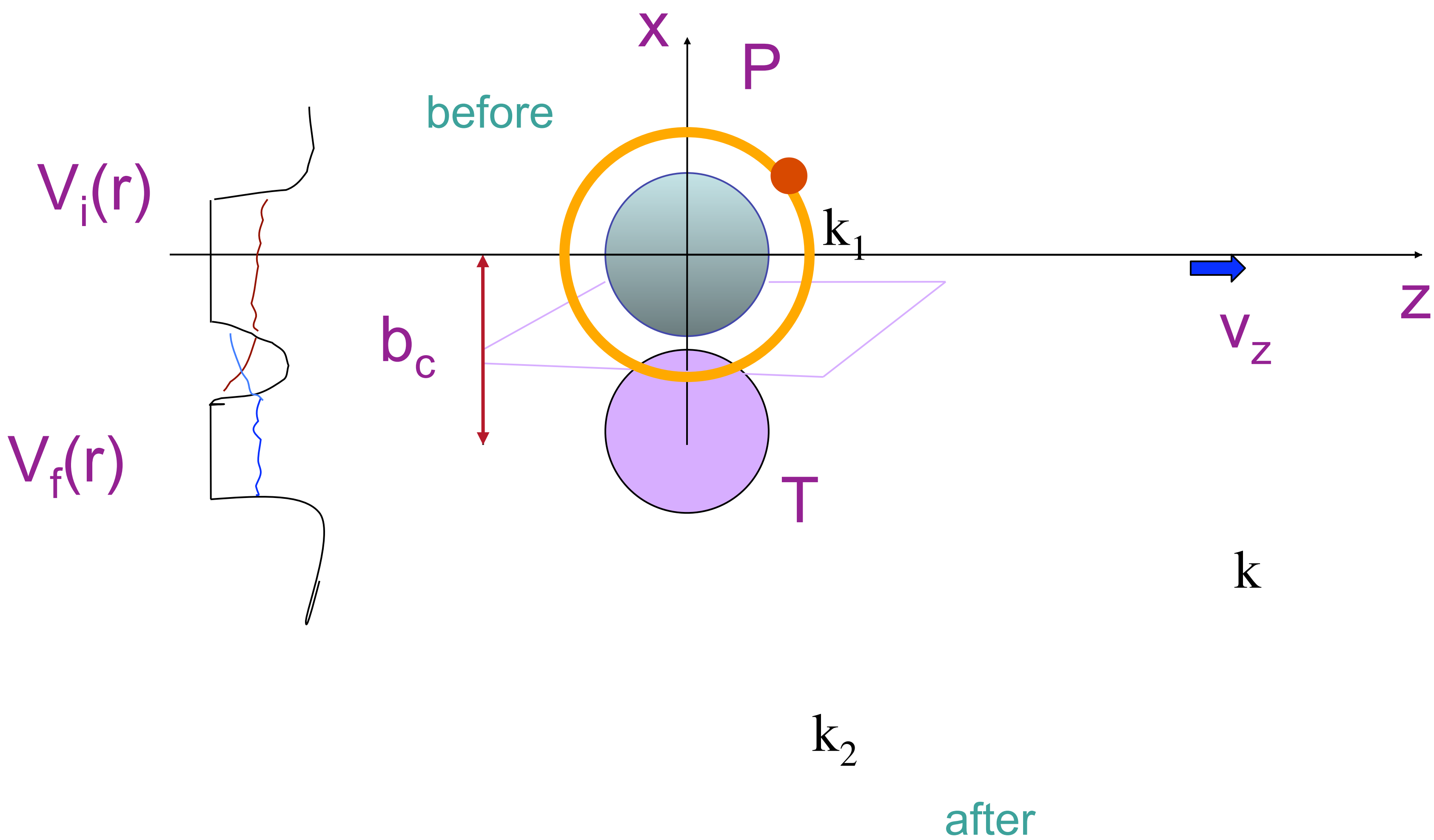

$k_2 - k_1 = k \quad \varepsilon_f - \varepsilon_i = mv^2/2$

diffraction and stripping

$\varepsilon_f^{opt} > 0$ for small ε_i

Transfer (...to the continuum) (inclusive breakup with final state interaction with the target)

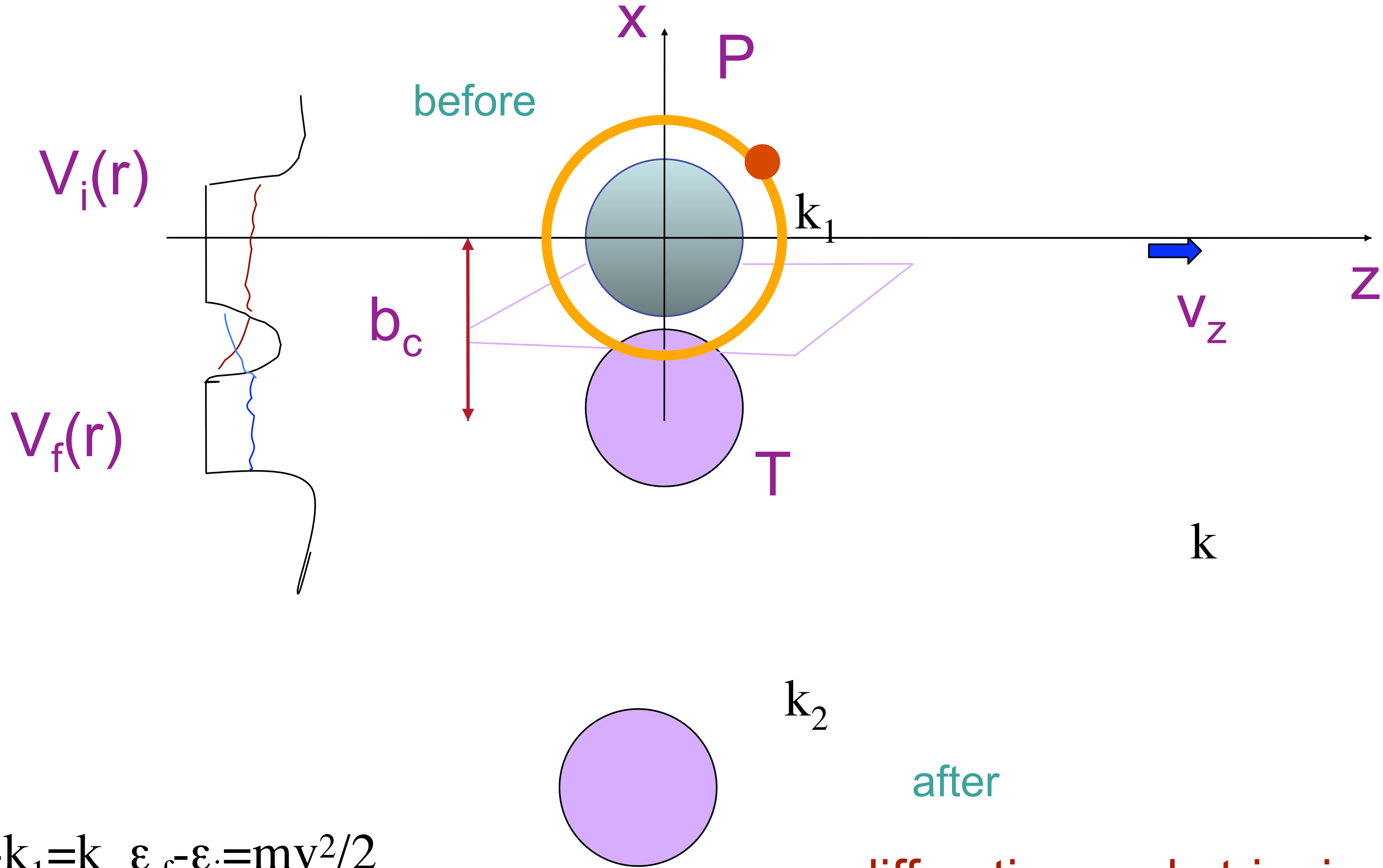

$k_2 - k_1 = k \quad \varepsilon_f - \varepsilon_i = mv^2/2$

diffraction and stripping

$\varepsilon_f^{opt} > 0$ for small ε_i

Transfer (...to the continuum)
(inclusive breakup with final state interaction with the target)

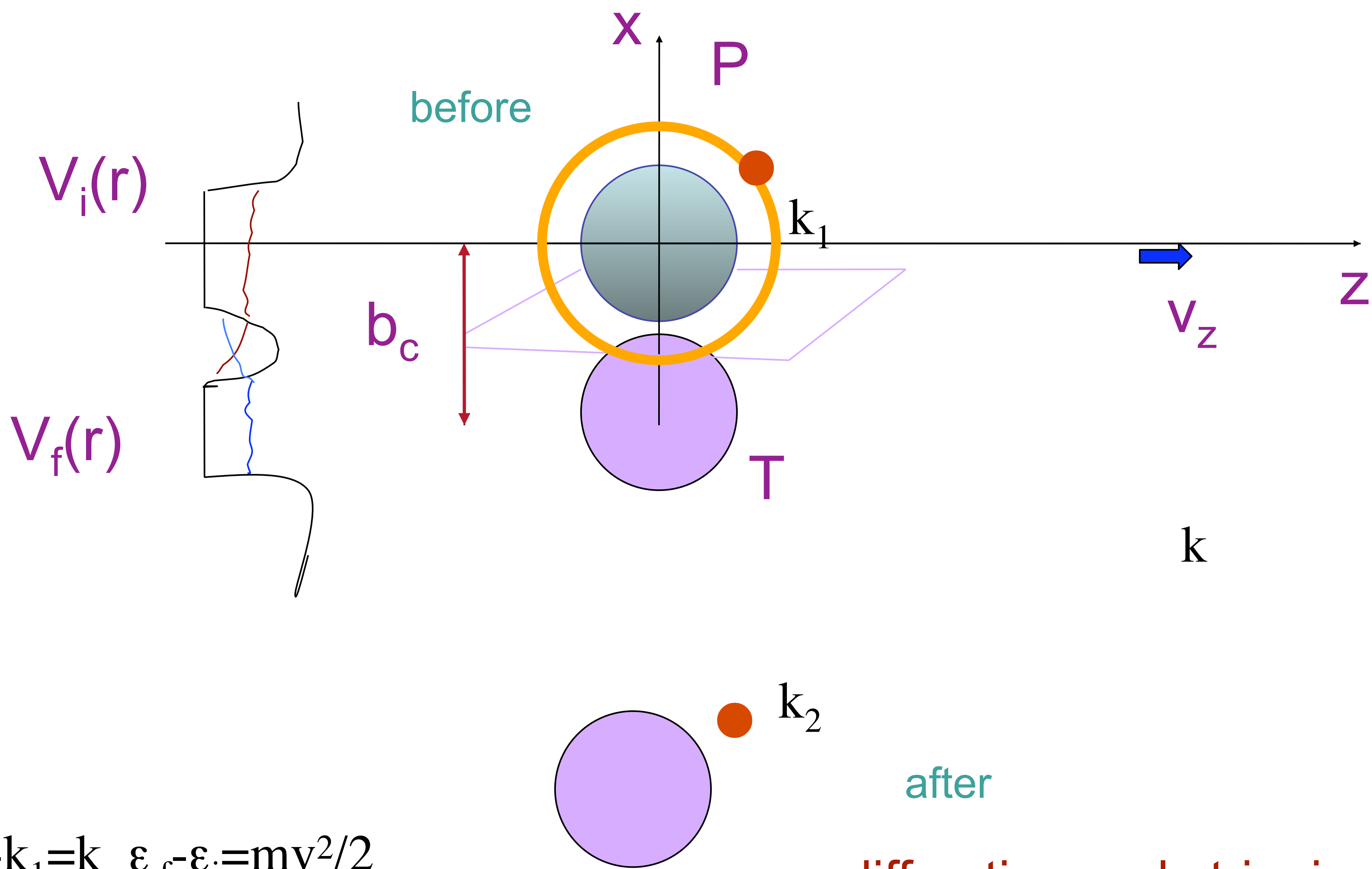

$k_2 - k_1 = k \quad \varepsilon_f - \varepsilon_i = mv^2/2$

$\varepsilon_f^{opt} > 0$ for small ε_i

diffraction and stripping

Transfer (...to the continuum)
(inclusive breakup with final state interaction with the target)

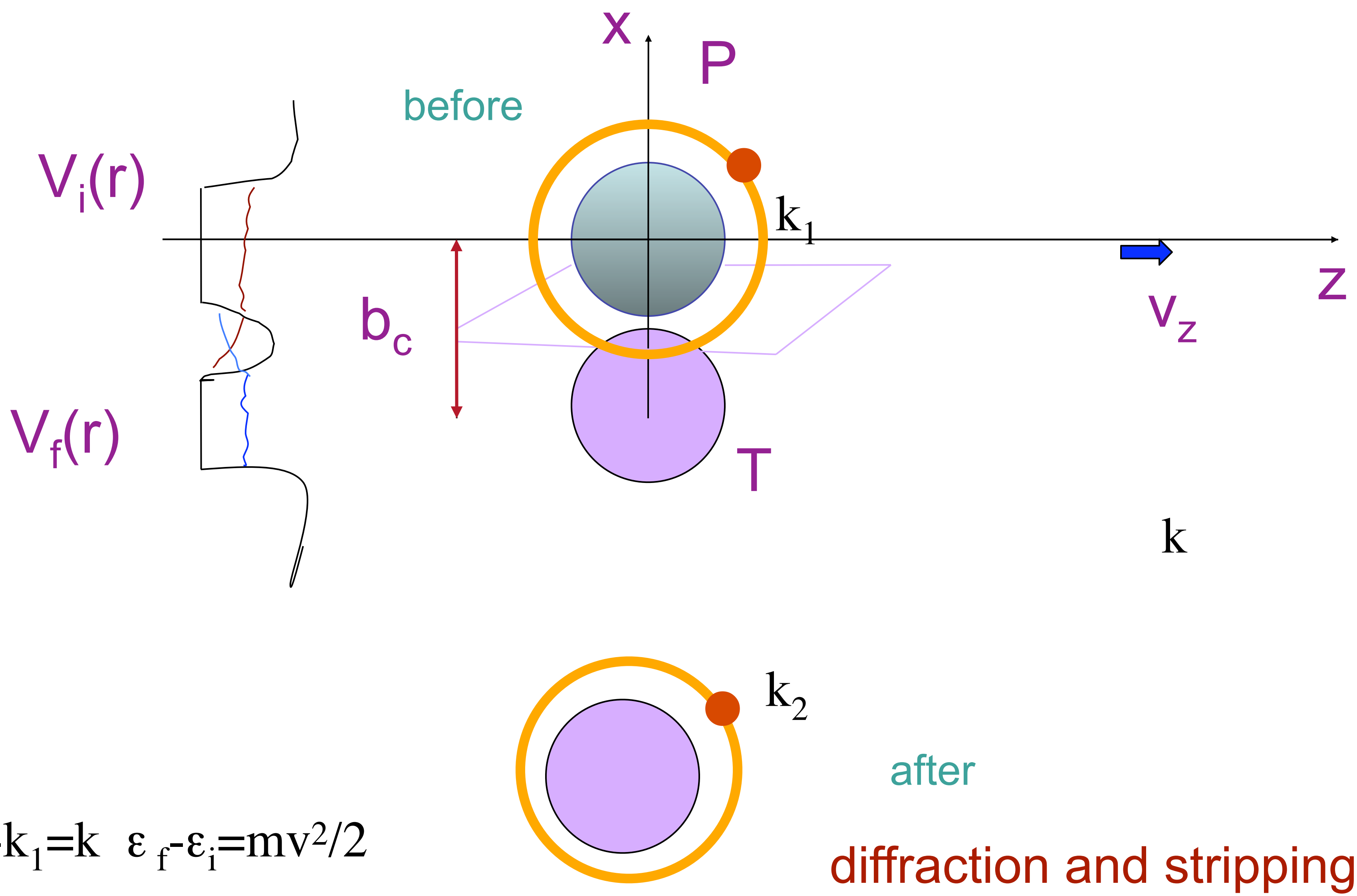

$k_2 - k_1 = k \quad \varepsilon_f - \varepsilon_i = mv^2/2$

diffraction and stripping

$\varepsilon_f^{opt} > 0$ for small ε_i

Transfer (...to the continuum) (inclusive breakup with final state interaction with the target)

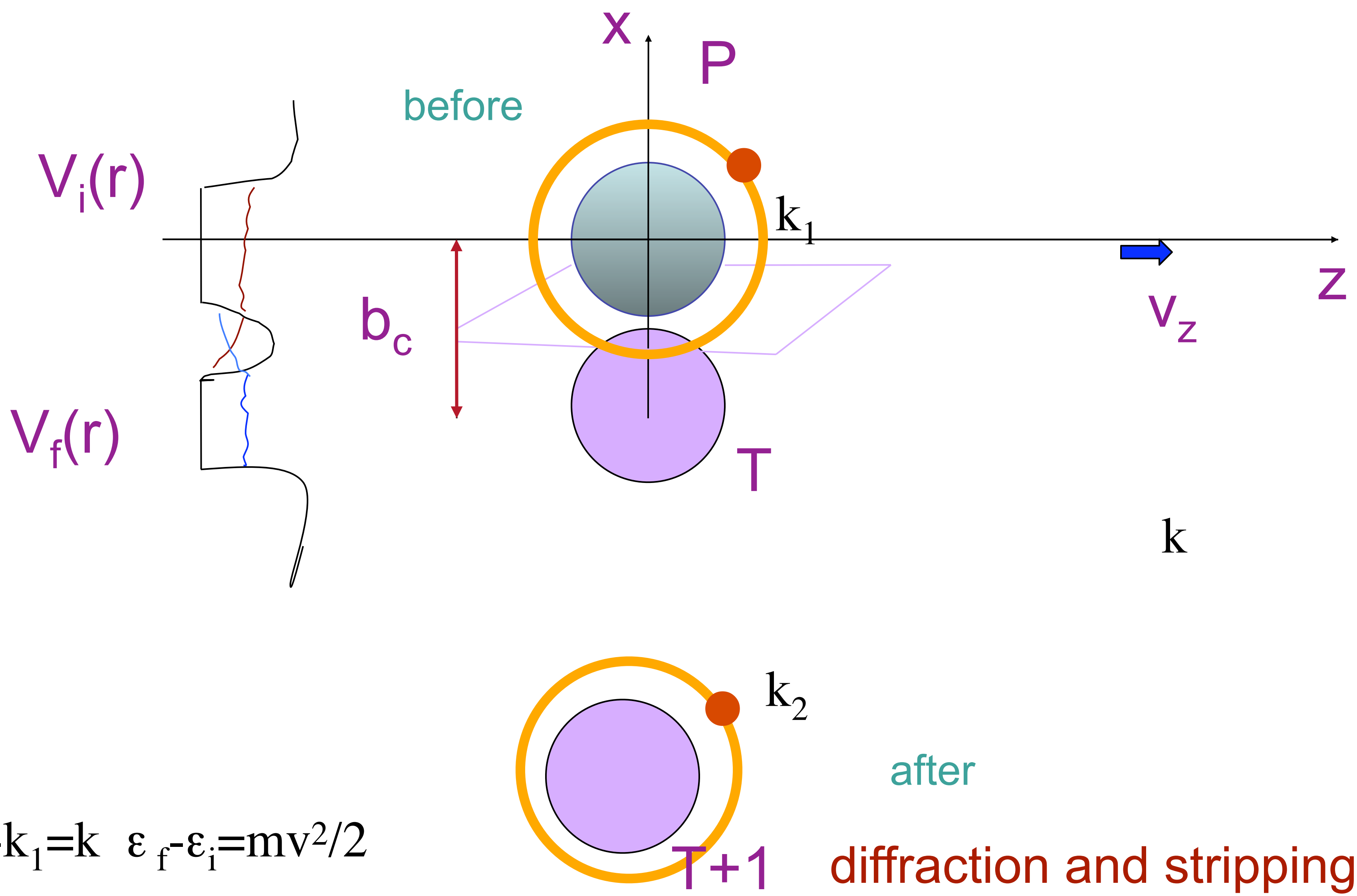

$k_2 - k_1 = k \quad \varepsilon_f - \varepsilon_i = mv^2/2$

diffraction and stripping

$\varepsilon_f^{opt} > 0$ for small ε_i

Transfer (...to the continuum)
(inclusive breakup with final state interaction with the target)

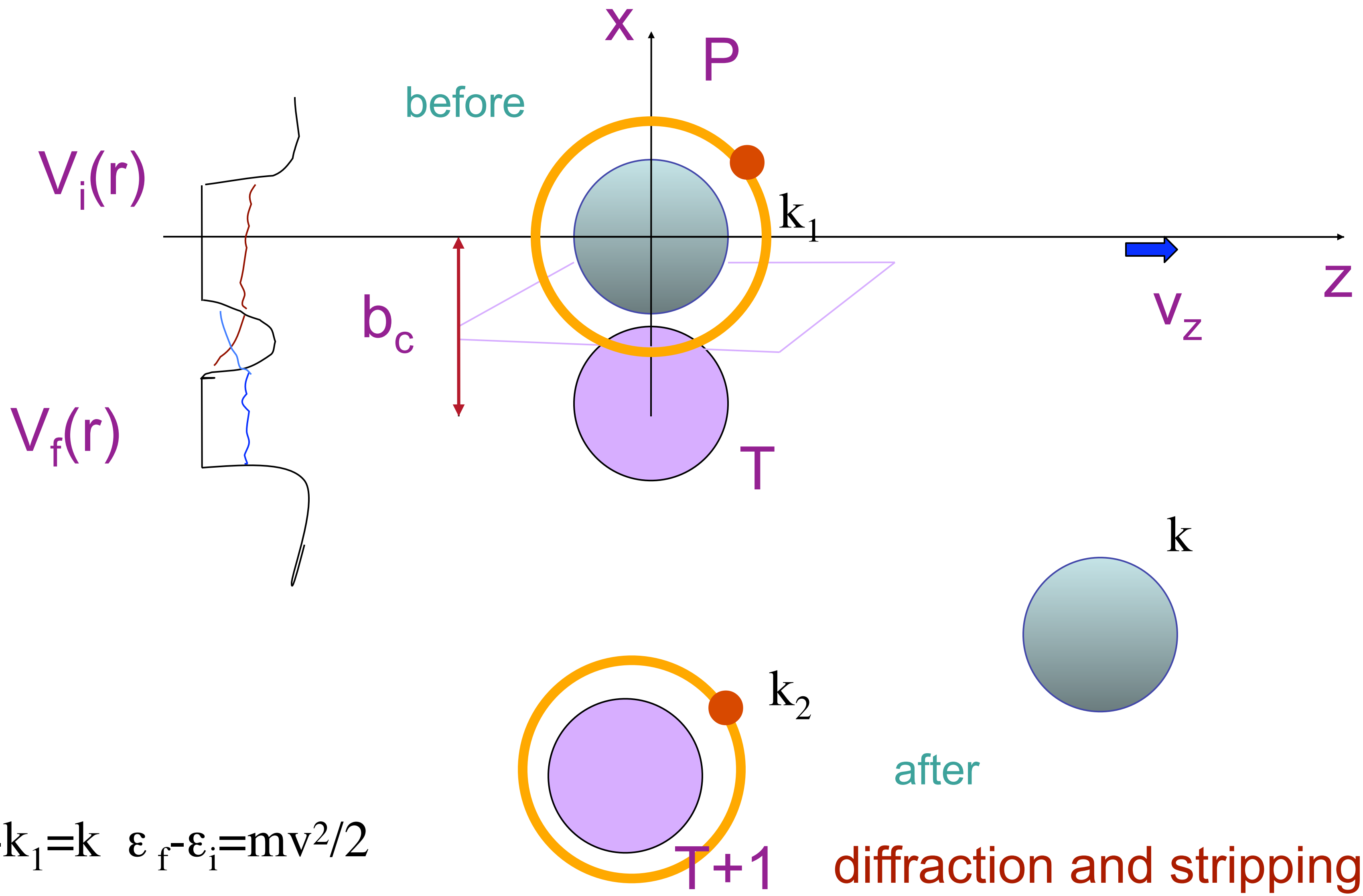

diffraction and stripping

$k_2 - k_1 = k \quad \varepsilon_f - \varepsilon_i = mv^2/2$

$\varepsilon_f^{opt} > 0$ for small ε_i

Transfer (...to the continuum)
(inclusive breakup with final state interaction with the target)

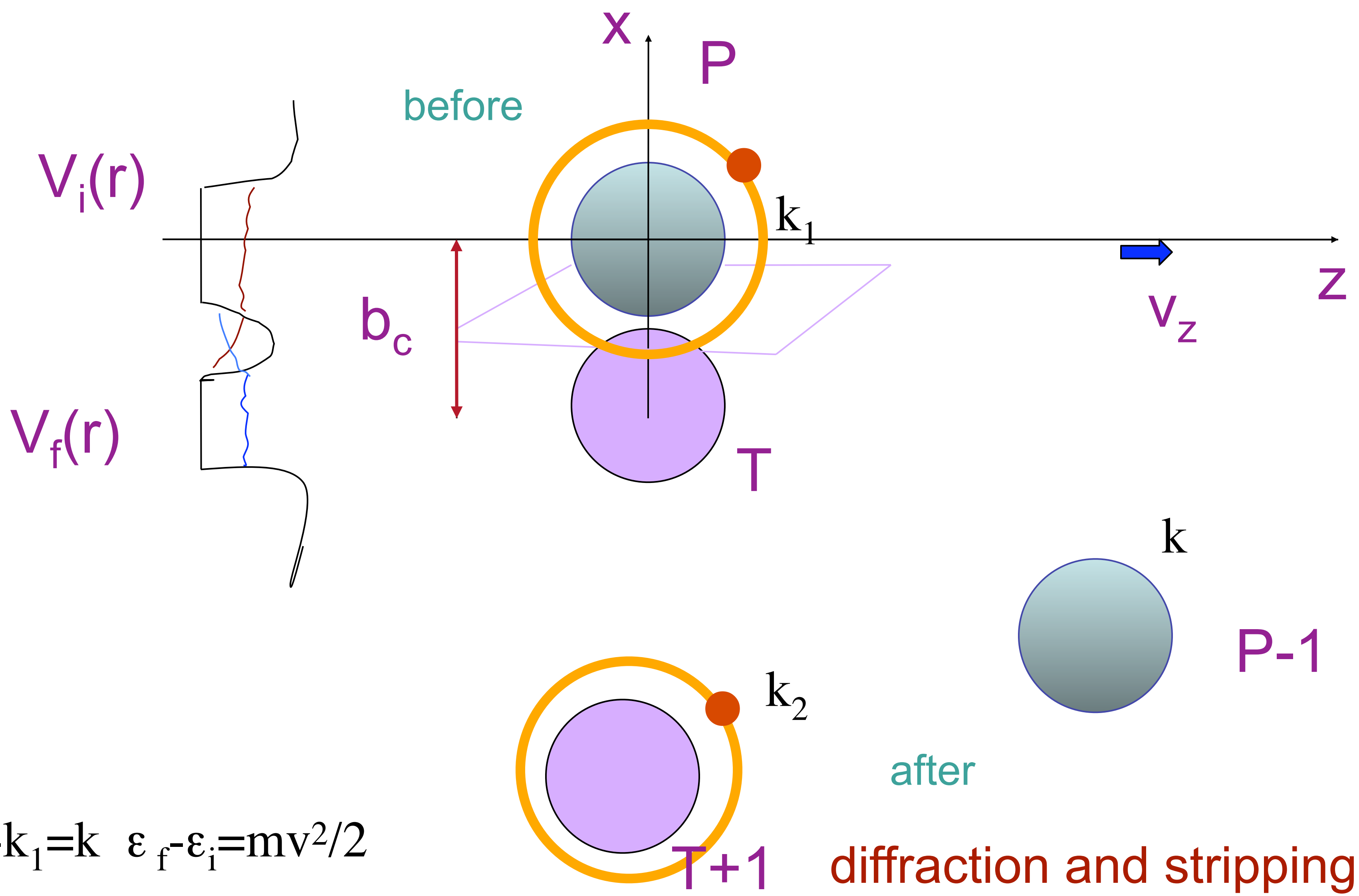

$k_2 - k_1 = k \quad \varepsilon_f - \varepsilon_i = mv^2/2$

diffraction and stripping

$\varepsilon_f^{opt} > 0$ for small ε_i

J.Enders et al.

PHYSICAL REVIEW C **65** 034318

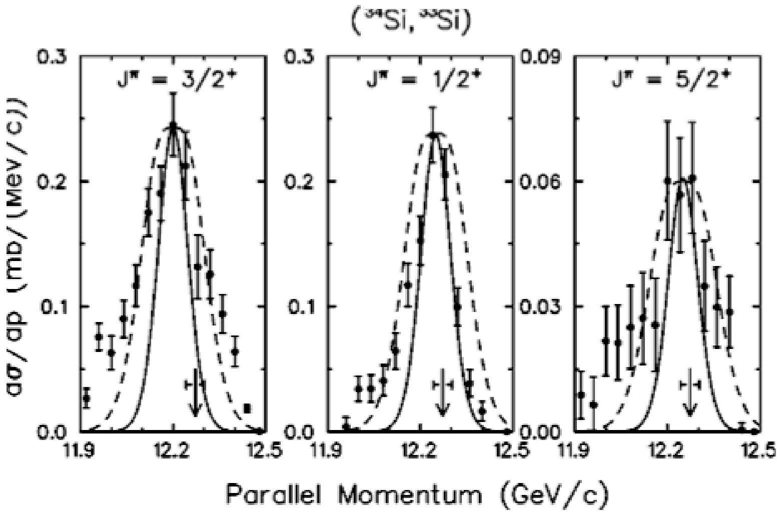

FIG. 3. Parallel-momentum distributions of the reaction residues

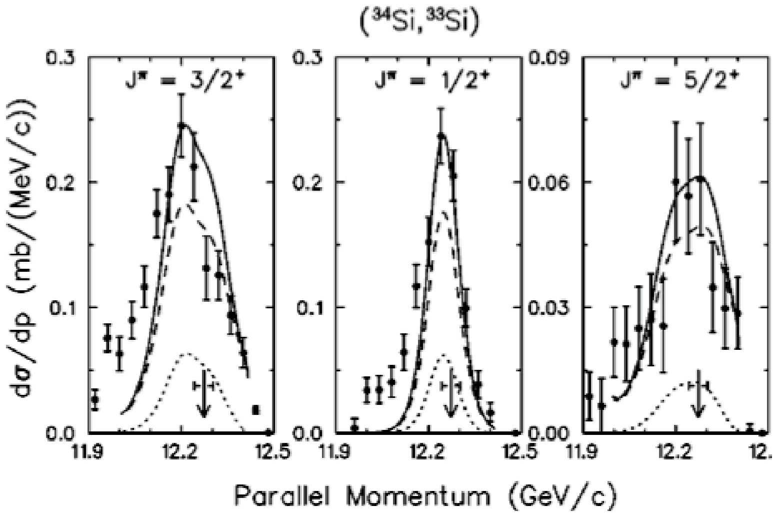

FIG. 4. Measured momentum distribution (full points) co

PHYSICAL REVIEW C VOLUME 49, NUMBER 1 JANUARY 1994

Inclusive spectra of stripping reactions induced by heavy ions

A. Bonaccorso
Istituto Nazionale di Fisica Nucleare, Sezione di Pisa, 56100 Pisa, Italy

I. Lhenry and T. Suomijärvi
Institut de Physique Nuclèaire, Centre National de la Recherche Scientifique–Institut National de Physique Nucleàire et de Physique des Particules F91406 Orsay, France

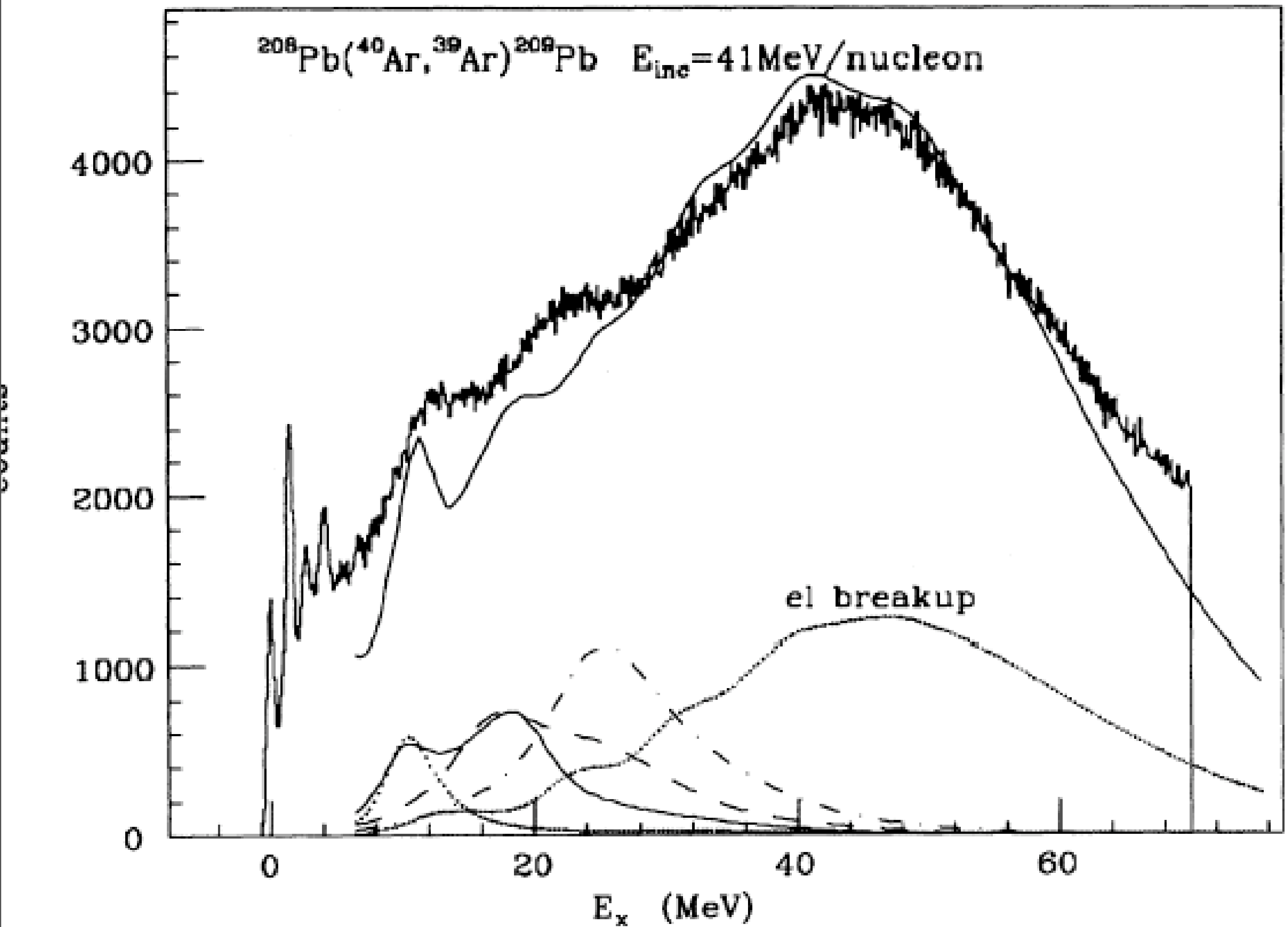

Projectile fragmentation

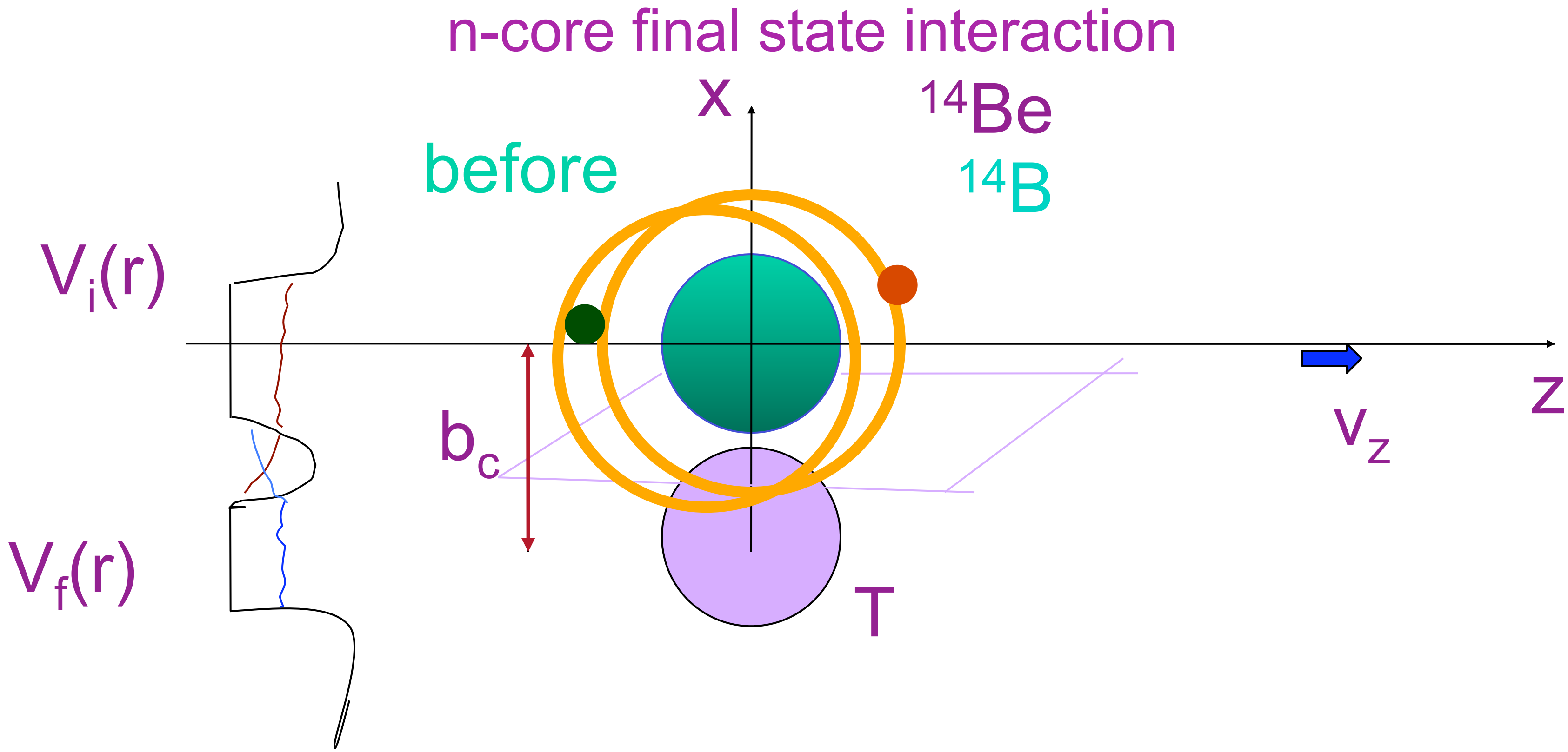

INFN Angela Bonaccorso

Projectile fragmentation

n-core final state interaction

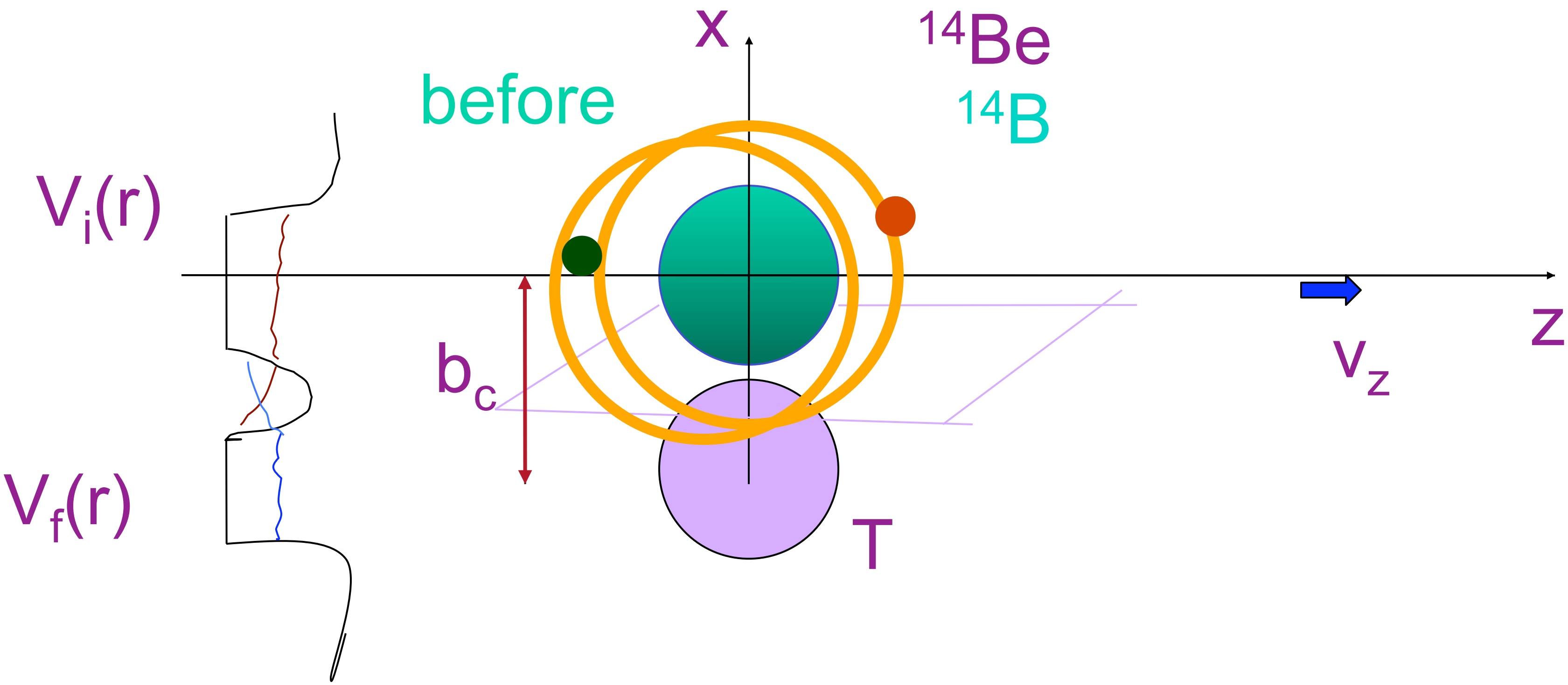

after

Projectile fragmentation

n-core final state interaction

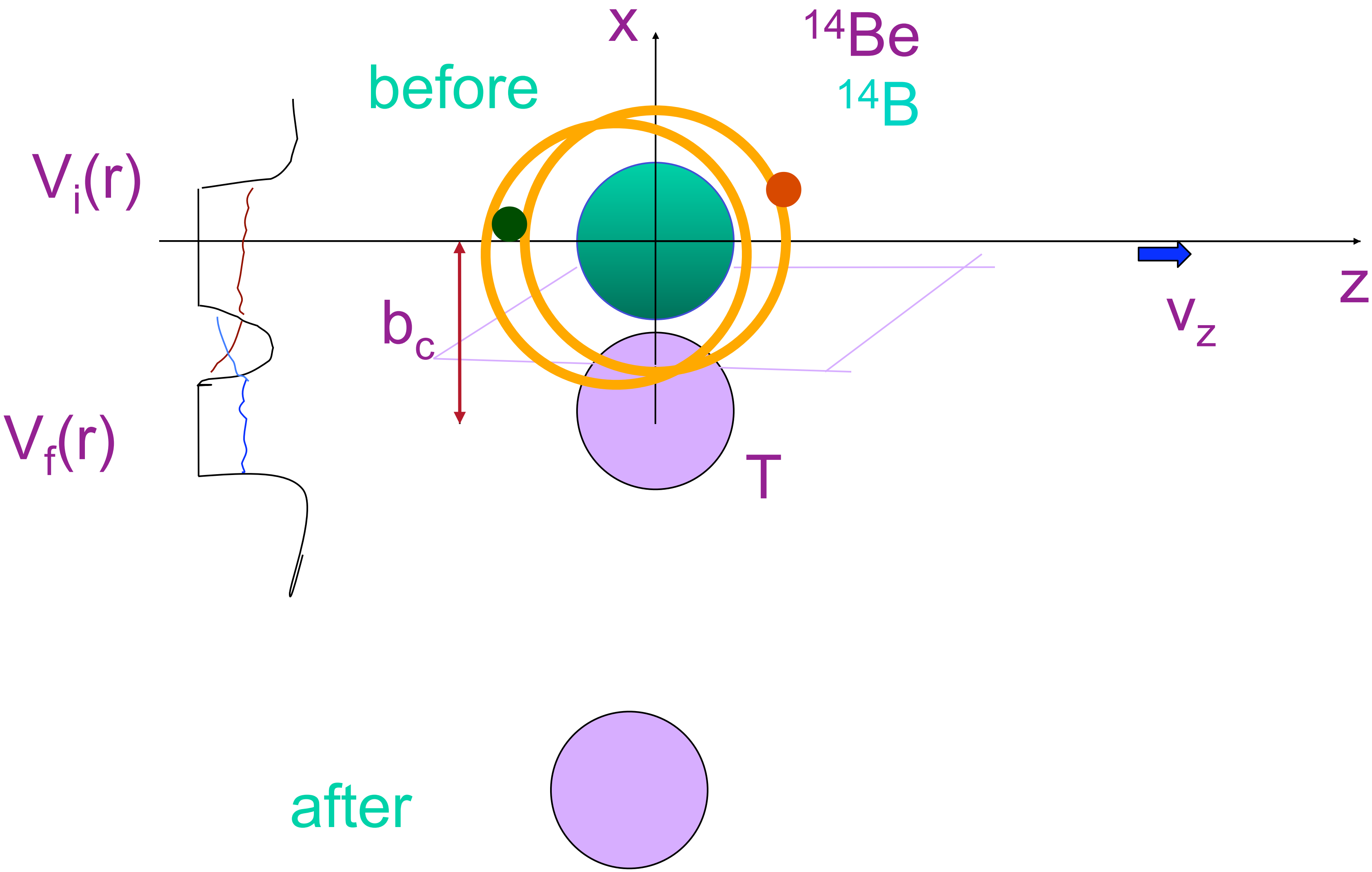

Projectile fragmentation

n-core final state interaction

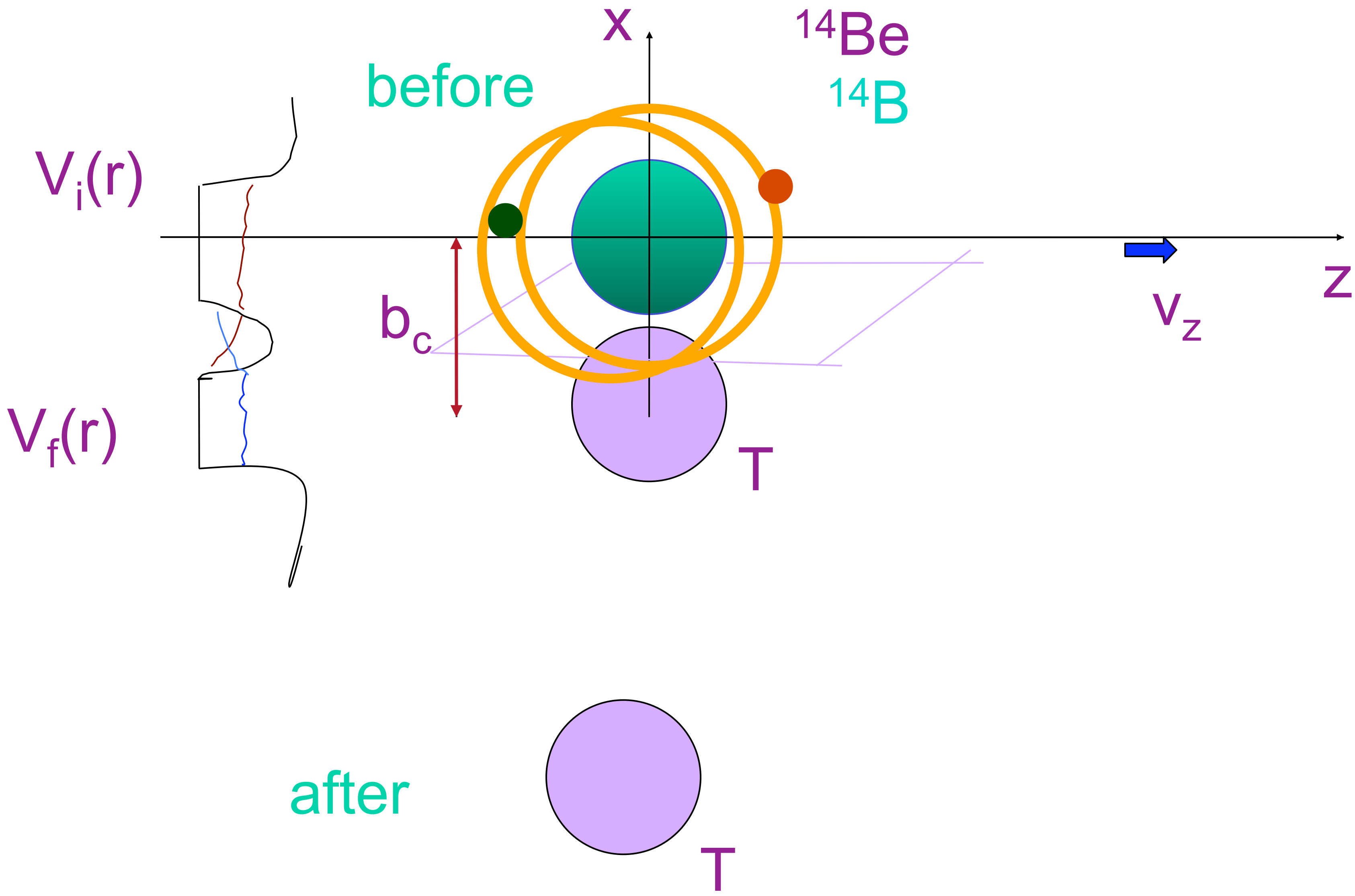

Projectile fragmentation

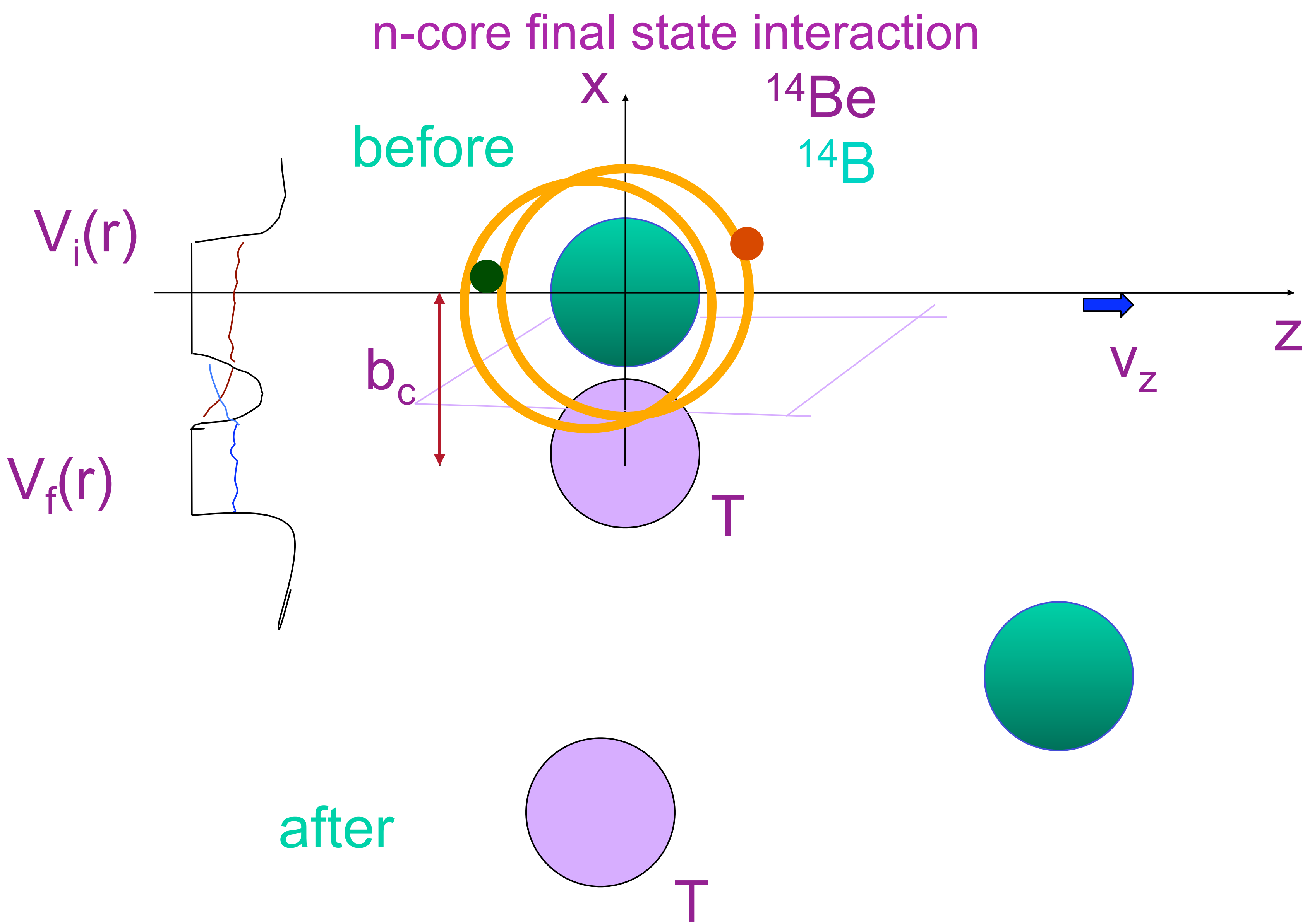

Projectile fragmentation

n-core final state interaction

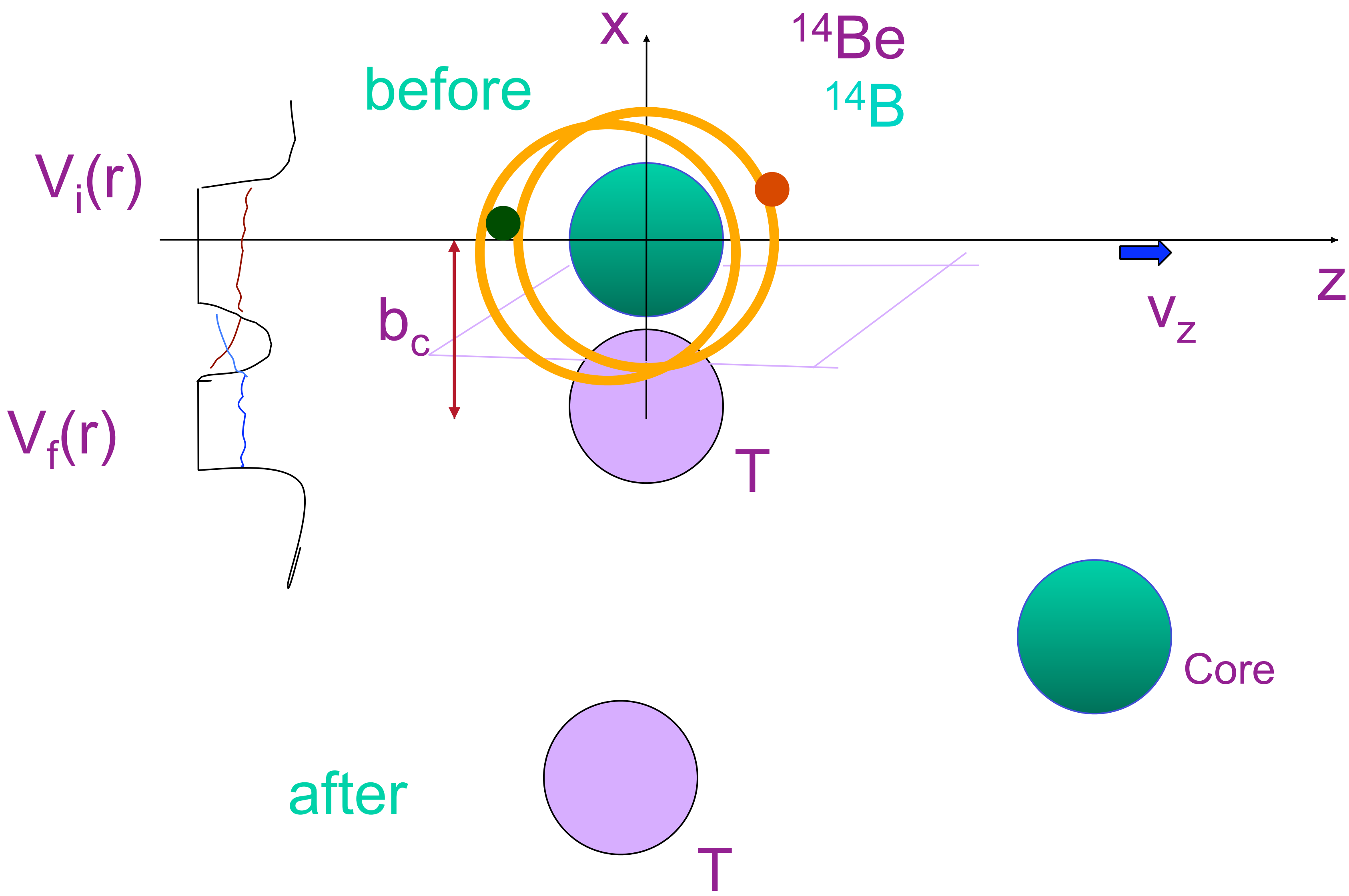

Projectile fragmentation

n-core final state interaction

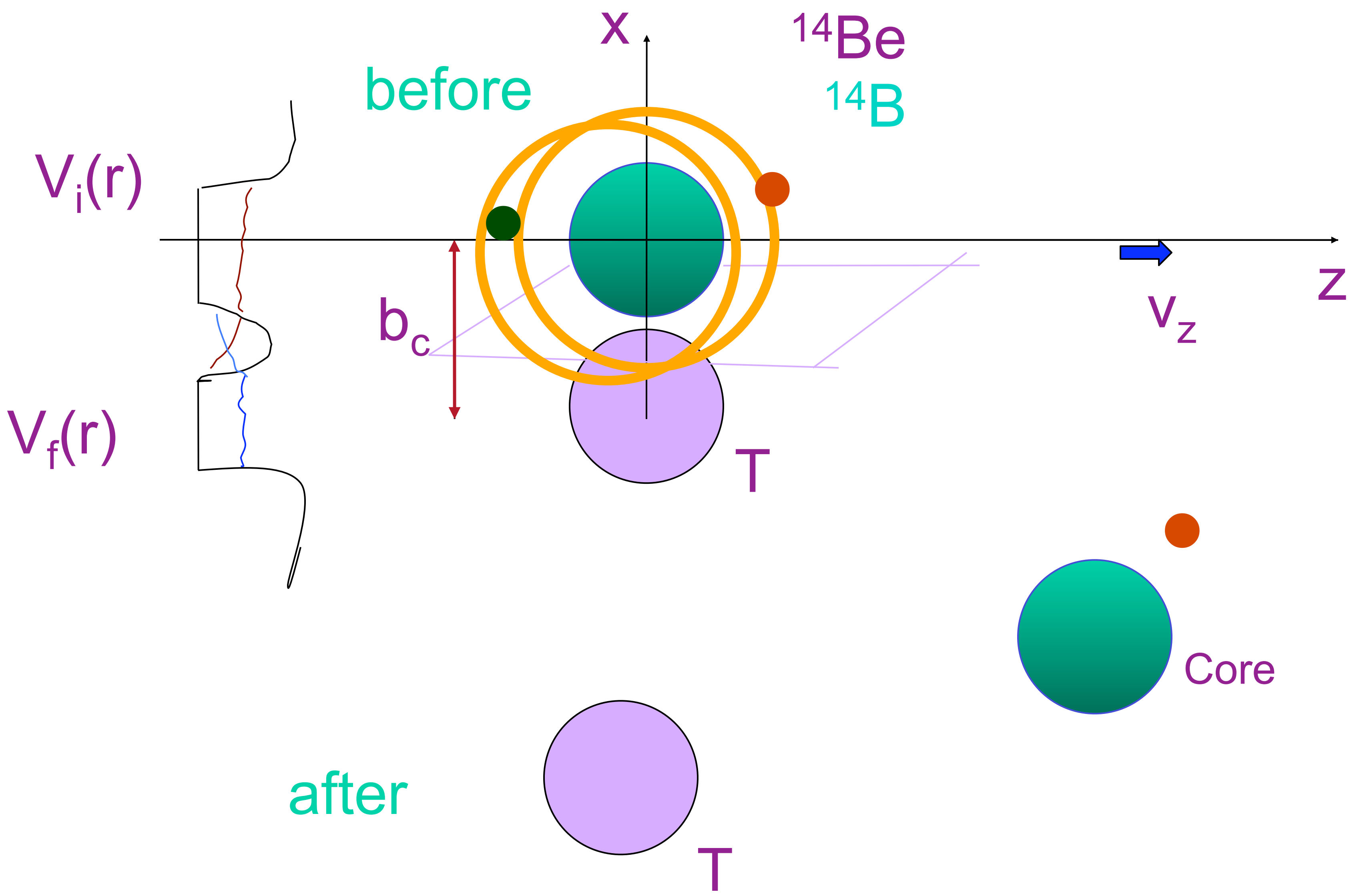

Projectile fragmentation

n-core final state interaction

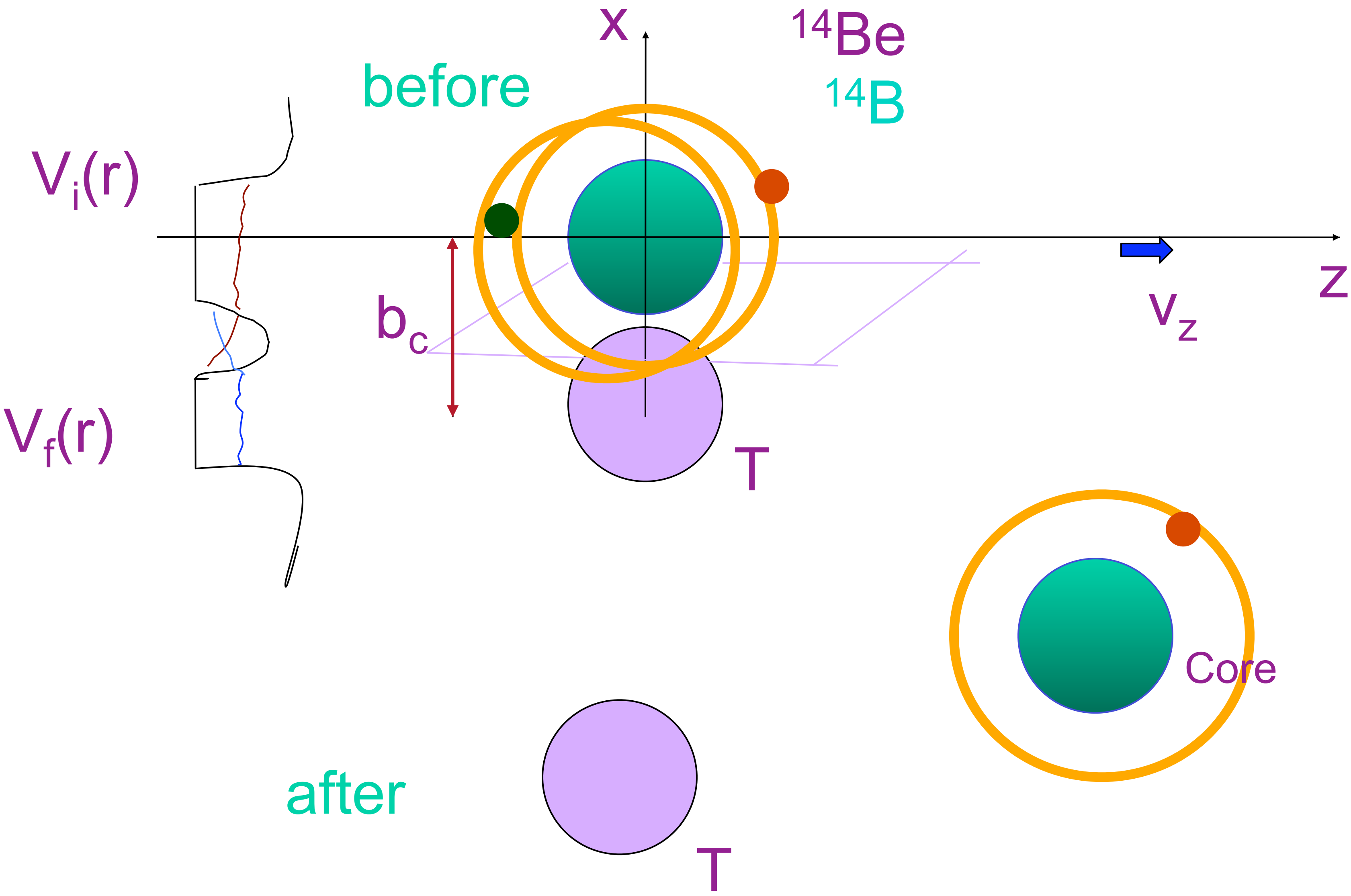

Projectile fragmentation

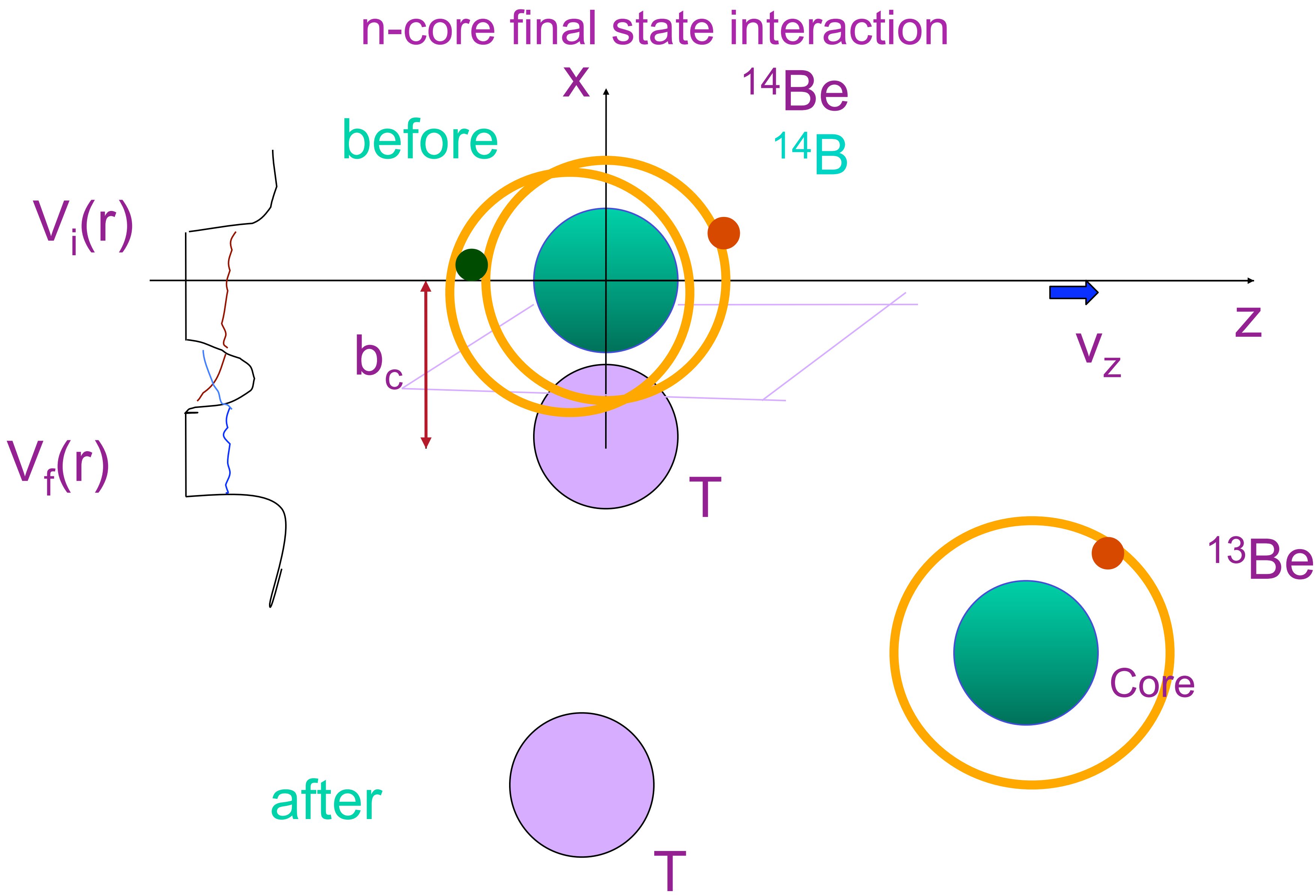

Projectile fragmentation

n-core final state interaction

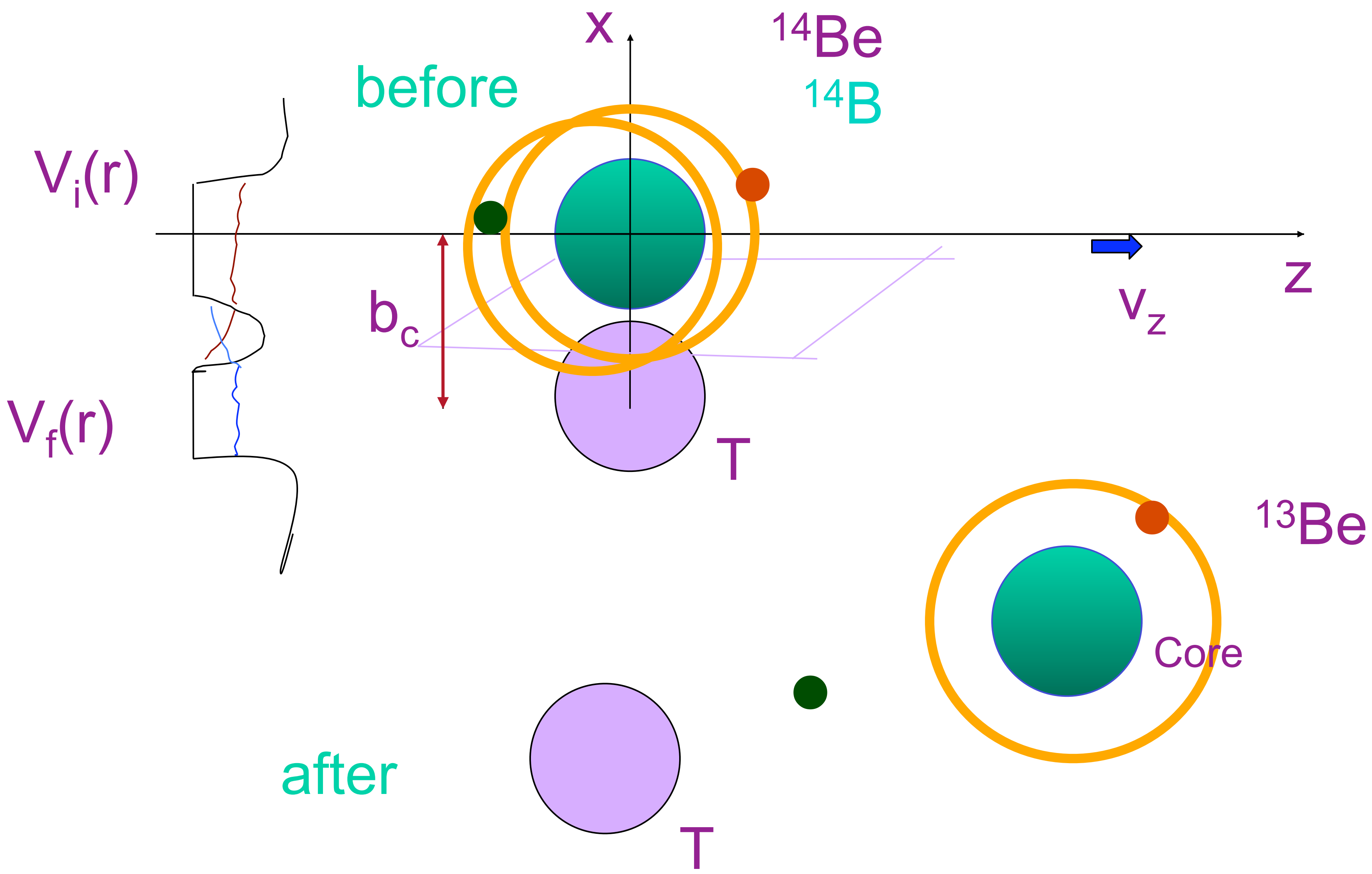

INFN Angela Bonaccorso

Projectile fragmentation

^{11}Be: a **simple** test case

from bound s-state to d-resonance: inelastic excitation to the continuum?

CAPEL, GOLDSTEIN, AND BAYE PHYSICAL REVIEW C 70, 064605 (2004)

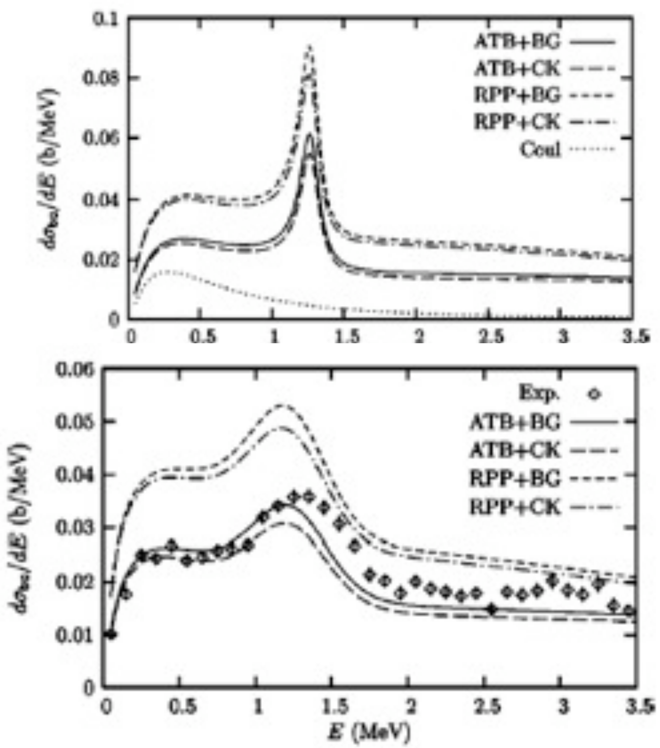

FIG. 4. Theoretical and experimental breakup cross sections as a function of the energy. The four curves correspond to the calculations performed with various combinations of the potentials of Table III convoluted with energy resolution. Experimental data are from Ref. [39].

[39] N. Fukuda *et al.*, Phys. Rev. C 70, 054606 (2004).

^{11}Be+^{12}C @ 67A.MeV

60 G. Blanchon et al. / Nuclear Physics A 784 (2007) 49–78

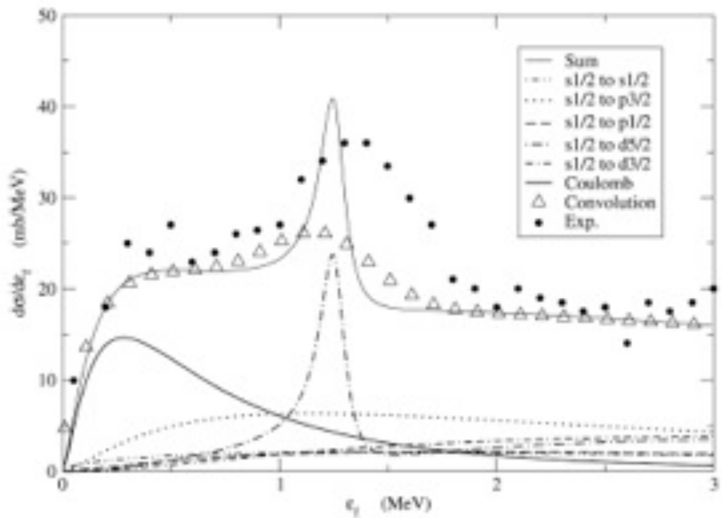

Fig. 3. n–^{10}Be relative energy spectrum, including Coulomb and nuclear breakup for the reac ^{11}Be + ^{12}C → n + ^{10}Be + X at 67*A* MeV. Only the contributions from an s initial state with spectroscopic tor $C^2S = 0.84$ are calculated. The triangles are the total calculated result after convolution with the experime resolution function. The dots are the experimental points from [1].

Analytical methods for transfer and breakup

$|S_{ct}|^2$

↑

$$\sigma = \int d^2 b_c P_{el}(b_c) P_{tr}(b_c);\; P_{tr} = |A|^2 \longrightarrow A = \frac{1}{i\hbar}\int dt \langle \psi_f(r,t) | V_2 | \psi_i(r - R(t), t) \rangle$$

Seaking a clear physical interpretation of DWBA (Brink et al. and Copenhagen school since 1978).

similar to Alder& Winther for Coulomb excitations.

Review of basic knowledge of core-target and nucleon-target interaction potentials and cross sections. This is necessary to ensure accuracy of absolute cross sections in spectroscopic studies.

Heavy-ion high energy scattering and the eikonal approximation.

Nuclear Physics A654 (1999) 235c-251c

ELSEVIER

Reactions with Radioactive Ion Beams

Isao Tanihata

RIKEN, 2-1 Hirosawa, Wako, Saitama 351-0198, Japan

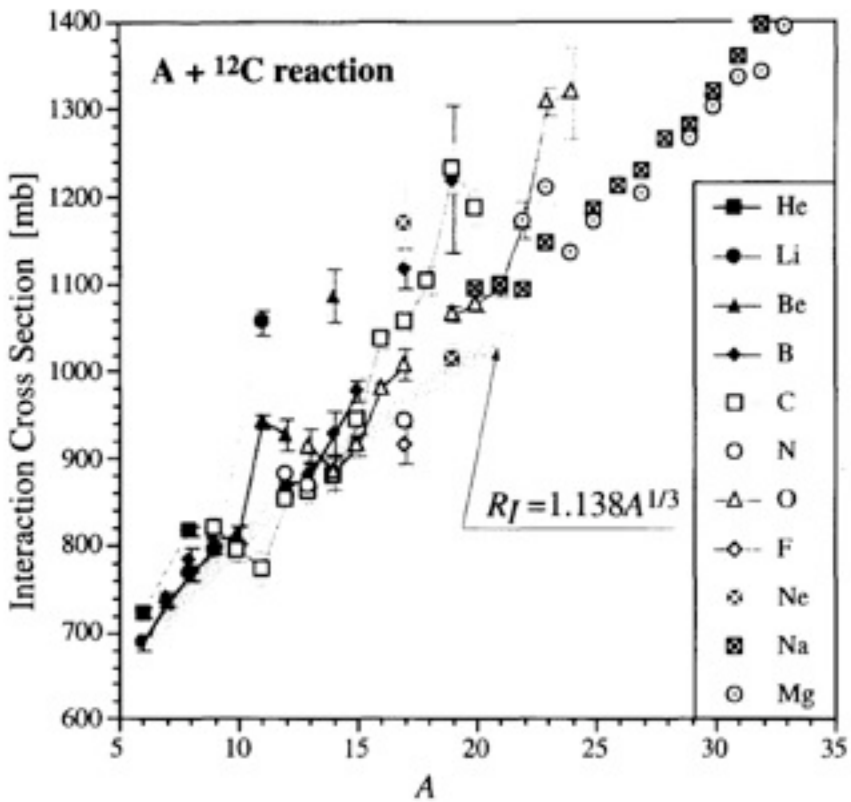

Fig. 2 Interaction cross sections of p and sd shell nuclei at the beam energy near 800A MeV. **He:** ref. 1, **Li, Be:** ref. 2, **B:** ref. 3-5, **Ne and A=17:** ref. 6, **A=20:** ref. 7, **Na:** ref. 8, **Mg:**ref. 9, and others ref.10.

Prog. Part. Nucl. Phys., Vol. 35, pp. 505–573, 1995
Pergamon
0146-6410(95)00046-1

Nuclear Structure Studies from Reaction Induced by Radioactive Nuclear Beams

I. TANIHATA

The Institute of Physical and Chemical Research (RIKEN), 2-1 Hirosawa, Wako, Saitama 351-01, Japan

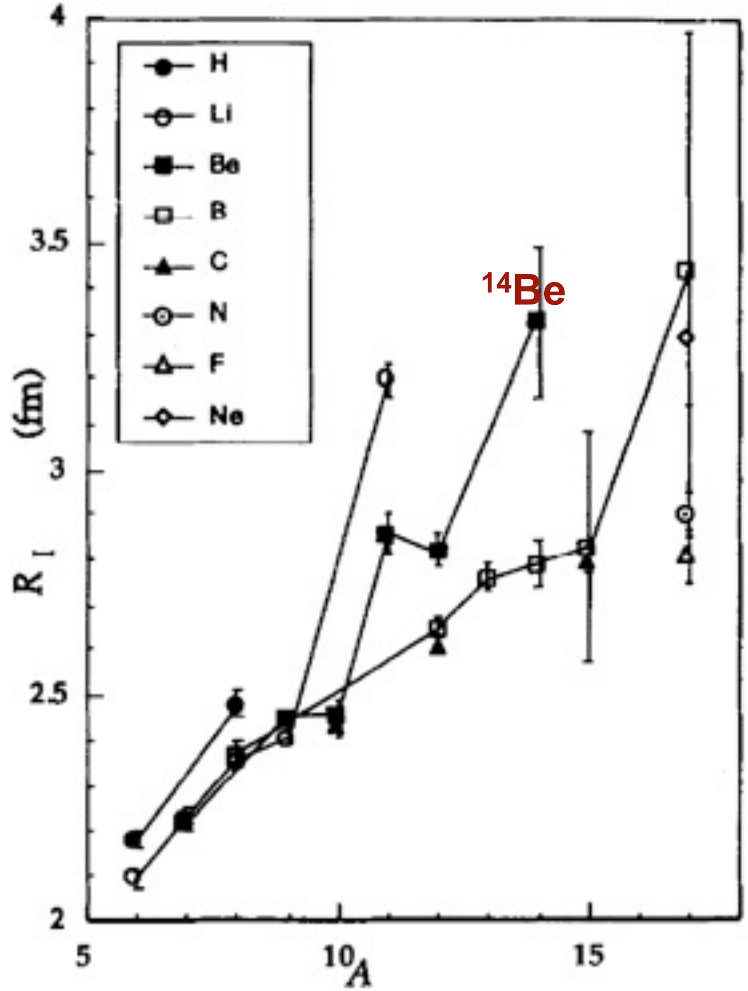

PHYSICAL REVIEW C VOLUME 35, NUMBER 5 MAY 1987

Trends of total reaction cross sections for heavy ion collisions in the intermediate energy range

S. Kox,[a] A. Gamp,*[a],[b] C. Perrin,[a] J. Arvieux,†[a] R. Bertholet,[c] J. F. Bruandet,[a] M. Buenerd,[a] R. Cherkaoui,‡[a] A. J. Cole,[a] Y. El-Masri,[a],[d] N. Longequeue,[a] J. Menet,[a] F. Merchez,[a] and J. B. Viano[a]

$$\sigma_R = \pi R_{\rm int}^2 \left[1 - \frac{B_C}{E_{\rm c.m.}} \right] , \qquad (13)$$

takes into account difference between impact parameter and distance of closest approach

where the term B_C is the Coulomb barrier of the projectile-target system. It is given by

$$B_C = \frac{Z_t Z_p e^2}{r_C (A_t^{1/3} + A_p^{1/3})} , \qquad (14)$$

$$R_{\rm int} = R_{\rm vol} + R_{\rm surf} .$$

$$R_{\rm surf} = r_0 \left[a \frac{A_p^{1/3} A_t^{1/3}}{A_p^{1/3} + A_t^{1/3}} - c \right] .$$

validity of the strong absorption model for heavy-ion reactions gives a simple way to treat the core-target interaction in halo nuclei scattering

INFN Angela Bonaccorso

From a fit of many data of σ_R from 30*A* to 2100*A* MeV reactions, the parameters r_0, a, c were determined. It was found that r_0 = 1.1 fm and a =1.85 are independent of the projectile-target combination and the beam energy. Only c was found to depend on the beam energy, as shown in Fig. 2.3.

These equations provide a simple way to compare the reaction cross sections at different energies. However, since they are purely empirical formula, one should be careful when applying them to an exotic nucleus because of a possible difference in the surface diffuseness as well as any proton-neutron density difference. When one measures σ_R using a β-unstable nucleus, only r_0 is expected to change. Although r_0 includes size information of both the projectile and the targets, it provides a simple mean to study the deviation of the radius

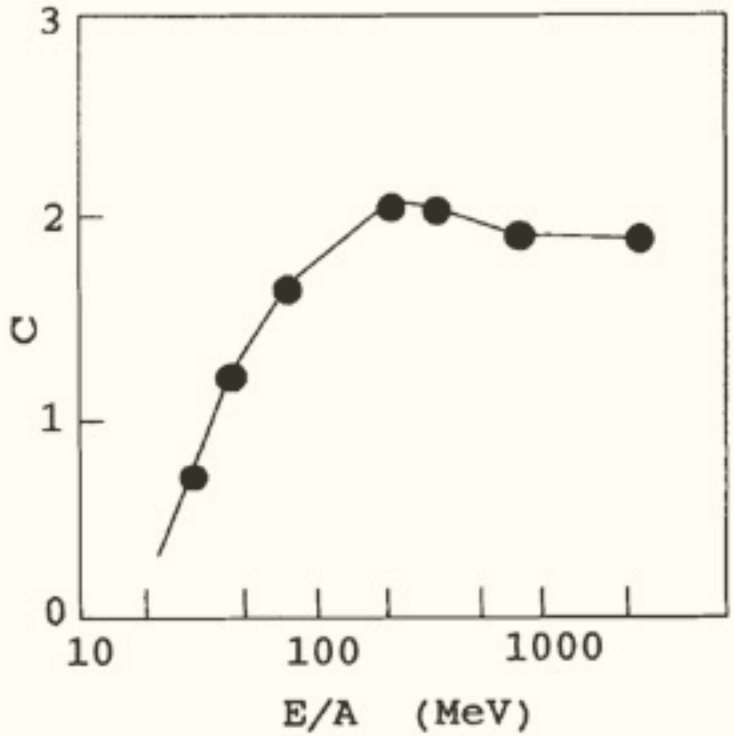

Fig. 2.3 Energy dependence of the parameter c in the empirical reaction cross sections.

INFN Angela Bonaccorso

Nucleon-target potential

A.B. & F. Carstoiu

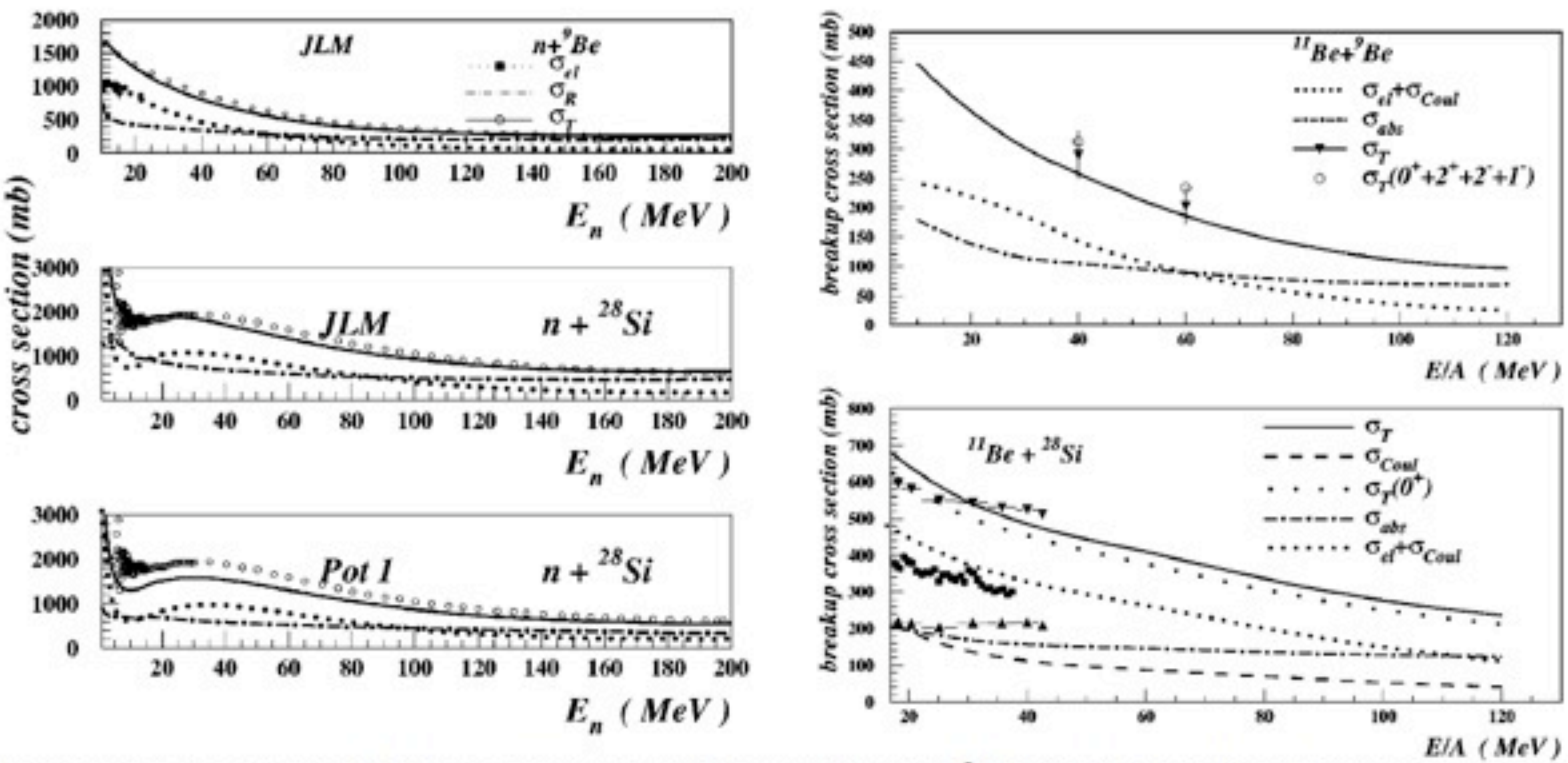

FIG. 1. Neutron-target cross sections as a function of the neutron incident energy. Top figure: ^{9}Be target. Dotted and dot-dashed curves are the elastic and reaction cross sections, respectively. Full curve is their sum. Data points from Ref. [18]. Center and bottom figure: ^{28}Si target with JLM potential and optical potential from Table I, respectively. Same notation as above. Data points from Ref. [18].

PHYSICAL REVIEW C VOLUME 47, NUMBER 1 JANUARY 1993

Neutron total cross sections at intermediate energies

R. W. Finlay, W. P. Abfalterer, G. Fink, E. Montei, and T. Adami
Department of Physics and Astronomy, Ohio University, Athens, Ohio 45701

P. W. Lisowski, G. L. Morgan, and R. C. Haight
P-Division, Los Alamos National Laboratory, Los Alamos, New Mexico 87545
(Received 30 September 1992)

http://www.nea.fr/html/dbdata/x4.

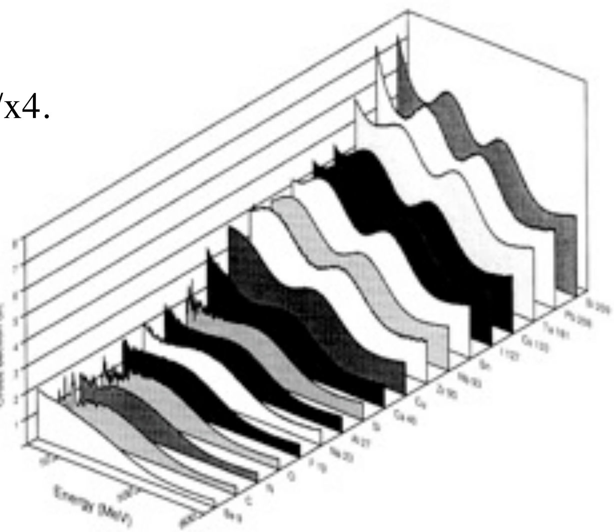

600MeV
3.03 b

PHYSICAL REVIEW C, VOLUME 62, 064612

Global analysis of proton nucleus reaction cross sections

A. de Vismes,[1] P. Roussel-Chomaz,[1] and F. Carstoiu[1,2]

Elastic scattering and the optical potential including breakup channel (cf. talks on FUSION)

Relevant papers in the past

[25] R. A. Broglia, and A. Winther, *Heavy Ion Reactions*, Benjamin, Reading, Mass, 1981.

[26] R. A. Broglia, G. Pollarolo and A. Winther, Nucl. Phys. **A361**, 307 (1981).

[27] A. Bonaccorso, G. Piccolo, D. M. Brink, Nucl. Phys. **A441** (1985) 555.

[28] Fl. Stancu and D. M. Brink, Phys. Rev. C **32**, 1937 (1985).

Elastic scattering and reaction mechanisms of the halo nucleus ^{11}Be around the Coulomb barrier

INFN Angela Bonaccorso

A.Di Pietro[1], G.Randisi[1,2*], V.Scuderi[1,2], L.Acosta[3], F.Amorini[1,2], M.J.G.Borge[4], P.Figuera[1], M.Fisichella[1,2], L.M.Fraile[5†], J.Gomez-Camacho[6], H.Jeppesen[5‡], M.Lattuada[1,2], I.Martel[3], M.Milin[7], A.Musumarra[1,8], M.Papa[1], M.G.Pellegriti[1,2], F.Perez-Bernal[3], R.Raabe[9], F.Rizzo[1,2], D.Santonocito[1], G.Scalia[1,2], O.Tengblad[4], D.Torresi[1,2], A.Maira Vidal[4], D. Voulot[5], F. Wenander[5], M.Zadro[10]

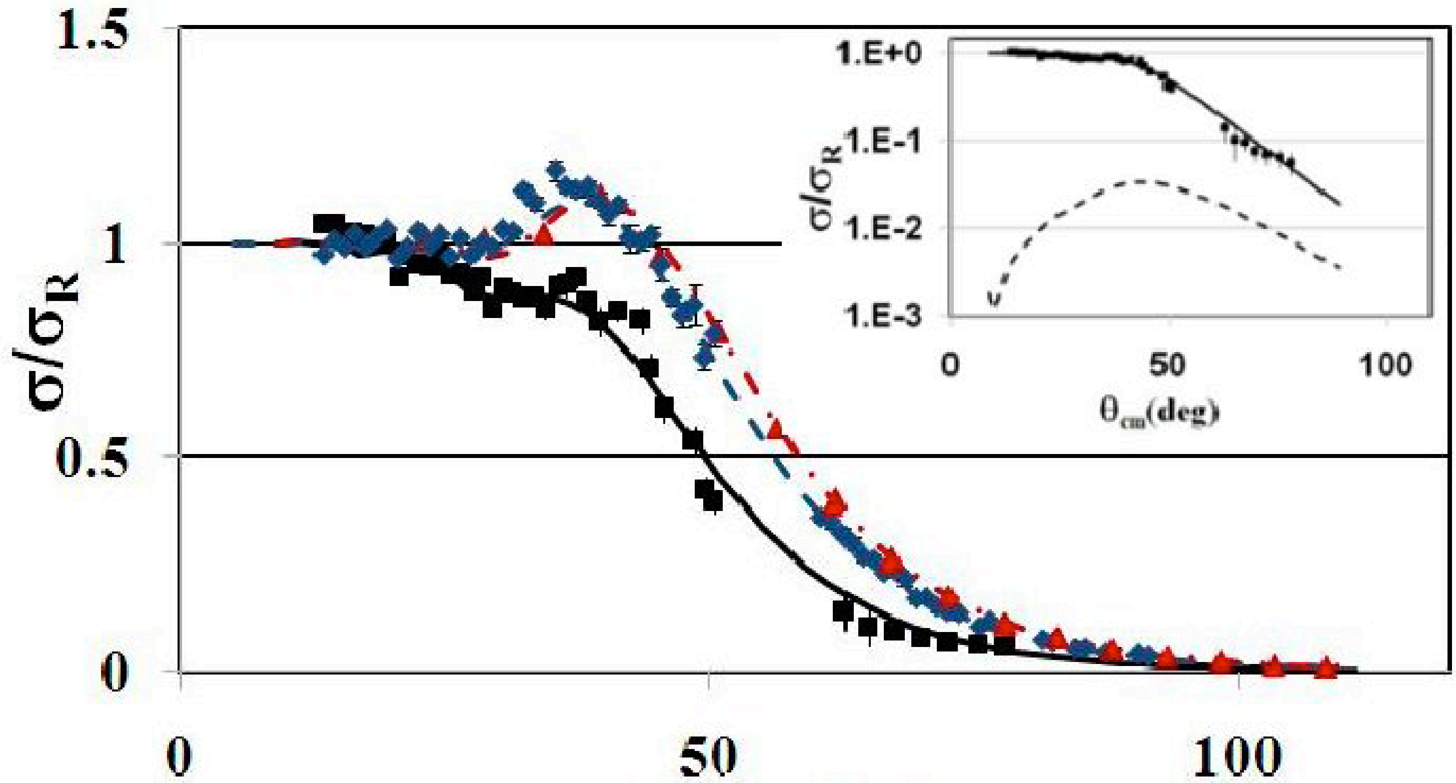

TABLE I: W-S Optical potentials obtained from the fit of the experimental data. The real potential radius parameter is r_0=1.1 fm and the imaginary one is r_i=1.2 fm, where $R_{0,i,si}=r_{0,i,si}(A_p^{1/3}+A_t^{1/3})$. The Coulomb radius parameter is r_C=1.25 fm.

Reaction	V(MeV)	a(fm)	V_i(MeV)	a_i(fm)	V_{si}(MeV)	r_{si}(fm)	a_{si}(fm)	J_V (MeV fm^3)	J_W (MeV fm^3)
^{9}Be+^{64}Zn	126	0.6	17.3	0.75				295	53
^{10}Be+^{64}Zn	86.2	0.7	43.4	0.7				193	124
^{11}Be+^{64}Zn	86.2	0.7	43.4	0.7	0.151	1.3	3.5	193	129

$$|S_{NN}(b)|^2 = e^{-4\delta_I(b)}$$

$$\delta_I(b) = -\frac{1}{2\hbar}\int_{-\infty}^{+\infty} \left(W_V(\mathbf{r}(t)) + W_S(\mathbf{r}(t))\right) dt$$

$$\int_{-\infty}^{+\infty} W_S(\mathbf{r}(t))dt = -\frac{\hbar}{2}P_{b_{up}} \quad \text{or } P_{transf}$$

$$\mathbf{r}(t) = \mathbf{b_c} + vt$$

$$|S_{NN}|^2 = |S_{CT}|^2 e^{-P_{b_{up}}}$$

$$W_S^N(r) = -\frac{\hbar v}{2} p_{b_{up}}^N(r) \frac{1}{\sqrt{2\pi a r}}$$

Appendix A. Connection to low energy approaches

In our formalism the imaginary part of the optical potential due to Coulomb breakup i given by

$$\int_{-\infty}^{+\infty} W_S(\mathbf{r}(t))\,dt = -\frac{\hbar}{2} p^C_{\text{b-up}}, \tag{A.1}$$

while Eq. (12) of Andrés et al. [14] reads

$$\int_{-\infty}^{+\infty} W_S(\mathbf{r}(t))\,dt = \hbar\alpha. \tag{A.2}$$

Where both $p^C_{\text{b-up}}$ and α depend on the incident energy and on the classical trajectory of relative motion. In our case such a trajectory is a straight line since our approach applies to incident energies well above the Coulomb barrier.

The two approaches are consistent if $\alpha \to -p^C_{\text{b-up}}/2$ in the high energy limit. To show that this is true we write explicitly the expression in Ref. [14]

$$\alpha = -\frac{\pi}{9}\left(\frac{Z_T e}{\hbar v a_c}\right)^2 \int d\varepsilon_k \left(I^2_{11}(\varpi) + I^2_{1-1}(\varpi)\right)\frac{dB(\text{E1}, \varepsilon_k)}{d\varepsilon_k}, \tag{A.3}$$

where $I_{1\pm 1}$ are the well known Coulomb integrals [46] which can be expressed in terms of Bessel functions of imaginary order. However, according to Eq. (28) of Ref. [50] in the high energy limit

$$I(\text{E1}, \pm 1) = I_{1\pm 1} = \frac{2a_c}{b_c}\varpi K_1(\varpi), \tag{A.4}$$

where a_c is the Coulomb length parameter and now K_1 is an ordinary Bessel function of real index.

On the other hand, considering Eq. (15) for $p^C_{\text{b-up}}$ we remark that it is well known and shown, for example, in Fig. 1 of Ref. [51] that $\varpi^2 K_0^2(\varpi)$ is much smaller than $\varpi^2 K_1^2(\varpi)$ for values of $\varpi \approx 0.1$, which happens for heavy ions at high energies. We can then write Eq. (15) as

$$p^C_{\text{b-up}}(b_c) \approx \frac{2\pi}{9}\left(\frac{Z_T e}{\hbar v b_c}\right)^2 \int d\varepsilon_k\, 2\left(2\varpi K_1(\varpi)\right)^2 \frac{dB(\text{E1}, \varepsilon_k)}{d\varepsilon_k}, \tag{A.5}$$

A.A. Ibraheem, A. Bonaccorso / Nuclear Physics A 748 (2005) 414–432

$$p^C_{\text{b-up}}(b_c) \approx \frac{32}{3\pi} C^2 S\left(\frac{C_0 C_i}{b_c}\right)^2 \int d\varepsilon_k \frac{m_n}{\hbar^2 k}\left(\varpi^2 K_1^2(\varpi) + \varpi^2 K_0^2(\varpi)\right)\frac{k^4}{(k^2+\gamma^2)^4}$$

ce for the case studied in this paper the explicit form of $B(\text{E1})$ is

$$\frac{dB(E1, \varepsilon_k)}{d\varepsilon_k} = C^2 S \frac{m_n}{\hbar^2 k}(C_i \beta_1 Z_P e)^2 \frac{6}{\pi^2}\frac{k^4}{(k^2+\gamma^2)^4}, \tag{A.6}$$

iich is the consistent with Eq. (6.5) of Ref. [51] or Eq. (7.24) of [28] and it is the explicit m of the $B(\text{E1})$ obtained for an s-initial state using the asymptotic form of the wave ıction.

Finally, using Eq. (A.4) in Eq. (A.3) and comparing with Eq. (A.5) we obtain that $\alpha =$ $p^C_{\text{b-up}}/2$ in the high energy, straight line trajectory limit. However, we remark that our ›bability Eq. (13) is more accurate than the high energy limit of α of Eq. (A.3) since it contains also the term representing longitudinal excitations, proportional to K_0 and to k_z, the parallel component of neutron momentum.

A. Bonaccorso and F. Carstoiu
Optical potentials of halo and weakly bound nuclei
Nucl. Phys. A706 (2002) 322.

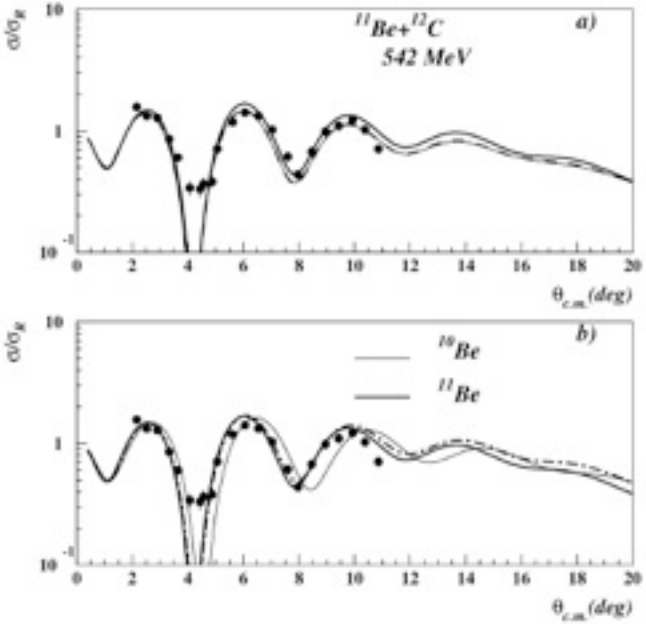

A.A. Ibraheem and A. Bonaccorso,
Recoil effects on the optical potentials of weakly bound nuclei
Nucl. Phys. A748 (2005) 414.

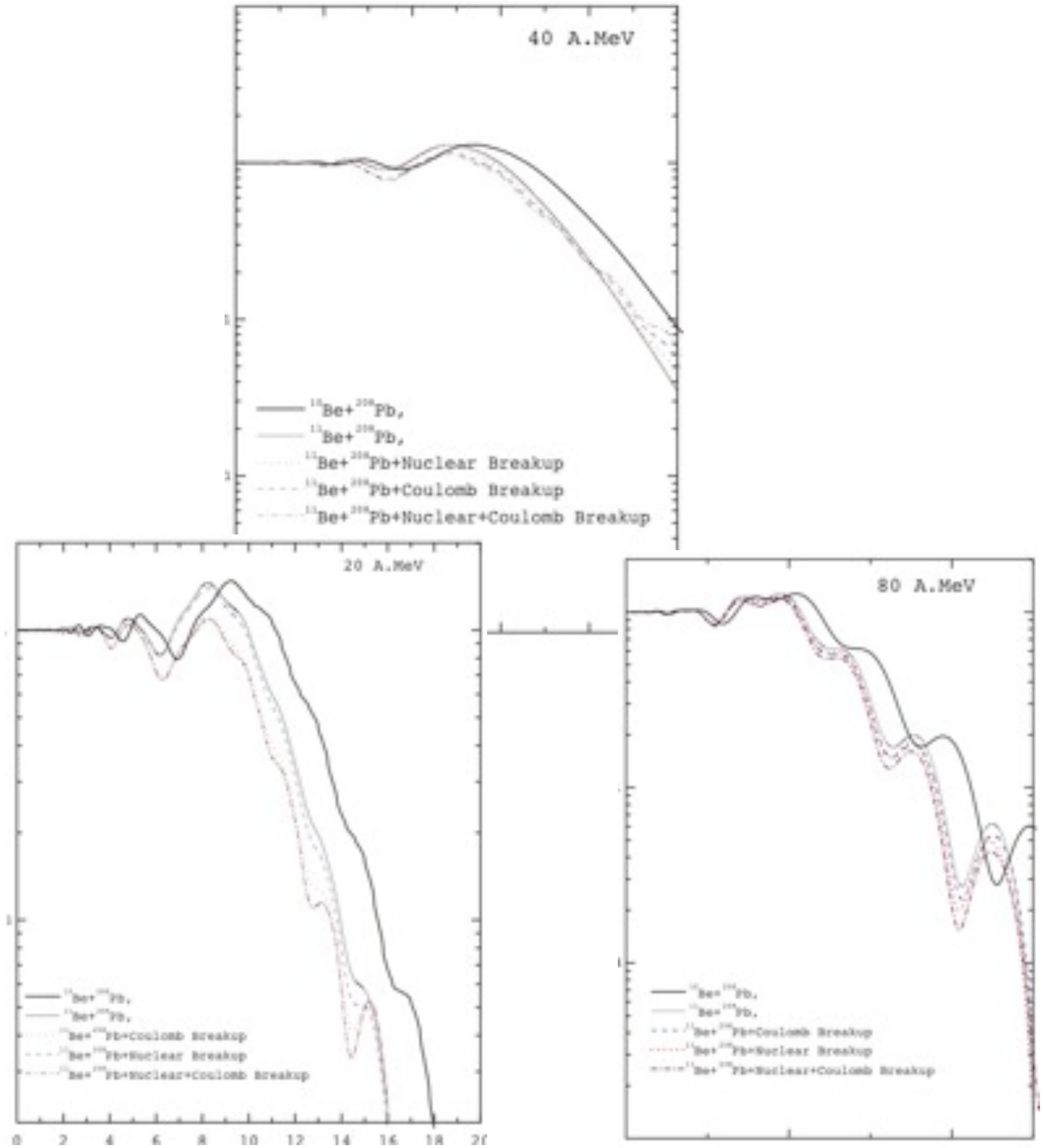

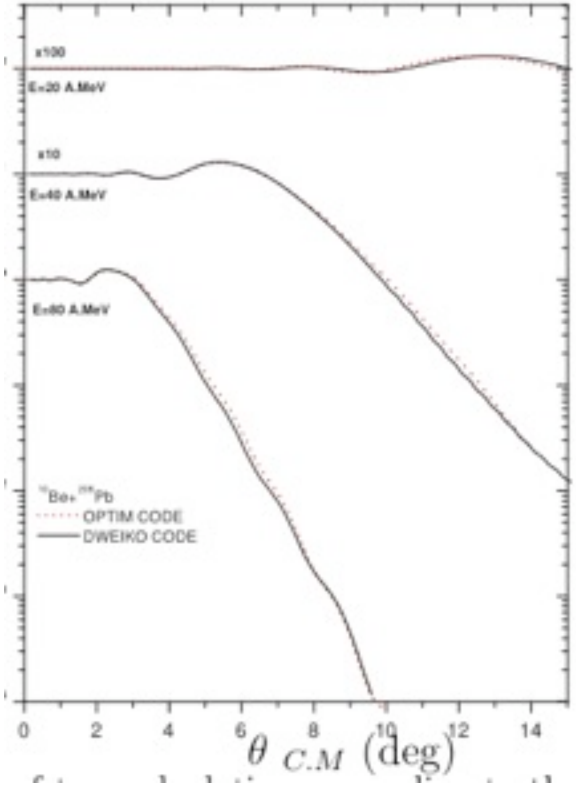
x100
E=20 A.MeV
x10
E=40 A.MeV
E=80 A.MeV
10Be+208Pb
OPTIM CODE
DWEIKO CODE
0 2 4 6 8 10 12 14
θ C.M (deg)

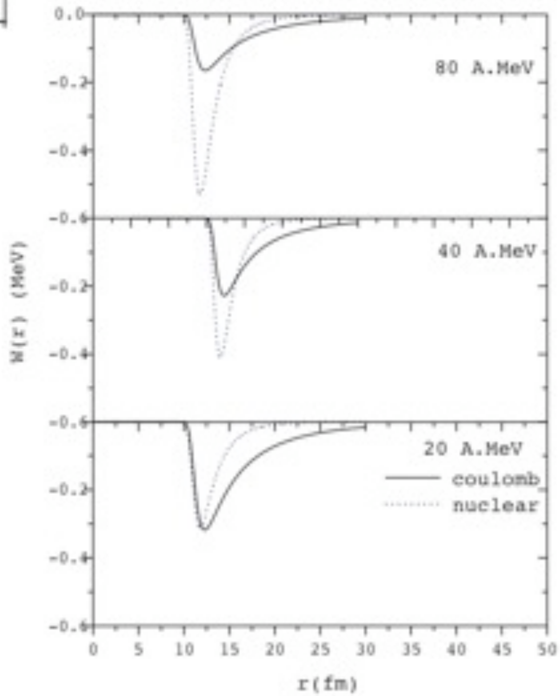
80 A.MeV
40 A.MeV
20 A.MeV
coulomb
nuclear
W(r) (MeV)
0.0 -0.2 -0.4 -0.6
0 5 10 15 20 25 30 35 40 45 50
r(fm)

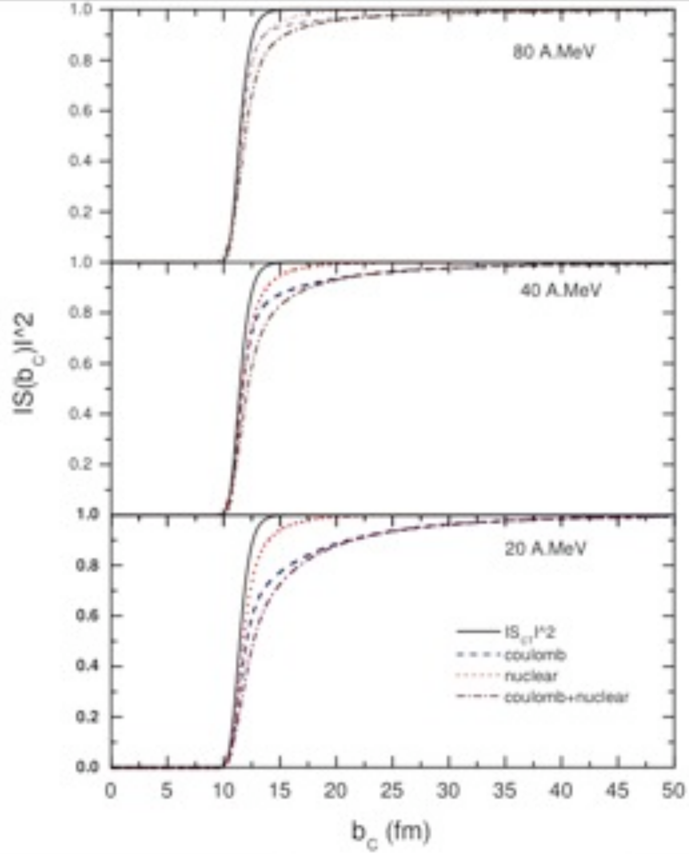
80 A.MeV
40 A.MeV
20 A.MeV
|S(b_C)|^2
|S_C|^2
coulomb
nuclear
coulomb+nuclear
0.0 0.2 0.4 0.6 0.8 1.0
0 5 10 15 20 25 30 35 40 45 50
b_C (fm)

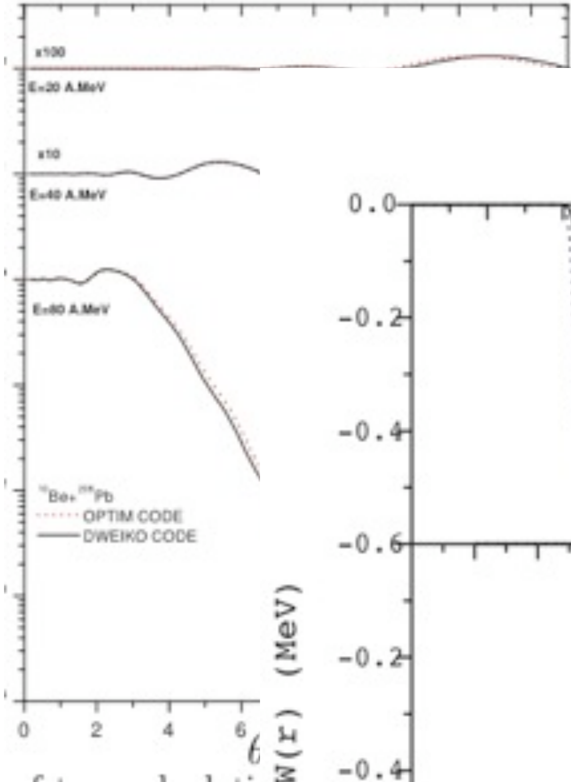
x100
E=20 A.MeV
x10
E=40 A.MeV
E=80 A.MeV
11Be+208Pb
OPTIM CODE
DWEIKO CODE
0
2
4
6

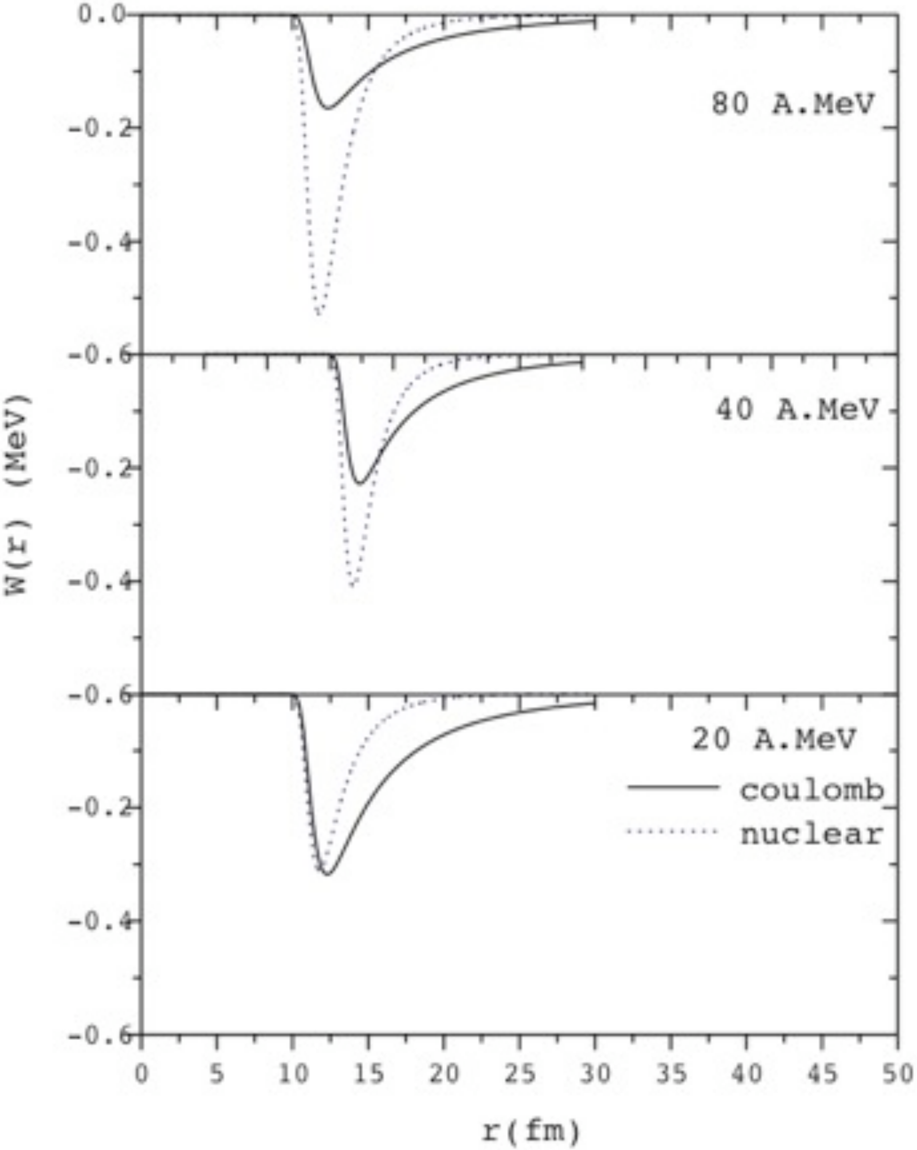
80 A.MeV
40 A.MeV
20 A.MeV
coulomb
nuclear
W(r) (MeV)
r(fm)

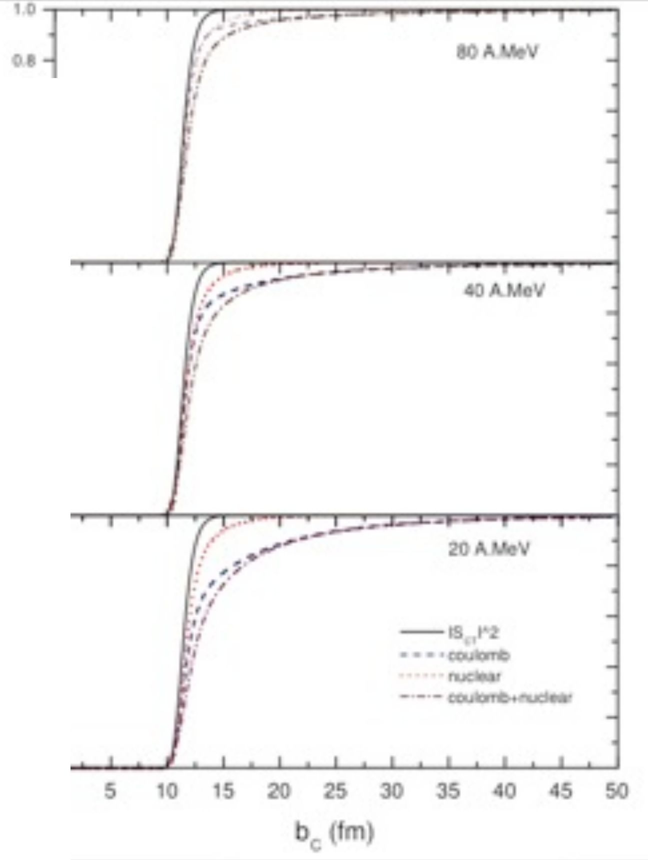
80 A.MeV
40 A.MeV
20 A.MeV
|S_C1|^2
coulomb
nuclear
coulomb+nuclear
b_C (fm)

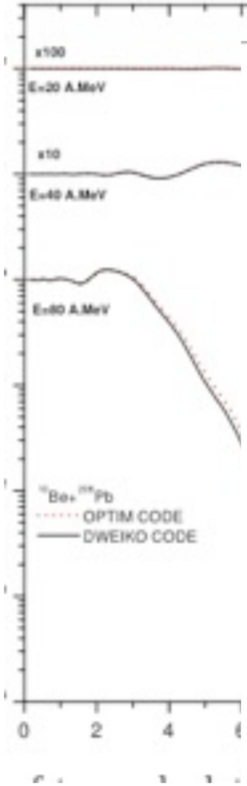
x100
E=20 A.MeV
x10
E=40 A.MeV
E=80 A.MeV
OPTIM CODE
DWEIKO CODE
0
2
4

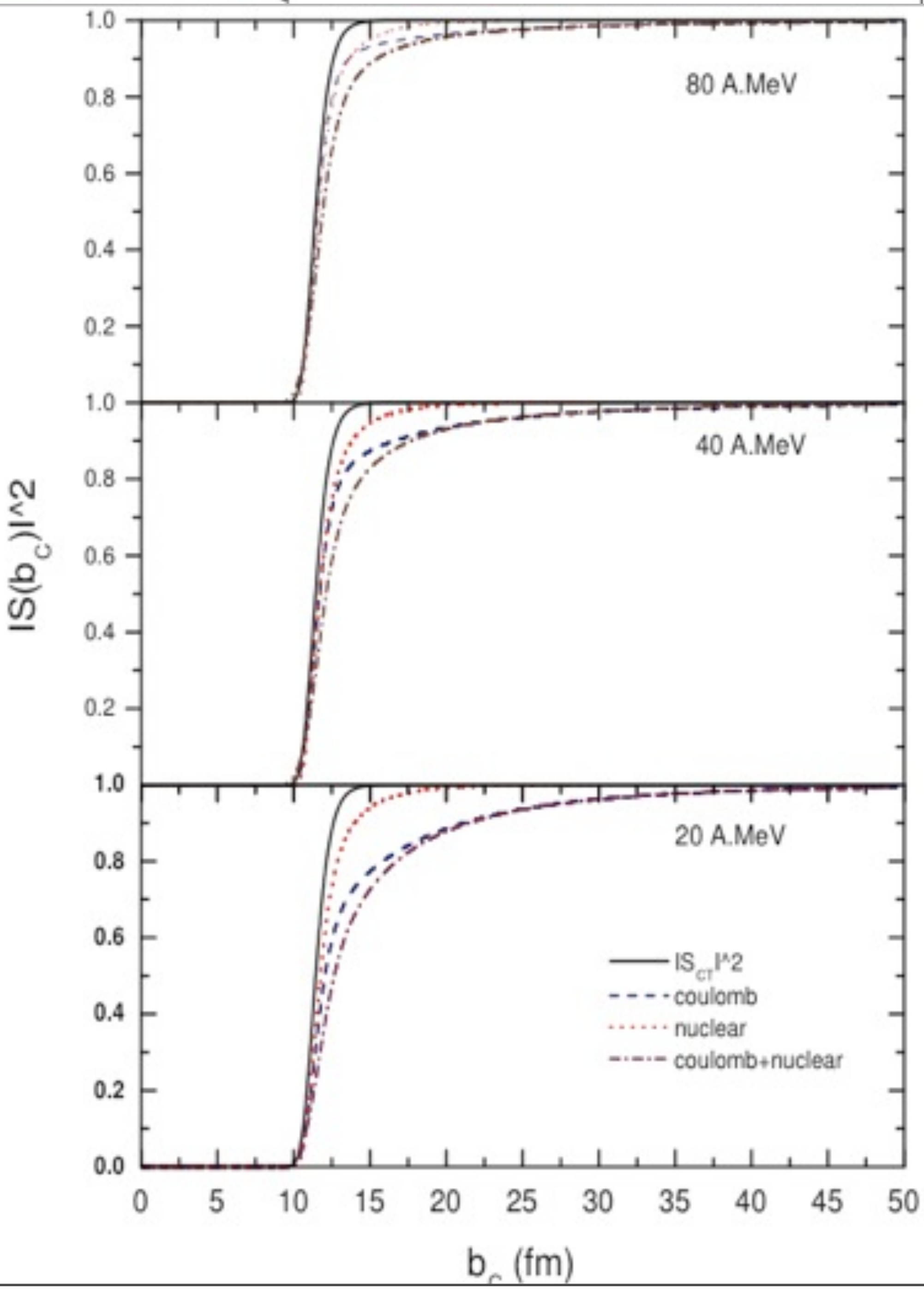
80 A.MeV
40 A.MeV
20 A.MeV
IS(b_C)I^2
IS_CTI^2
coulomb
nuclear
coulomb+nuclear
b_C (fm)

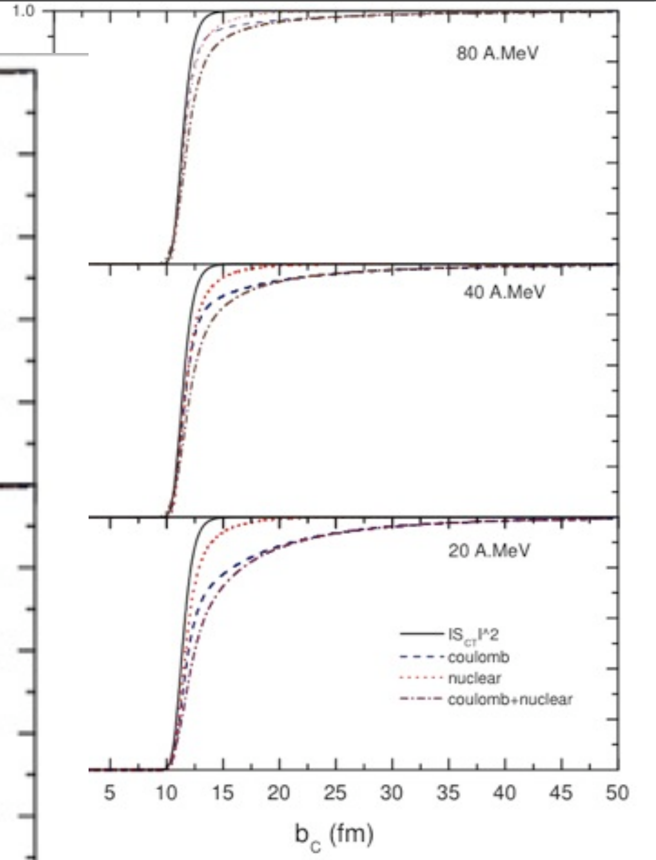
80 A.MeV
40 A.MeV
20 A.MeV
IS_CTI^2
coulomb
nuclear
coulomb+nuclear
b_C (fm)

Nuclear and Coulomb breakup potentials can be compared by using the parameterization :

$$W_S^N(r) = -\frac{\hbar v}{2} P_0 \sum_n A_n \exp\left(-r/\alpha_n\right) \frac{1}{\sqrt{2\pi\alpha_n r}}.$$

$$W_S^C(r) = -\frac{\hbar v}{2} P_0 \sum_n B_n \exp\left(-r/\beta_n\right) \frac{1}{\sqrt{2\pi\beta_n r}}.$$

The core survival probability has been parameterized as

$$P_0(b_c) = |S_{CT}|^2 = \exp(-\ln 2 e^{[(R_s - b_c)/a_0]}),$$

$\alpha_2 \approx 1/2\gamma$, $\gamma = \sqrt{2\mu\varepsilon_i}/\hbar$ $\beta_3 \approx (\varepsilon_f - \varepsilon_i)/\hbar v$

the most relevant parameter is the diffusness whose physical interpretation is

decay length of initial state wave function adiabaticity parameter of Coulomb

$$
\begin{aligned}
1-|S_{NN}(b_c)|^2 &\approx 1-|S_{CT}(b_c)|^2 e^{-P_{bup}(b_c)} \\
&= 1-|S_{CT}(b_c)|^2 + \\
&\quad +|S_{CT}(b_c)|^2 (p^N_{b_{up}}(b_c)+p^C_{b_{up}}(b_c))
\end{aligned}
$$

$$
\begin{aligned}
\sigma_{NN} &= 2\pi \int b_c db_c \left(1-|S_{NN}(b_c)|^2\right) \\
&\approx \sigma_{CT}+\sigma^N_{b_{up}}+\sigma^C_{b_{up}}.
\end{aligned}
$$

Projectile fragmentation and resonances (near threshold).

- During scattering at low energy a quasi-stationary system is formed (compound nucleus). Link the properties of the unperturbed “target” nucleus (wave functions of stationary states, underlying potential) to the experimentally measured scattering quantity.
- This is usually s-state (sometime p-state) scattering. Higher angular momentum resonances need an energy dependent optical potential (channel coupling).

INFN Angela Bonaccorso

Transfer to the continuum vs. Projectile fragmentation: a model for diffractive breakup in which the observable studied is the n-core relative energy spectrum and its resonances

$$A_{fi} = \frac{1}{i\hbar}\int_{-\infty}^{\infty} dt \langle \psi_f(\mathbf{r},t)|V_2(\mathbf{r}-\mathbf{R}(t))|\psi_i(\mathbf{r},t)\rangle,$$

$$\begin{aligned}\frac{dP_t(b_c)}{d\varepsilon_f} &= \frac{1}{8\pi^3}\frac{mk_f}{\hbar^2}\frac{1}{2l_i+1}\Sigma_{m_i}|A_{fi}|^2 \\ &\approx \frac{4\pi}{2k_f^2}\Sigma_{j_f}(|1-S_{j_f}|^2+1-|S_{j_f}|^2)(2j_f+1)(1+F_{l_f,l_i,j_f,j_i})B_{l_f,l_i} \\ &= \sigma_{nN}(\varepsilon_f)\mathcal{F},\end{aligned}$$

diffraction + stripping → inclusive breakup (

$$\frac{dP_{in}}{d\varepsilon_f} = \frac{2}{\pi}\frac{v_2^2}{\hbar^2 v^2}C_i^2\frac{m}{\hbar^2 k}\frac{1}{2l_i+1}\Sigma_{m_i,m_f}|1-\bar{S}_{m_i,m_f}|^2|I_{m_i,m_f}|^2,$$

→ exclusive breakup

diffraction

$$B_{l_f,l_i} \approx \frac{e^{-2\eta b_c}}{b_c}$$ **Knockout**

$$\bar{S} = Se^{2i\nu} = e^{2i(\delta+\nu)}$$

$\bar{S}$ *off-shell*

S *on shell*

$$I_{l_f,l_i} \approx \frac{e^{-2\gamma b_c}}{b_c^3}$$ **Fragmentation**

$$A_{bup} = \frac{1}{i\hbar}\int_{-\infty}^{\infty} dt < \psi_2(t)|V_{nt}(r)|\psi_1(t) >$$
$$\approx \int dk_y \sqrt{k_y^2+\eta^2}\,\bar{\psi}_i(d_1,k_y,k_1)\bar{\psi}_f^*(d_2,k_y,k_2)$$

$$A_{fi} = \frac{v_2}{i\hbar v}\int_{-\infty}^{\infty} \mathrm{d}z\ \psi_f^*(b_c,0,z)\psi_i(b_c,0,z)e^{iqz}.$$

$$A_{fi} = \frac{v_2}{i\hbar v}\int_{-\infty}^{\infty} \mathrm{d}z\ \psi_f^*(b_c,0,z)\psi_i(b_c,0,z)e^{iqz}.$$

TRANSFER
Stripping &
Diffraction
Overlap of momentum distribution (Fourier transforms)

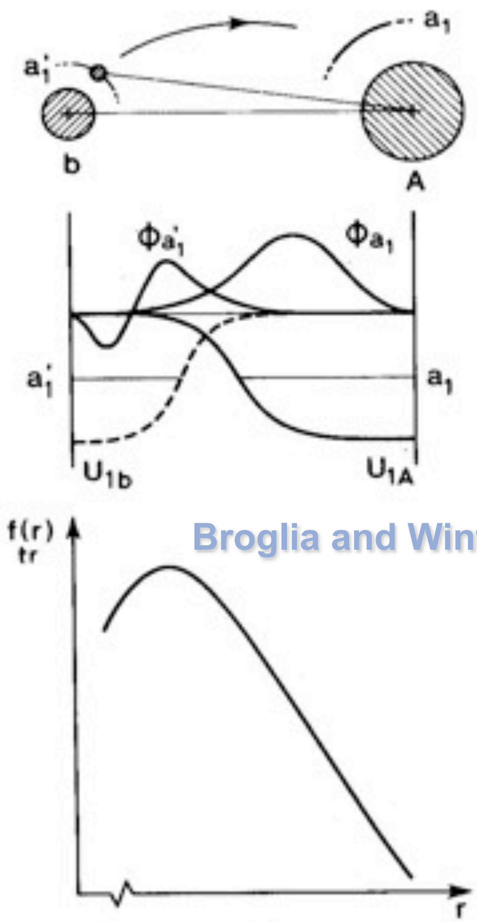

(a)

Broglia and Winther book

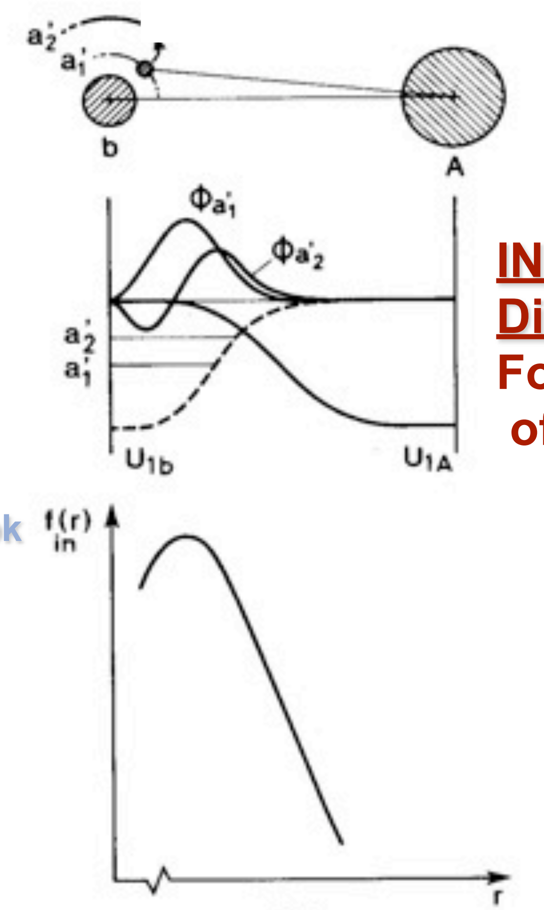

(b)

INELASTIC
Diffraction
Fourier transform of the overlap

Comparison to R-matrix theory

AB, DM Brink, PRC38 , 1776(1988)

$$|\sin\delta_{l_f}|^2=\frac{\Gamma}{2}\frac{\Gamma/2}{(\varepsilon-\varepsilon_{res})^2+\Gamma^2/4}\simeq\frac{\Gamma}{2}\pi\delta(\varepsilon-\varepsilon_{res}) \qquad (3.1)$$

and

$$P(l_f,l_i)=\int\frac{dP}{d\varepsilon}(l_f,l_i)d\varepsilon$$
$$\simeq\frac{\Gamma}{2}\pi\int d\varepsilon\,\delta(\varepsilon-\varepsilon_{res})4B(l_{res},l_i)$$
$$=\frac{\pi}{2}\left[\frac{\hbar}{mv}\right]^2\frac{m\Gamma}{\hbar^2 k_{res}}|C_i|^2(2l_f+1)$$
$$\times P_{l_i}\left[1+2\frac{k_1^2}{\gamma^2}\right]P_{l_f}\left[2\frac{k_2^2}{k_{res}^2}-1\right]\frac{e^{-2\eta R}}{\eta R}, \qquad (3.2)$$

where $B(l_{res},l_i)$ is given by Eq. (2.29).

In the case of transfer between bound states [cf. Eq. (3.15) of Ref. 4] the equivalent of Eq. (3.2) was

$$P(l_2,l_1)=\frac{\pi}{2}\left[\frac{\hbar}{mv}\right]^2|C_1C_2|^2(2l_2+1)P_{l_1}\left[1+2\frac{k_1^2}{\gamma_1^2}\right]$$
$$\times P_{l_2}\left[2\frac{k_2^2}{\gamma_2^2}+1\right]\frac{e^{-2\eta R}}{\eta R}. \qquad (3.3)$$

The place of the asymptotic normalization constant of the final state C_2 is then taken by the term $m\Gamma/\hbar^2 k_{res}$.

To understand this we use the definition of Γ given in R-matrix theory[14]

$$\Gamma=\frac{\hbar^2 k_{res}}{m}\frac{u_l^2(R)}{[k_{res}O_l(k_{res}R)]^2}, \qquad (3.4)$$

where u_l is the neutron radial wave function calculated in the potential of the target at the resonance energy and $O_l(k_{res}R)=h_l^{(+)}(k_{res}R)$ is its asymptotic form outside a radius R beyond which the nuclear potential vanishes. Then we have

$$\frac{m\Gamma}{\hbar^2 k_{res}}=\frac{u_l^2(R)}{[k_{res}O_l(k_{res}R)]^2}. \qquad (3.5)$$

$$|C_2|^2=\frac{\psi_{num}^2(R)}{[\gamma_2 h_l^{(+)}(i\gamma_2 R)]^2}, \qquad (3.6)$$

where ψ_{num} is the numerical solution of the single-particle Schrödinger equation at the experimental binding energy and $h_l^{(+)}(i\gamma_2 R)$ is a Hankel function of complex argument imposed as its asymptotic form. C_2 is independent from the radius R when this is taken well outside the nuclear potential.

[14] A. M. Lane, R. G. Thomas, and E. P. Wigner, Phys. Rev. 98, 639 (1955).

Angela Bonaccorso

Istituto Nazionale di Fisica Nucleare

•^{14}B fragmentation on C

JL Lecouey LPCC 02-03; Few-Body Systems 34 (2004) 21

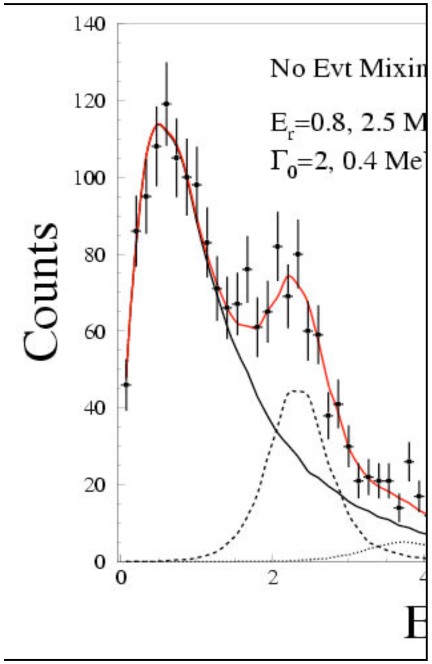

•GSI-U. Datta Pramanik-2004)

•Unpublished

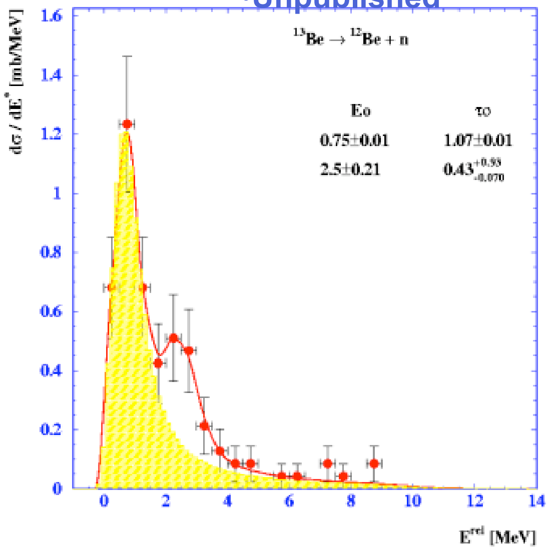

H.Simon et al, NPA791 (2007)267

^{14}Be fragmentation on C

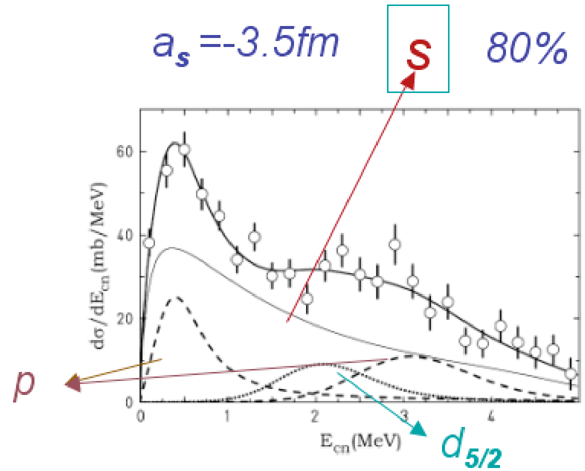

Fig. 10. Differential cross section as a function of the relative energy between ^{12}Be and a neutron. The data points are the same as those in Fig. 4, panel 3. The thin-solid line corresponds to the $1/2^+$ virtual state, the dotted line is the contribution from the $5/2^+$ state. Dashed lines display the $1/2^-$ state and its satellite at low energy. The thick-solid line is the sum of the reaction branches.

^{14}B fragmentation on H, Kondo et al., proton target

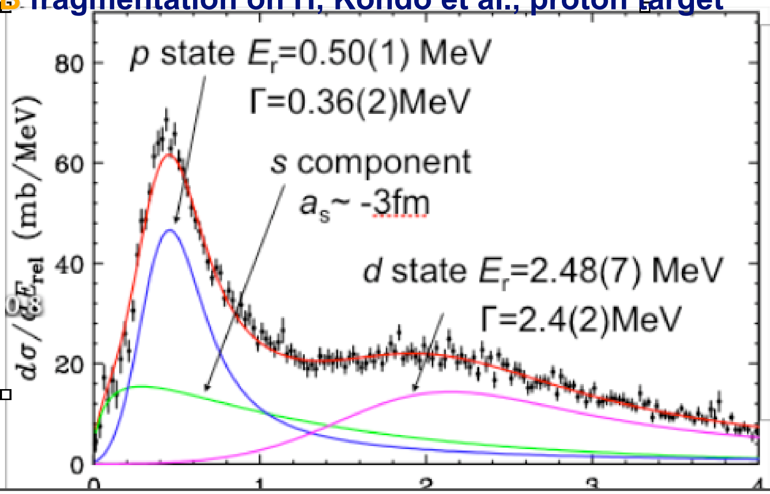

Systematic investigation of the drip-line nuclei ^{11}Li and ^{14}Be and their unbound subsystems ^{10}Li and ^{13}Be.

Nucl. Phys. A791 (2007) 267.

H. Simon [a,b], M. Meister [a,c], T. Aumann [b,d], M.J.G. Borge [e], L.V. Chulkov [b,f], Th. W. Elze [g], H. Emling [b], C. Forseén [h,c], H. Geissel [b], M. Hellström [b], B. Jonson [c], J. V. Kratz [d], R. Kulessa [i], Y. Leifels [b], K. Markenroth [c], G. Münzenberg [b], F. Nickel [b], T. Nilsson [a,c], G. Nyman [c], A. Richter [a], K. Riisager [j], C. Scheidenberger [b], G. Schrieder [a], O. Tengblad [e] and M. V. Zhukov [c]

INFN Angela Bonaccorso

^{14}Be $T_{1/2}$=4.35ms±0.17

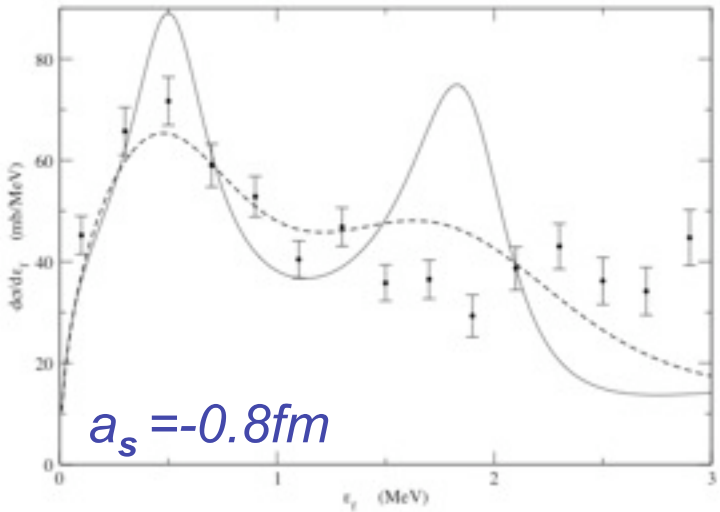

Figure 12: Sum of all transitions from the s initial state with ε_f=-1.85 MeV (solid line). Experimental points from L. Chulkov et al. [56]. Dashed line is the folding of the calculated spectrum with the experimental resolution curve.

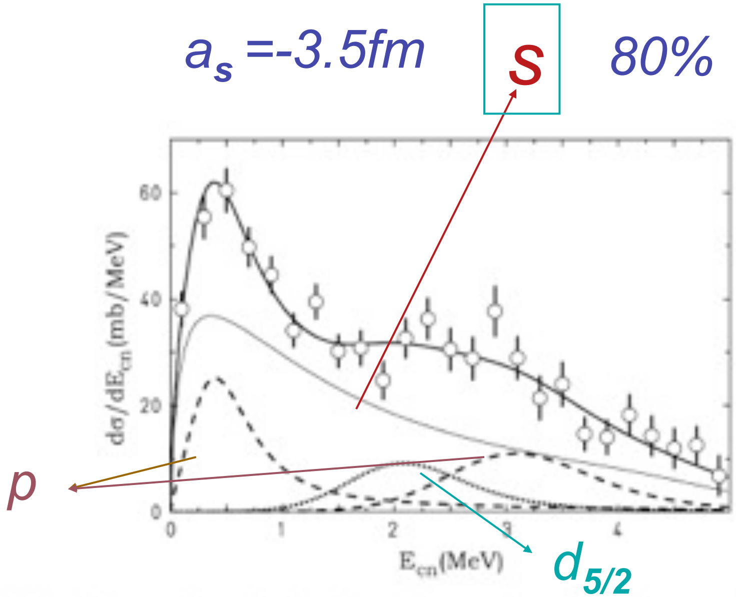

Fig. 10. Differential cross section as a function of the relative energy between ^{12}Be and a neutron. The data points are the same as those in Fig. 4, panel 3. The thin-solid line corresponds to the $1/2^+$ virtual state, the dotted line is the contribution from the $5/2^+$ state. Dashed lines display the $1/2^-$ state and its satellite at low energy. The thick-solid line is the sum of the reaction branches.

Systematic investigation of the drip-line nuclei ^{11}Li and ^{14}Be and their unbound subsystems ^{10}Li and ^{13}Be.

Nucl. Phys. A791 (2007) 267.

H. Simon [a,b], M. Meister [a,c], T. Aumann [b,d], M.J.G. Borge [e], L.V. Chulkov [b,f], Th. W. Elze [g], H. Emling [b], C. Forssén [h,c], H. Geissel [b], M. Hellström [b], B. Jonson [c], J. V. Kratz [d], R. Kulessa [i], Y. Leifels [b], K. Markenroth [c], G. Münzenberg [b], F. Nickel [b], T. Nilsson [a,c], G. Nyman [c], A. Richter [a], K. Riisager [j], C. Scheidenberger [b], G. Schrieder [a], O. Tengblad [e] and M. V. Zhukov [c]

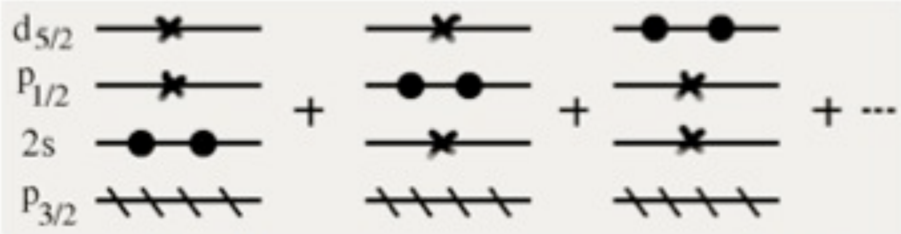

Figure 3.5: Formation of ^{13}Be with one neutron (crosses) added to an open shell ^{12}Be. Only one neutron is added in each configuration, but the cross indicates states which can be populated.

M. Labiche, F. M. Marqués, O. Sorlin, and N. Vinh Mau, Phys. Rev. C **60**, 027303 (1999).
J. C. Pacheco and N. Vinh Mau, Phys. Rev. C **65**, 044004 (2002).

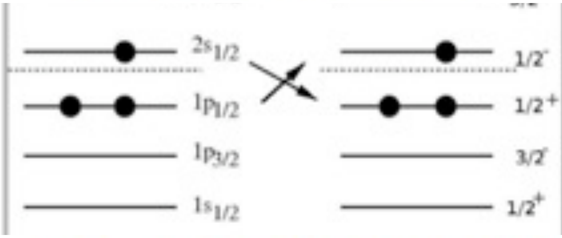

TABLE III: Theoretical and experimental values of S_{2n} (MeV) in ^{12}Be and ^{14}Be (from Ref.[22]), $\langle r^2\rangle^{1/2}_{A+2}$ (fm), $\langle \boldsymbol{\lambda}^2\rangle^{1/2}$ (fm) and $\langle \boldsymbol{\rho}^2\rangle^{1/2}$ (fm) in ^{14}Be (from Ref. [23, 37], $\boldsymbol{\lambda}$ deduced using Eq.10) in the two cases of non-inversion (A) and inversion (B) of the $2s_{1/2}$ and $1p_{1/2}$ shells.

	$S_{2n}(^{12}\mathrm{Be})$	$S_{2n}(^{14}\mathrm{Be})$	$\langle r^2\rangle^{1/2}_{A+2}$	$\langle \boldsymbol{\rho}^2\rangle^{1/2}$	$\langle \boldsymbol{\lambda}^2\rangle^{1/2}$
A	2.91	0.51	3.45	8.45	5.45
B	3.71	1.29	2.91	4.56	4.02
Exp.	3.673±0.015	1.26 ± 0.01	3.10±0.15	5.4±1.0	4.2±1.7

Particle-particle random phase approximation applied to Beryllium isotopes

G. Blanchon[(1)], N. Vinh Mau[(1,2)], A. Bonaccorso[(3)], M. Dupuis[(1)], and N. Pillet[(1)]

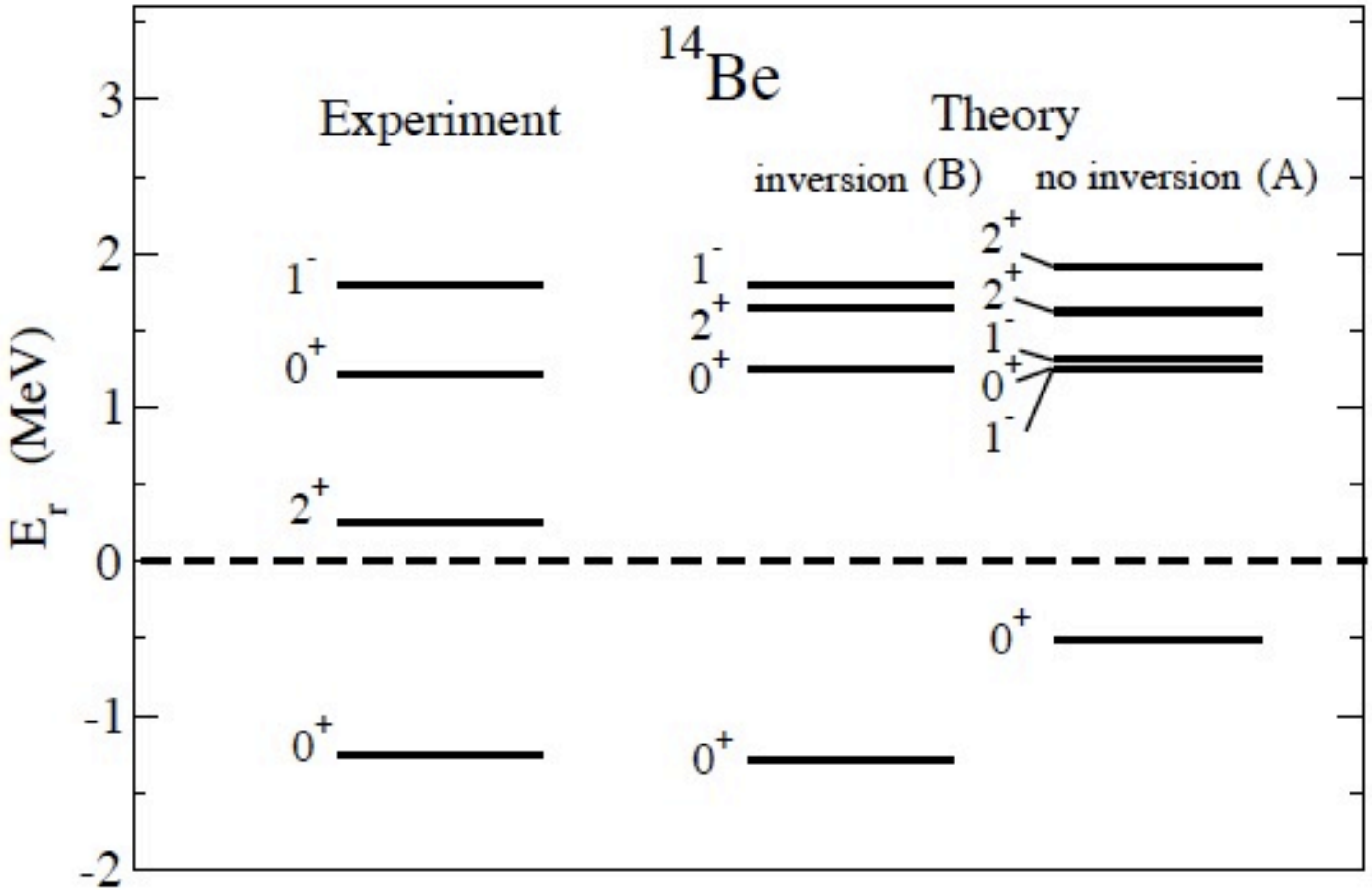

FIG. 2: Low lying spectra of ^{14}Be obtained with pp-RPA without (A) and with (B) inversion in ^{13}Be compared to experiment.

PRC, in press, 1007.2719v1-nucl-th

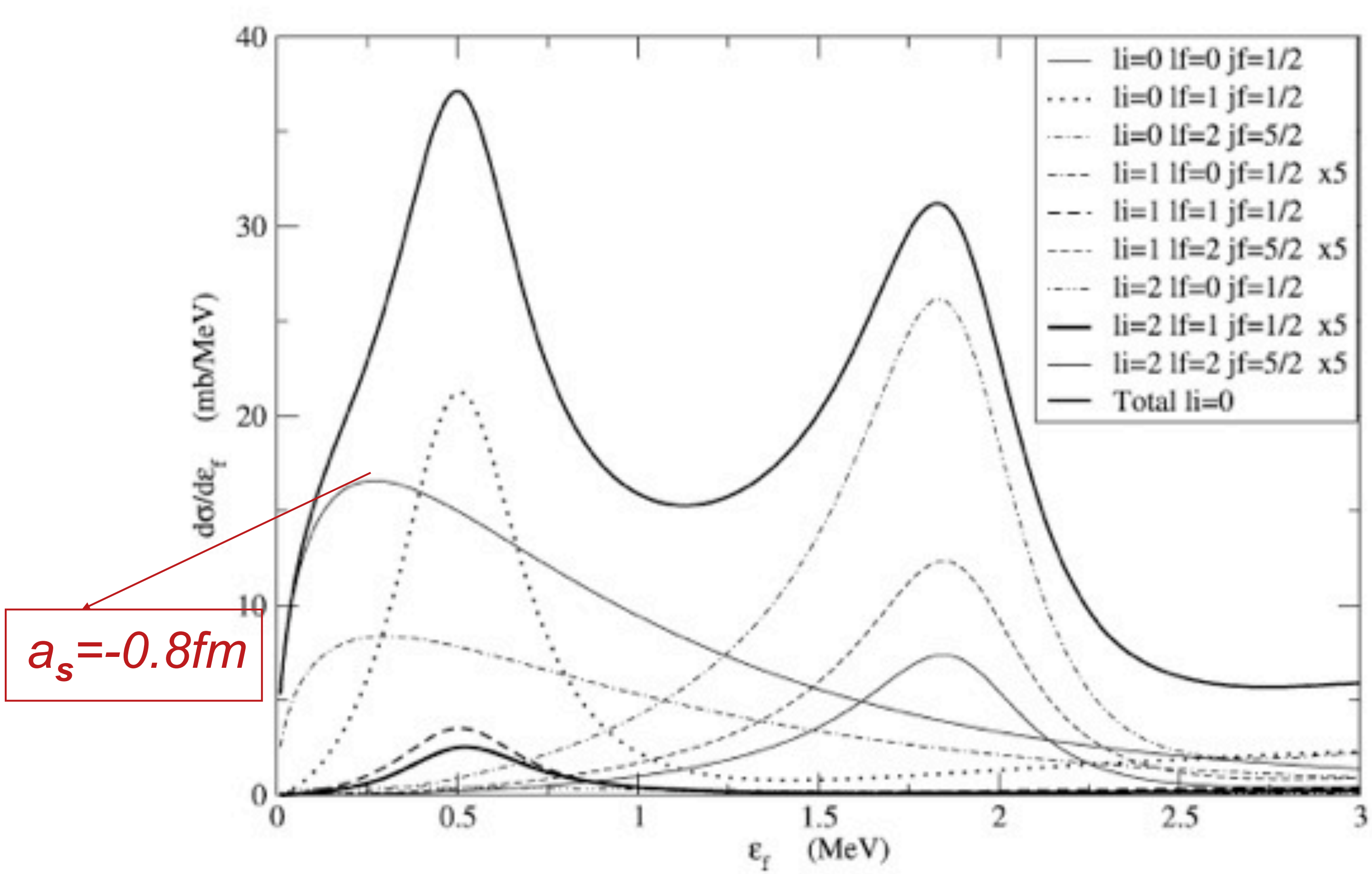

Fig. 8. Results obtained including the s, p and d states. Each curve corresponds to just one transition as indicated. The solid curve is the sum of all transitions from the s-bound state. To make them visible some curves have been multiplied by a factor of five as indicated in the legend.

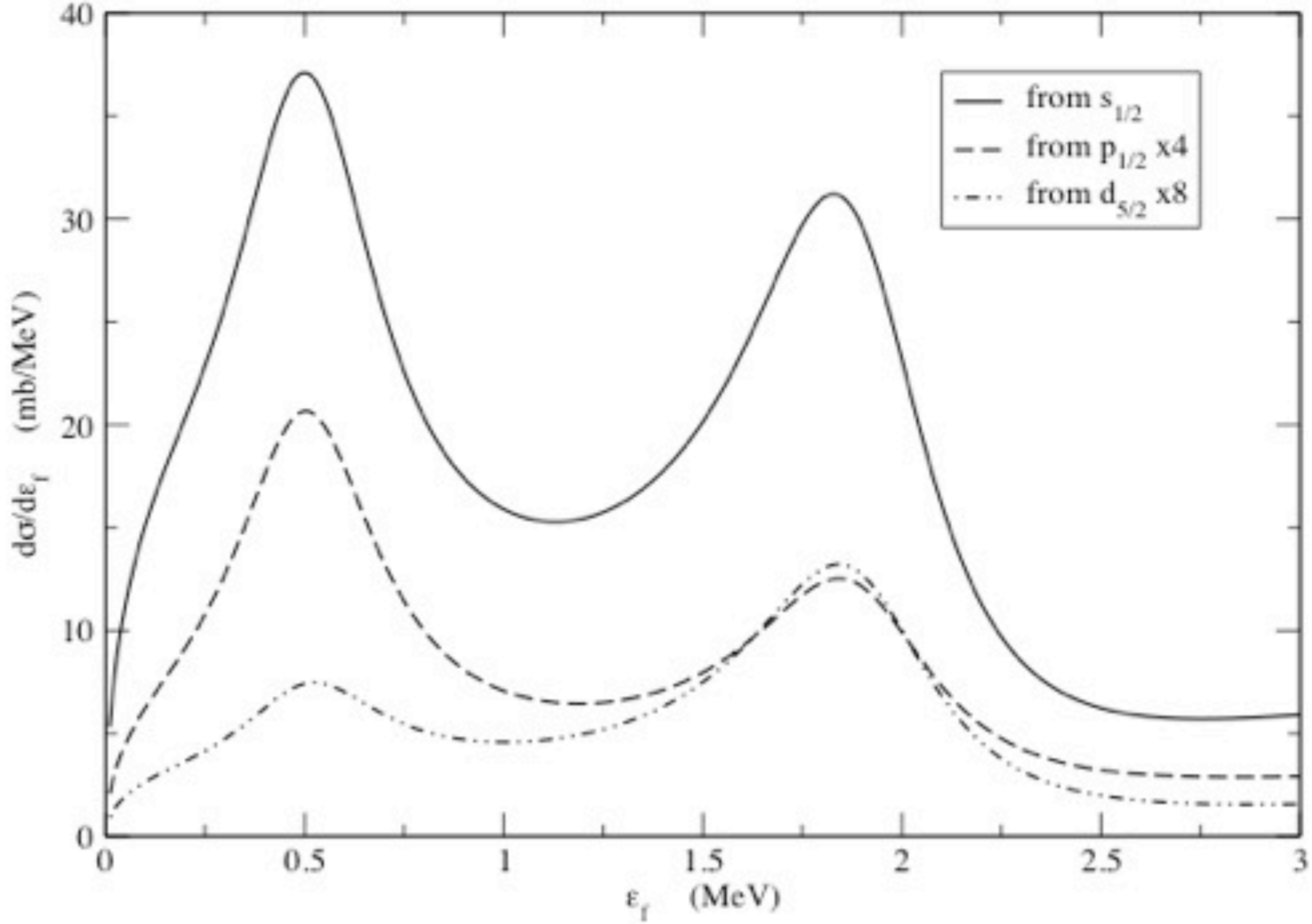

Figure 11: Check of the dependence from the initial state angular momentum. Full curve: sum of transitions from s-initial state. Dashed and dotdashed lines: sum of transitions from p and d-initial states respectively.

In projectile fragmentation reactions it is the lowest angular momentum initial state to dominate the transition process

Strengths of the s-state δV potential in Eq. (40) and corresponding scattering lengths, effective range parameter and *energy parameter* ϵ. The strength of the central Woods–Saxon part is $V_0 = -39.8$ MeV in all cases (cf. Table 3)

α (MeV)	a_s (fm)	r_e (fm)	$\|\epsilon\|$ (MeV)
8.0	−0.8	117.0	
4.0	−3.5	17.9	
2.0	−6.6	11.8	
−1.0	−26.1	7.58	
−5.0	22.4	5.9	0.06
−15.0	7.1	3.8	1.34
−35.0	4.5	2.7	6.49

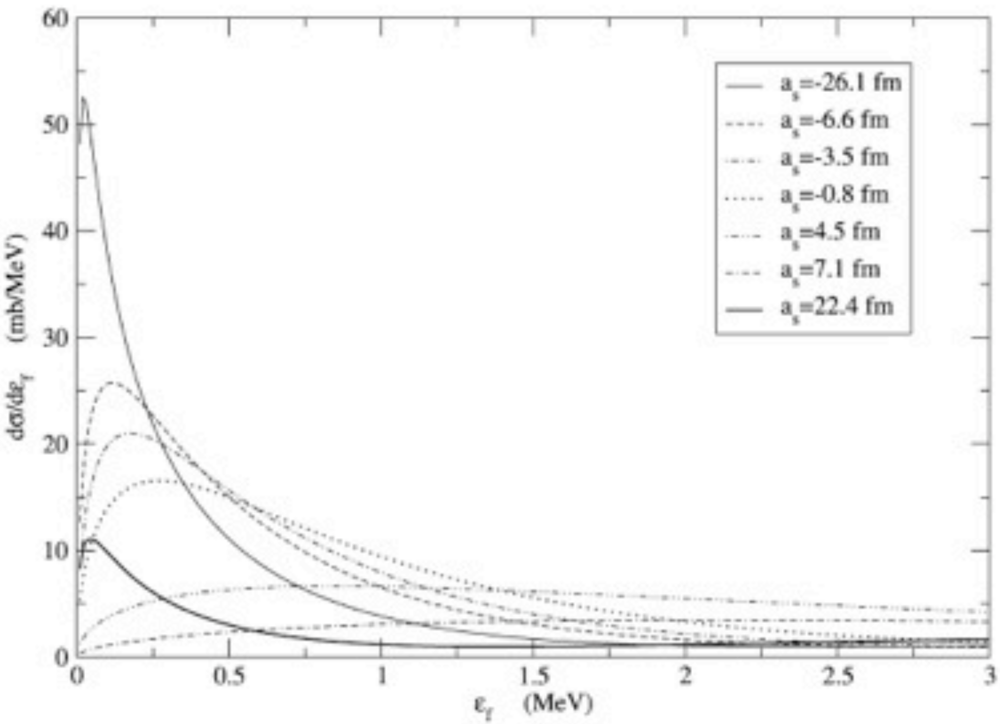

Conclusions

- A time dependent theory for projectile fragmentation reaction has been established which contains the sudden approximation and R-matrix theories as limiting cases.
- 2p correlations and particle-vibration couplings play a fundamental role.
- Importance of coupling to core excited states.
- For the ***first time the shell ordering of ^{13}Be has been established*** **theoretically** on a firm basis and ***parity inversion across threshold has been proved to persist for N=9 isotones***
- Much care is needed in analyzing experimental results in order not to draw misleading or unphysical conclusions: sudden approximation vs. time dependent, use of Breit-Wigner resonance form (vs. exact S-matrix or R-matrix),importance of various initial state components.

Coulomb breakup. All orders vs first order approximation. The proton vs neutron case.

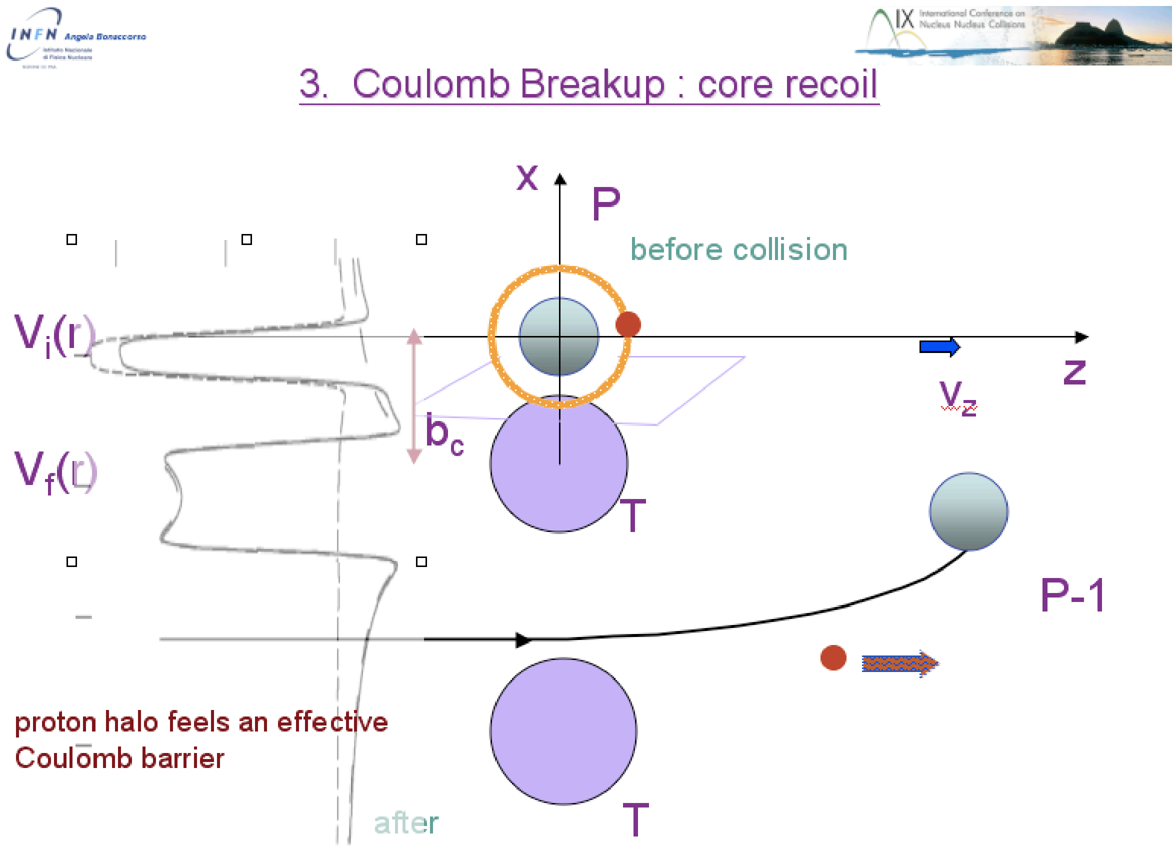

Proton Coulomb Breakup : core recoil + direct term

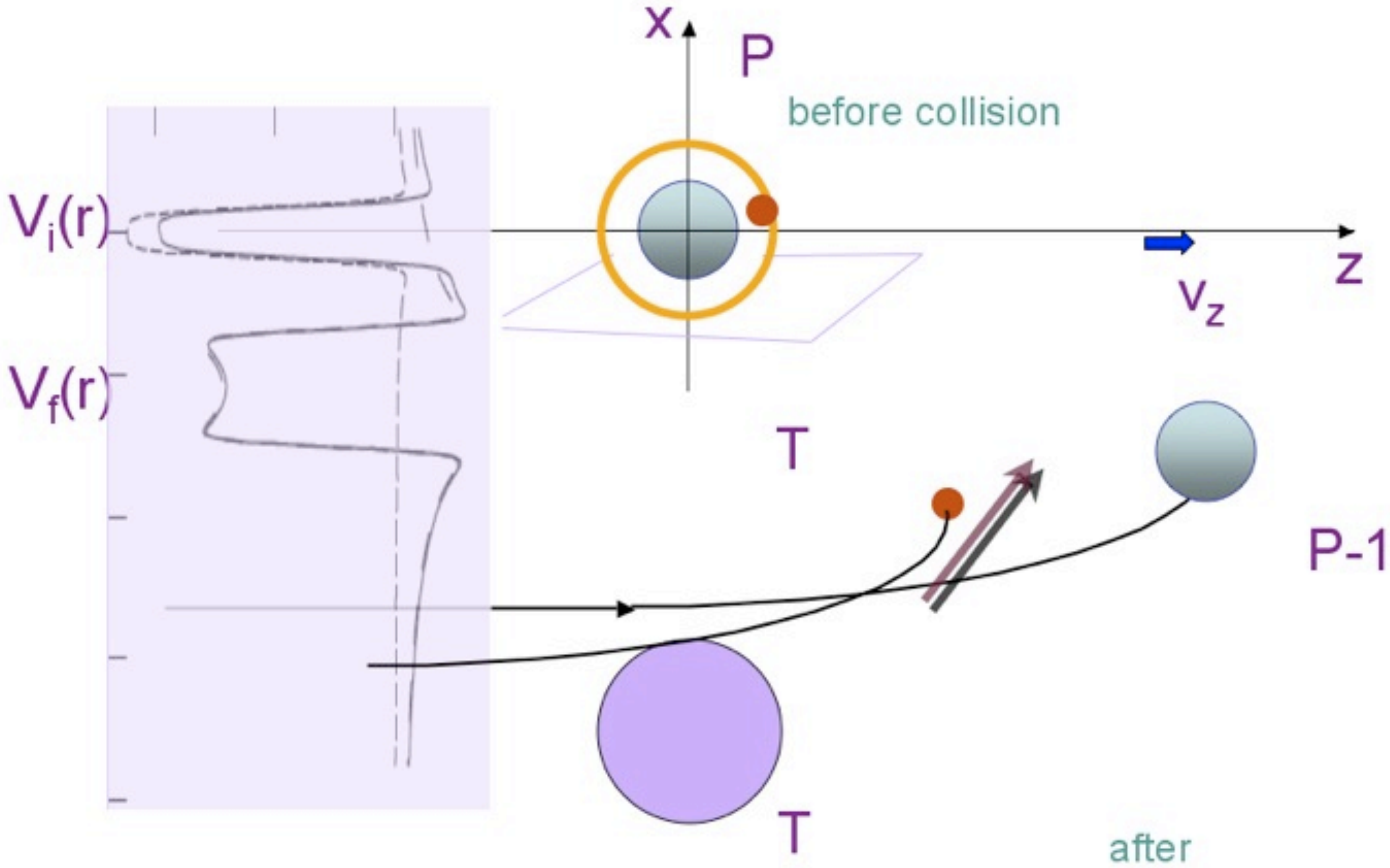

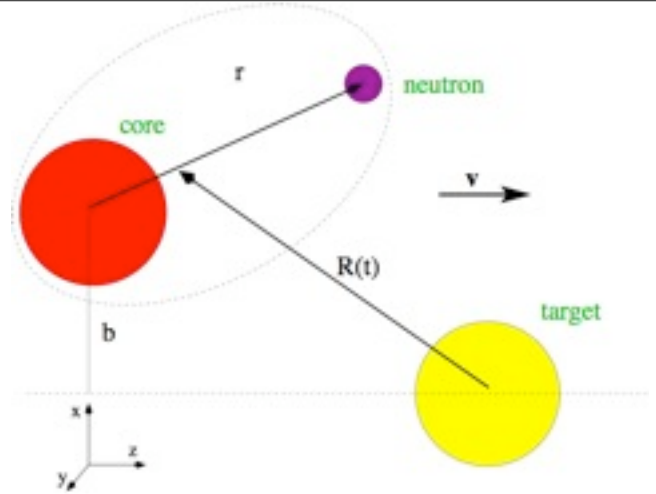

$$V_{\rm nt}(\beta_2\mathbf{r}+\mathbf{R}) \approx V_{\rm nt}(\mathbf{r}+\mathbf{R}),$$
$$V_{\rm ct}(\mathbf{R}-\beta_1\mathbf{r}) \approx V_{\rm ct}(\mathbf{R})+\mathbf{V}_{\rm eff}(\mathbf{r},\mathbf{R})$$

where

$$\mathbf{V}_{\rm eff}(\mathbf{r},\mathbf{R}) = \beta_1\mathbf{r}\cdot\mathbf{F}_{\rm ct}(\mathbf{R}) \quad \text{and} \quad \mathbf{F}_{\rm ct}(\mathbf{R}) = -\nabla V_{\rm ct}(\mathbf{R}).$$

$$\begin{aligned} V_{\rm eff}\big(\mathbf{r},\mathbf{R}(t)\big) &= +\beta_1 Z_P Z_T e^2\left(\frac{\mathbf{r}\cdot\mathbf{R}(t)}{R(t)^3}\right) \\ &= +\beta_1 Z_P Z_T e^2 \frac{xd+zvt}{(d^2+(vt)^2)^{3/2}}. \end{aligned}$$

The breakup amplitude becomes

$$g_{lm}(\mathbf{k},\mathbf{d}) = \frac{1}{i\hbar}\int d^3\mathbf{r}\int dt\, e^{-i\mathbf{k}\cdot\mathbf{r}+i\omega t} e^{\left(\frac{1}{i\hbar}\int_t^\infty \overline{V_2}(\mathbf{r},t')\,dt'\right)}\overline{V_2}(\mathbf{r},t)\phi_{lm}(\mathbf{r})$$

where $\omega = (\varepsilon_{\mathbf{k}}-\varepsilon_0)/\hbar$.

$$V(\vec{r},\vec{R}) = \frac{V_c}{|\vec{R}-\beta_1\vec{r}|} + \frac{V_v}{|\vec{R}+\beta_2\vec{r}|} - \frac{V_0}{R} \qquad (1)$$

where $V_c = Z_c Z_t e^2$, $V_v = Z_v Z_t e^2$ and $V_0 = (Z_v + Z_c) Z_t e^2$. β_1 and β_2 are the mass ratios of proton and core, respectively, to that of the projectile. The coordi-

Our expression for the differential cross-section is

$$\frac{d\sigma}{d\vec{k}} = \frac{1}{8\pi^3}\int d\vec{b}_c |S_{ct}(b_c)|^2 |g^{rec} + g^{dir} + g^{nuc}|^2. \qquad (6)$$

where $S_{ct}(b_c)|^2$ is the core-target elastic scattering probability discussed later and the probability amplitude has been written as the sum of three pieces: the recoil term,

$$g^{rec} = \int d\vec{r} e^{-i\vec{k}\cdot\vec{r}} \phi_i(\vec{r}) (e^{i\frac{2V_c}{\hbar v}\log\frac{b_c}{R_\perp}} - 1 - i\frac{2V_c}{\hbar v}\log\frac{b_c}{R_\perp} + i\chi(\beta_1, V_c)), \qquad (7)$$

where, according to the discussions in [1, 25, 26, 27], the sudden limit has been used in order to include all orders in the interaction. Similarly, the second term in our probability amplitude is the direct proton Coulomb interaction. It has the same form as Eq.(7) but for the substitution $V_c \to V_v$, $b_c \to b_v$ and $\beta_1 \to -\beta_2$.

Finally, the nuclear part is

$$g^{nuc} = \int d\vec{r} e^{-i\vec{k}\cdot\vec{r}} \phi_i(\vec{r}) \left(e^{i\chi_{nt}(b_v)} - 1\right). \qquad (8)$$

PHYSICAL REVIEW C **76**, 014607 (2007)

All orders proton breakup from exotic nuclei

A. García-Camacho,[1] G. Blanchon,[1] A. Bonaccorso,[1] and D. M. Brink[2]

[1] *INFN, Sezione di Pisa and Dipartimento di Fisica, Università di Pisa, Largo Pontecorvo 3, I-56127 Pisa, Italy*

[2] *Department of Theoretical Physics, 1 Keble Road, Oxford OX1 3NP, United Kingdom*

(Received 12 February 2007; published 11 July 2007)

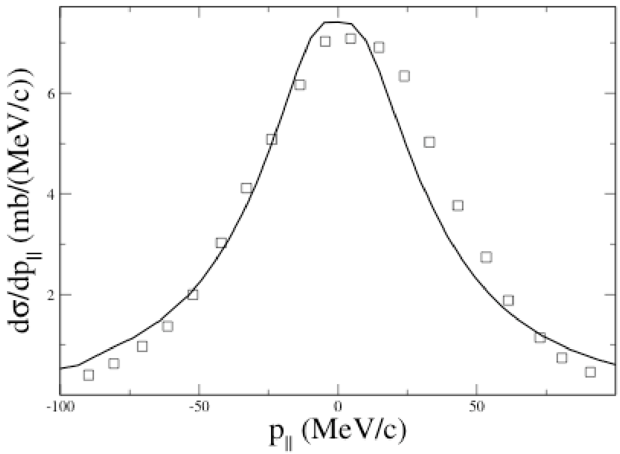

Figure 2: Calculated inclusive momentum distribution of ^{7}Be fragments after proton-removal from ^{8}B against Pb at 936 MeV/A. Data are from [46].

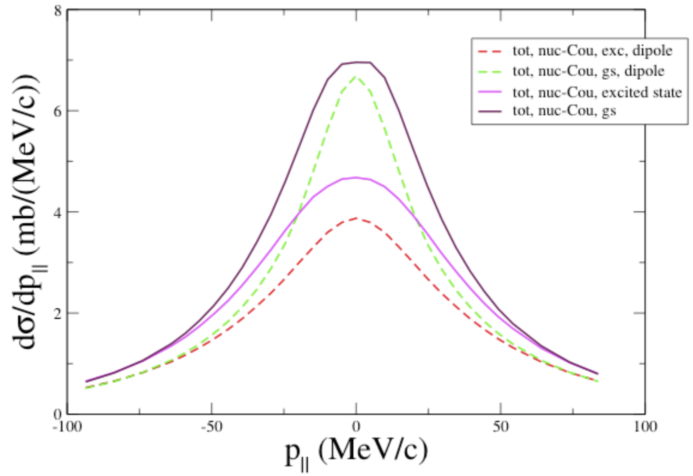

Figure 4: For the same reaction of Fig 2, proton momentum distribution in both dipole and full-multipole approximations, for both ground and excited state.

Physics Letters B 681 (2009) 22–25

Dynamic polarization in the Coulomb breakup of loosely bound ^{17}F

J.F. Liang[a,*], J.R. Beene[a], A.L. Caraley[b], H. Esbensen[c], A. Galindo-Uribarri[a], C.J. Gross[a], P.E. Mueller
K.T. Schmitt[d], D. Shapira[a], D.W. Stracener[a], R.L. Varner[a]

[a] Physics Division, Oak Ridge National Laboratory, Oak Ridge, TN 37831, USA
[b] Department of Physics, State University of New York at Oswego, Oswego, NY 13126, USA
[c] Physics Division, Argonne National Laboratory, Argonne, IL 60439, USA
[d] Department of Physics and Astronomy, University of Tennessee, Knoxville, TN 37966, USA

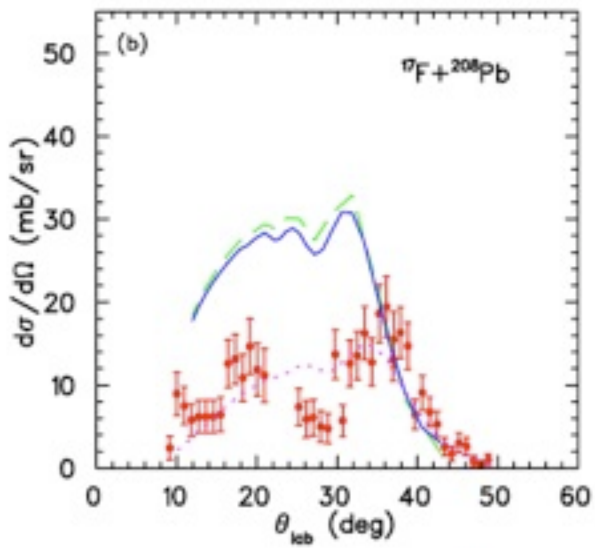

Fig. 4. Angular distributions of exclusive breakup for (a) $^{17}F + {}^{58}Ni$ and (b) $^{17}F + {}^{208}Pb$. The dynamical calculation including the proton-target Coulomb field is shown by the dashed curves and the combined Coulomb and nuclear fields is shown by the solid curves. The dotted curve in (b) is for the perturbation calculation using an effective binding energy of 1.2 MeV (see text).

INFN Angela Bonaccorso
Istituto Nazionale di Fisica Nucleare
SEZIONE DI PISA

Δ

$$\tilde{\varepsilon}_i = \varepsilon_i - \frac{Z_p e^2}{R_i} - Z_t e^2 \left(\frac{1}{2}\left(\frac{1}{|b_c + R_i|} + \frac{1}{|b_c - R_i|}\right) - \frac{1}{b_c}\right)$$

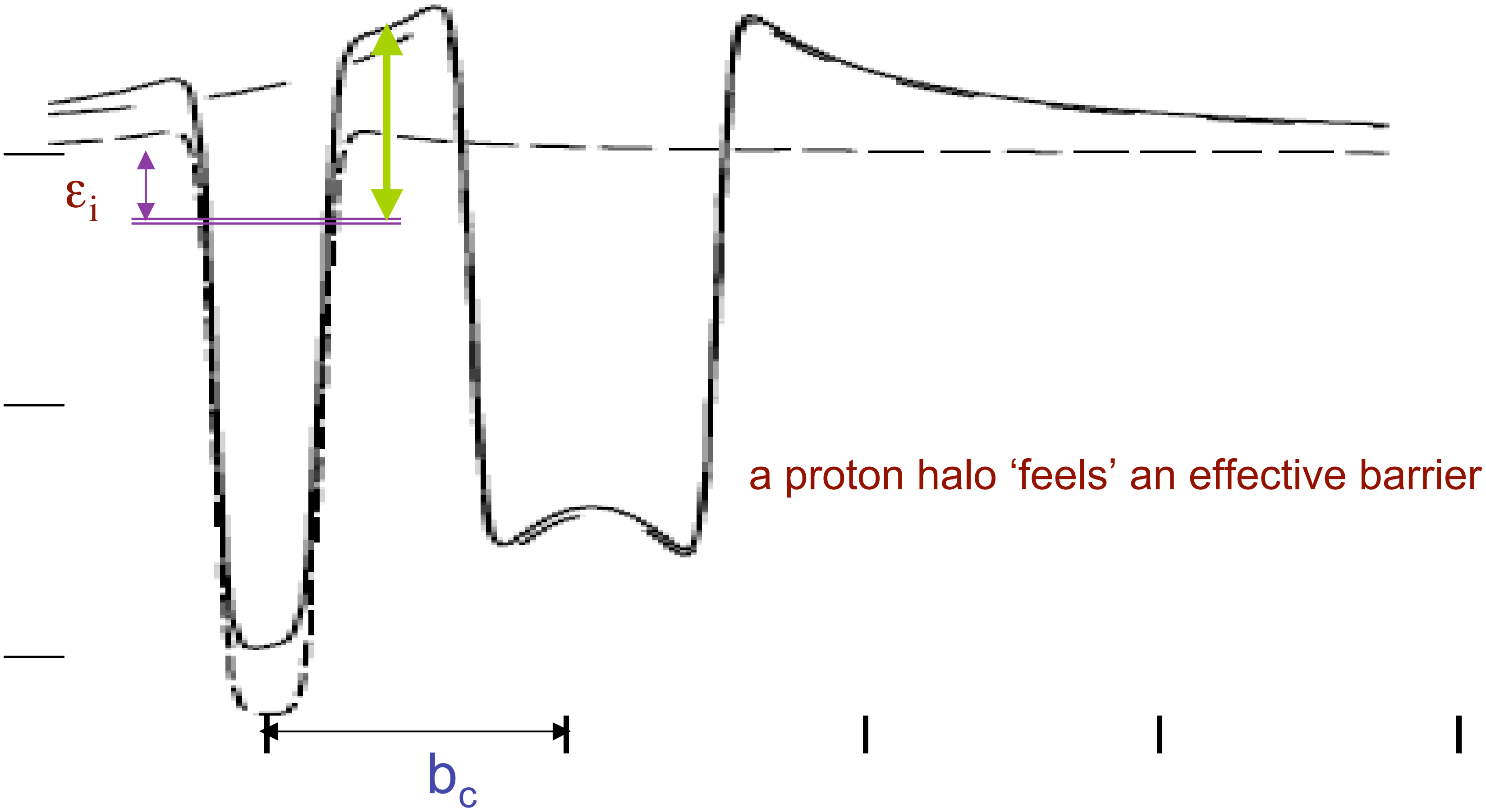

INFN Angela Bonaccorso
Istituto Nazionale di Fisica Nucleare
SEZIONE DI PISA

The proton vs neutron case.

BONACCORSO, BRINK, AND BERTULANI — PHYSICAL REVIEW C **69**, 024615 (2004)

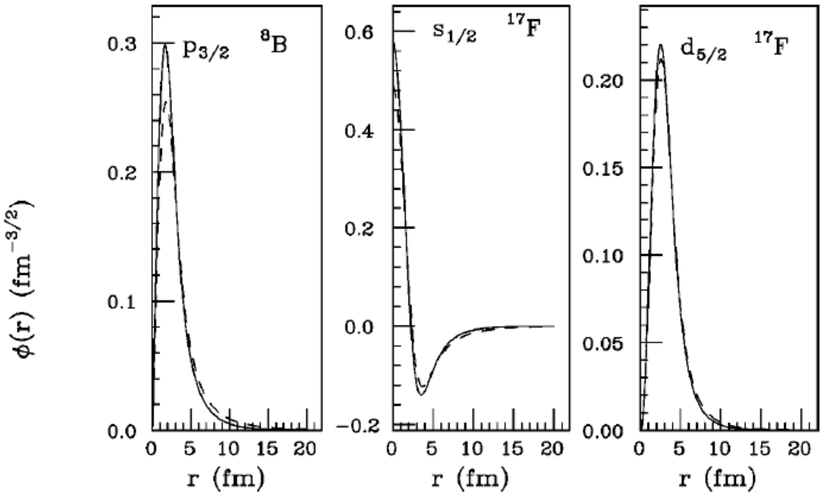

FIG. 3. Proton (dashed) and neutron (solid) wave functions for ^{8}B, ^{17}F as indicated. Neutron wave functions obtained for effective energies as in Table II, in the case of the ^{58}Ni target.

	^{8}B	J^π	^{17}F	J^π
$R_i(fm)$	6.0		6.5	
$\varepsilon_i(MeV)$	-0.14	$1p_{3/2}$	-0.6	$1d_{5/2}$
$\varepsilon_i^*(MeV)$	-0.57	$1p_{1/2}$	-0.1	$2s_{1/2}$

TABLE II. Effective parameters.

	^{8}B+^{58}Ni	^{8}B+^{208}Pb	^{17}F+^{58}Ni	^{17}F+^{208}Pb
Δ_i (MeV)	−1.85	−2.29	−2.7	−3.2
$\tilde{\varepsilon}_i$ (MeV)	−1.99	−2.43	−3.3	−3.8
$\tilde{\gamma}_i$ (fm^{-1})	0.29	0.34	0.39	0.42
$\tilde{C}_i$ (fm$^{-1/2}$)	0.69	0.79	0.75	0.89
$\tilde{\varepsilon}_i^*$ (MeV)			−2.8	−3.3
$\tilde{\gamma}_i^*$ (fm^{-1})			0.36	0.39
$\tilde{C}_i^*$ (fm$^{-1/2}$)			3.06	3.5

INFN Angela Bonaccorso
Istituto Nazionale di Fisica Nucleare
SEZIONE DI PISA

8B+208Pb (gs $p_{3/2}$) at 72 Mev/n multipole Vs dipole

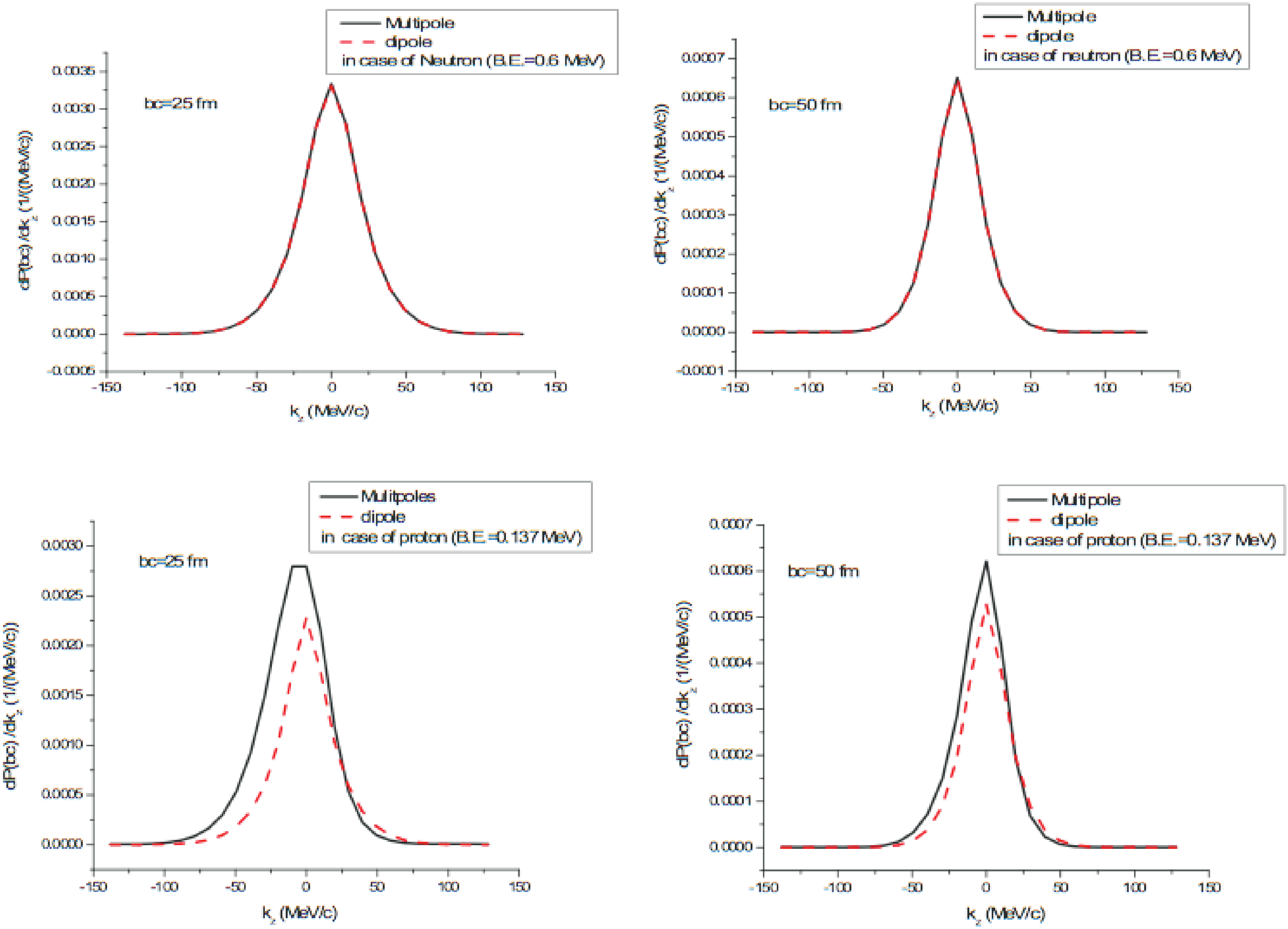

INFN Angela Bonaccorso
Istituto Nazionale di Fisica Nucleare
SEZIONE DI PISA

First order pert. results

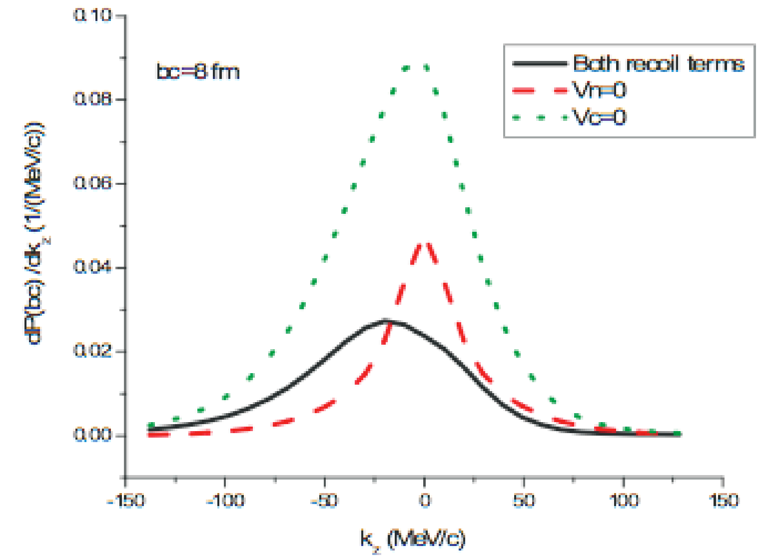

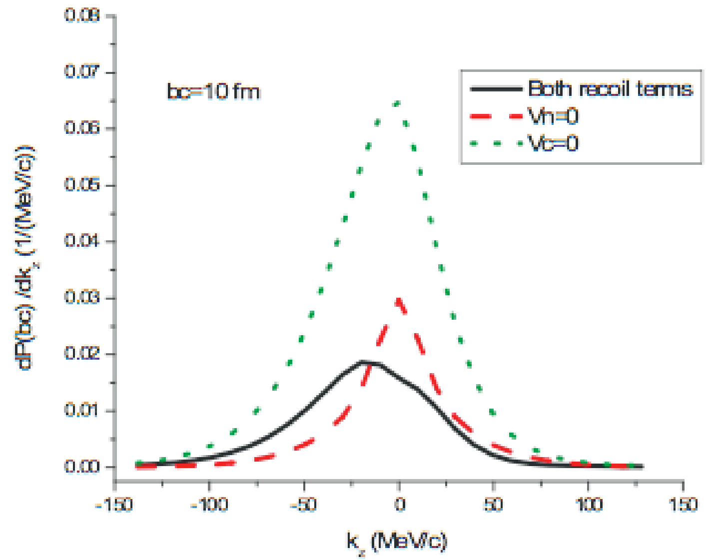

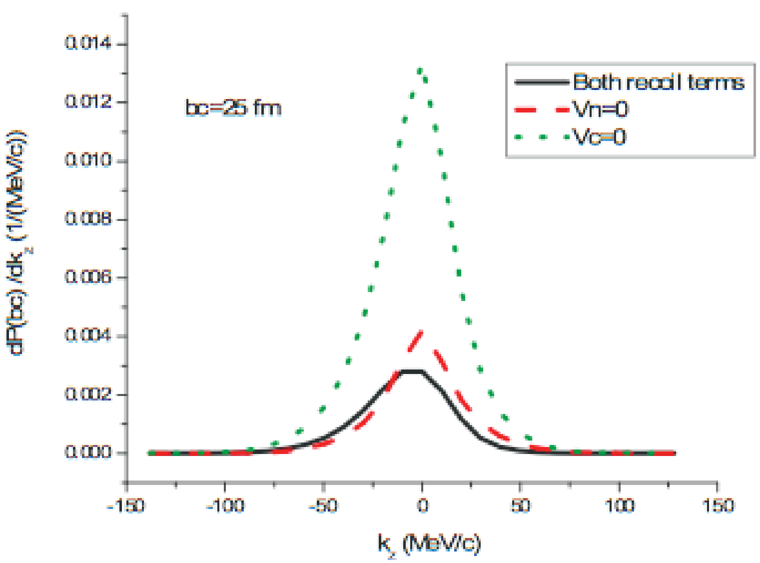

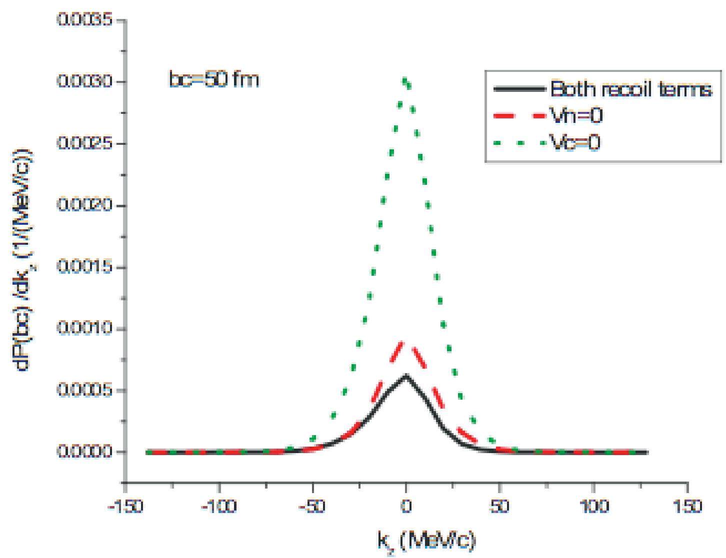

INFN Angela Bonaccorso
Istituto Nazionale di Fisica Nucleare
SEZIONE DI PISA

8B+208Pb (ground state) at 72 MeV/n Proton Vs Neutron

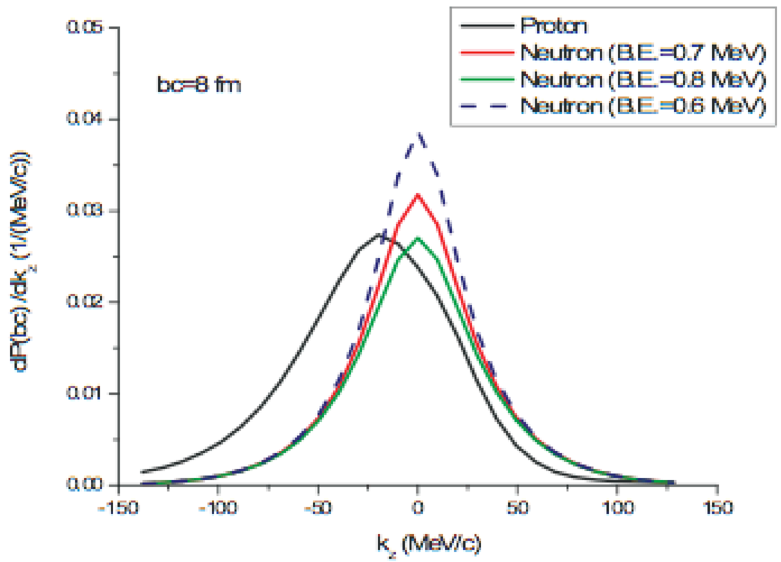

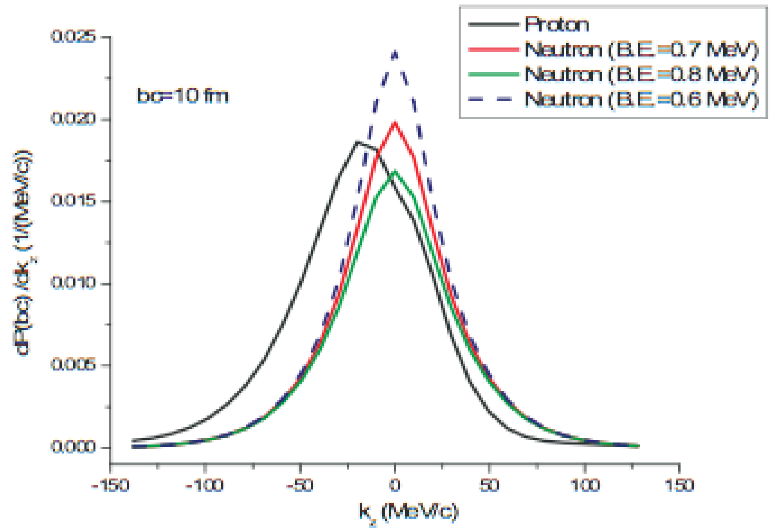

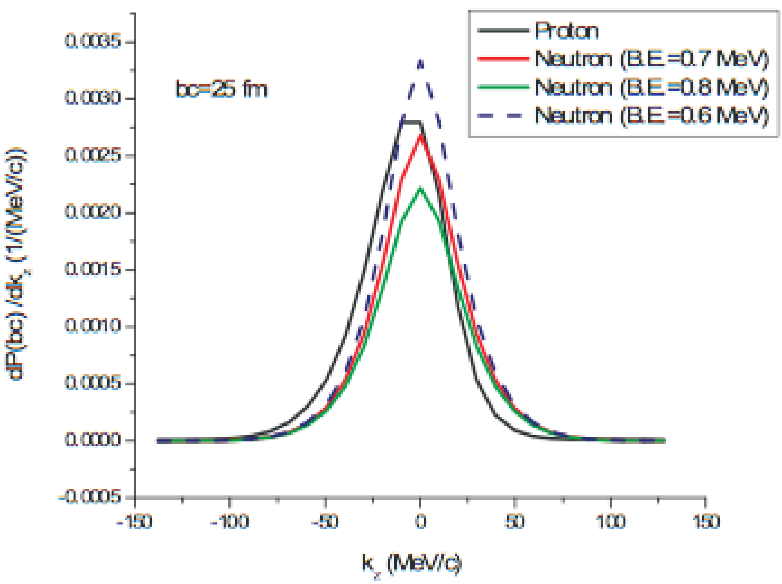

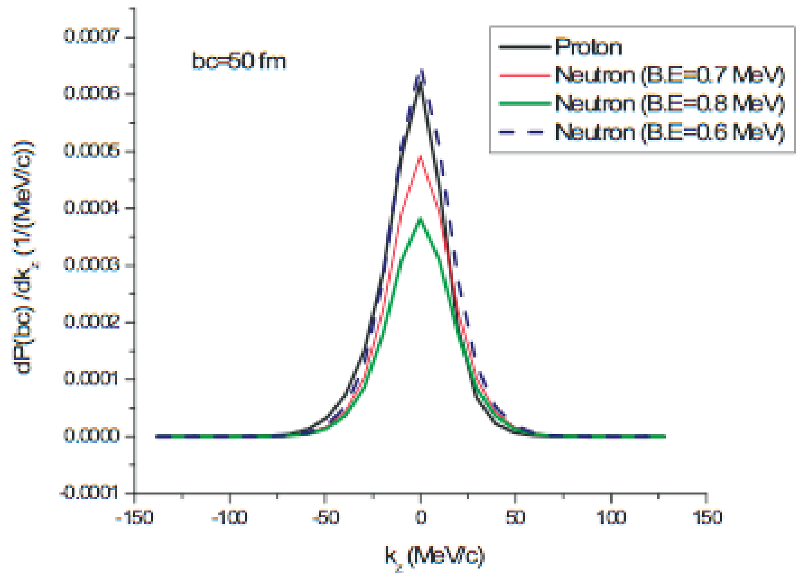

Accuracy of reaction theory and experimental data analysis vs structure theory.

$$\sigma_{\text{el.bup}} = \int \langle \phi_0 | \widehat{S}_v^* \widehat{S}_c^* | \phi_{\mathbf{k}} \rangle \langle \phi_{\mathbf{k}} | \widehat{S}_v \widehat{S}_c | \phi_0 \rangle \, \mathrm{d}\mathbf{k}$$

$$= \langle \phi_0 | \left| \widehat{S}_v \right|^2 \left| \widehat{S}_c \right|^2 | \phi_0 \rangle - \left| \langle \phi_0 | \widehat{S}_v \widehat{S}_c | \phi_0 \rangle \right|^2 .$$

$$\sigma_{\text{in.bup}} = \frac{\pi}{k^2} \sum \langle \phi_0 | \left(1 - \widehat{T}_c \right) \widehat{T}_v | \phi_0 \rangle .$$

T_v with $1 - |\widehat{S}_v|^2$

$$\sigma_{\exp} = R_s \left(\frac{A}{A-1} \right)^2 C^2 S_j \, \sigma_{sp},$$

PHYSICAL REVIEW C 77, 044306 (2008)

Reduction of spectroscopic strength: Weakly-bound and strongly-bound single-particle states studied using one-nucleon knockout reactions

A. Gade,[1,2] P. Adrich,[1] D. Bazin,[1] M. D. Bowen,[1,2] B. A. Brown,[1,2] C. M. Campbell,[1] J. M. Cook,[1,2] T. Glasmacher,[1,2] P. G. Hansen,[1,2] K. Hosier,[3] S. McDaniel,[1,2] D. McGlinchery,[3] A. Obertelli,[1] K. Siwek,[1,2] L. A. Riley,[3] J. A. Tostevin,[4] and D. Weisshaar[1]

reaction theory. The reduction of the experimentally deduced spectroscopic strengths, relative to the predictions of shell-model calculations, is of order 0.8–0.9 in the removal of weakly bound protons and 0.3–0.4 in the knockout of the strongly bound neutrons. These results support previous studies at the extremes of nuclear binding and provide further evidence that in asymmetric nuclear systems the nucleons of the deficient species, at the more-bound Fermi surface are more strongly correlated than those of the more weakly bound excess species.

TABLE I. Summary of the results for the one-proton and one-neutron knockout from ^{24}Si and ^{28}S projectiles. Given are the excitation energy of the final states in the projectile-like knockout residues, the spin and parity, the experimental branching ratios, the measured cross sections, the shell-model single-particle orbitals, the single-particle cross sections from the eikonal theory and their composition into stripping and diffractive contributions, the shell-model spectroscopic factors (USDB effective interaction), the resulting theoretical cross sections from Eq. (1), the theoretical branching ratios, and the deduced reduction factors.

Res.	E_x (keV)	J^π ($\hbar$)	BR^{exp} (%)	σ (mb)	Conf. SM	σ_{sp} (mb)	σ_{sp}^{str} (mb)	σ_{sp}^{dif} (mb)	C^2S SM	σ^{th} (mb)	BRth (%)	R_s
						Projectile ^{24}Si						
^{23}Al	0	$5/2^+$	100	67.3(35)	$d_{5/2}$	22.74	17.56	5.18	3.42	84.68	100	0.79(4)
^{23}Si	0	$5/2^+$	100	9.8(10)	$d_{5/2}$	13.43	10.96	2.47	1.71	25.01	100	0.39(4)
						Projectile ^{28}S						
^{27}P	0	$1/2^+$	82(7)	31(3)	$s_{1/2}$	28.57	20.73	7.84	0.832	25.56	60.4	
	1100	$3/2^+$	18(3)	6.8(11)	$d_{3/2}$	19.01	14.61	4.40	0.82	16.76	39.6	
Inc.				38(3)						42.32		0.90(7)
^{27}S	0	$5/2^+$			$d_{5/2}$	11.09	8.99	2.10	3.136	37.40	96.5	
	$\leqslant$100	$3/2^+$			$d_{3/2}$	10.75	8.72	2.03	0.119	1.37	3.5	
Inc.				11.9(12)						38.77		0.31(3)

VOLUME 93, NUMBER 4 PHYSICAL REVIEW LETTERS week ending 23 JULY 2004

Reduced Occupancy of the Deeply Bound $0d_{5/2}$ Neutron State in ^{32}Ar

A. Gade,[1] D. Bazin,[1] B. A. Brown,[1,2] C. M. Campbell,[1,2] J. A. Church,[1,2,*] D. C. Dinca,[1,2] J. Enders,[1,†] T. Glasmacher,[1,2] P. G. Hansen,[1,2,‡] Z. Hu,[1] K. W. Kemper,[3] W. F. Mueller,[1] H. Olliver,[1,2] B. C. Perry,[1,2] L. A. Riley,[4] B. T. Roeder,[3] B. M. Sherrill,[1,2] J. R. Terry,[1,2] J. A. Tostevin,[5] and K. L. Yurkewicz[1,2]

[1]*National Superconducting Cyclotron Laboratory, Michigan State University, East Lansing, Michigan 48824, USA*
[2]*Department of Physics and Astronomy, Michigan State University, East Lansing, Michigan 48824, USA*
[3]*Department of Physics, Florida State University, Tallahassee, Florida 32306, USA*
[4]*Department of Physics and Astronomy, Ursinus College, Collegeville, Pennsylvania 19426, USA*
[5]*Department of Physics, School of Electronics and Physical Sciences, University of Surrey, Guildford, Surrey GU2 7XH, United Kingdom*

(Received 13 February 2004; published 19 July 2004)

The ^{9}Be(^{32}Ar, ^{31}Ar)X reaction, leading to the $\frac{5}{2}^+$ ground state of a nucleus at the proton drip line, has a cross section of 10.4(13) mb at a beam energy of 65.1 MeV/nucleon. This translates into a spectroscopic factor that is only 24(3)% of that predicted by the many-body shell-model theory. We introduce refinements to the eikonal reaction theory used to extract the spectroscopic factor to clarify that this very strong reduction represents an effect of nuclear structure. We suggest that it reflects correlation effects linked to the high neutron separation energy (22.0 MeV) for this state.

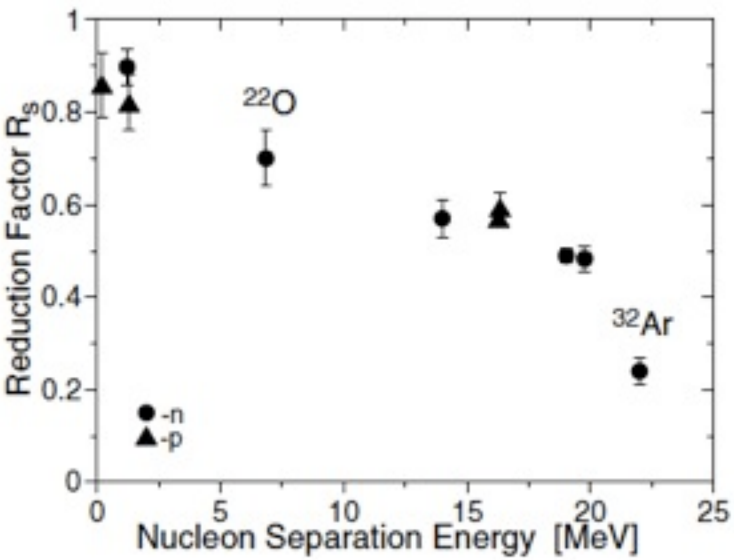

FIG. 3. Measured reduction factors R_s as a function of nucleon separation energy. The points, taken from the left, use data from ^{8}B, ^{9}C, ^{15}C, ^{57}Ni, ^{12}C, and ^{16}O [4,5,26]. The labeled $N = 14$ nuclei are discussed in the present Letter.

http://www.eurisol.org/usergroup/

EURISOL User Group

2nd Topical Meeting, Valencia, Spain

Neutron deficient exotic nuclei and the Physics of the "proton rich side" of the nuclear chart

7-9 February 2011 Colegio Rector Peset

Main organizer: Berta Rubio rubio@ific.uv.es

FUTURE:

EURISOL NET

Physics & Instrumentation

2. Effect of particle–vibration coupling on individual energies

Let us start with the Hartree–Fock(HF) potential for a neutron in the mean field of the core nucleus and calculate the correction to this HF potential due to the coupling of single particle states to the RPA collective one-phonon states of the core. Neglecting the antisymmetrisation between the single particle and the particles of the core, one can write this correction δV as [26,28]:

$$\delta V(r,r';E) = \lim_{\eta\to+0} \sum_{N,\lambda} \left[\frac{1-n_\lambda}{E-\epsilon_\lambda - E_N + i\eta} + \frac{n_\lambda}{E-\epsilon_\lambda+E_N-i\eta} \right] \times V^*_{0N}(r) V_{0N}(r') \phi^*_\lambda(r') \phi_\lambda(r). \quad (1)$$

λ and N characterise respectively the HF single particle state of energy ϵ_λ and wave function ϕ_λ and the RPA collective state of the core of excitation energy E_N; n_λ is the occupation number of the state λ in the HF ground state of the core and V_{0N} the transition amplitude between the ground state and the excited state N. V_{0N} can be written as:

$$V_{0N}(r) = \sum_{i,j} [n_i(1-n_j) + n_j(1-n_i)] x^{(N)}_{ij} \rho_{ij}(r) = \langle \Psi_N | v | \Psi_0 \rangle, \quad (2)$$

where $x^{(N)}_{ij}$ are the RPA amplitudes, $\rho_{ij}(r)$ the transition density for the unperturbed particle-hole state (ij), v the two body interaction and Ψ_N and Ψ_0 the RPA wave functions of the excited state and the ground state respectively. In the summation over N we keep only natural parity states with multipolarity L and define amplitudes $f_{NL}(r)$ such that:

$$V_{0N}(r) = \frac{1}{\sqrt{2L+1}} f_{NL}(r) Y^{M*}_L(\hat{r}). \quad (3)$$

The correction of Eq. (1) to the HF potential induces a modification of the single particle energies which, in first approximation, can be calculated as the average of δV over the HF state of interest, replacing in Eq. (1) the energy E by the corresponding HF energy. For an HF state n of energy ϵ_n we get the modified energy e_n as:

$$e_n = \epsilon_n + \delta\epsilon_n, \quad (4)$$

$$\delta\epsilon_n = \sum_{N,\lambda} F_{N\lambda} \frac{2j_\lambda+1}{4\pi} \begin{pmatrix} j_n & L & j_\lambda \\ -1/2 & 0 & 1/2 \end{pmatrix}^2 \left| \int_0^\infty r^2 \, dr \, \mathcal{R}_\lambda(r) \mathcal{R}_n(r) f_{NL}(r) \right|^2 \quad (5)$$

with

$$F_{N\lambda} = \frac{1-n_\lambda}{\epsilon_n - \epsilon_\lambda - E_N} + \frac{n_\lambda}{\epsilon_n - \epsilon_\lambda + E_N}. \quad (6)$$

$\mathcal{R}_\lambda$ and $\mathcal{R}_n$ are the radial wave functions.

$$f_{NL}(r) = \beta_{NL} R_0 \frac{dU(r)}{dr}.$$

Pacheco & N. Vinh Mau,
PRC 65 (2002) 044004
Labiche et al. PRC 60 027303 (1999)

TABLE IV: Main pp-RPA amplitudes for ^{14}Be ground state without (A) and with (B) inversion of $2s_{1/2}$-$1p_{1/2}$ shells.

	X_{ab}			$X_{\alpha\beta}$	
	$(2s_{1/2})^2$	$(1d_{5/2})^2$		$(1p_{3/2})^2$	$(1p_{1/2})^2$
A	-0.93	-0.49		0.32	0.36
	$(1d_{5/2})^2$	$(1p_{1/2})^2$	$(1p_{1/2}\ 2p_{1/2})$	$(1p_{3/2})^2$	$(2s_{1/2})^2$
B	0.69	-0.73	0.52	-0.61	0.45